SIO 92-11
NDP-044

Surface Water and Atmospheric Carbon Dioxide and Nitrous Oxide Observations by Shipboard Automated Gas Chromatography: Results From Expeditions Between 1977 and 1990

R. F. Weiss · F. A. Van Woy · P. K. Salameh

Scripps Institution of Oceanography

Carbon Dioxide Information Analysis Center
Oak Ridge National Laboratory

SIO 92-11
ORNL/CDIAC-59
NDP-044

SURFACE WATER AND ATMOSPHERIC CARBON DIOXIDE AND NITROUS OXIDE OBSERVATIONS BY SHIPBOARD AUTOMATED GAS CHROMATOGRAPHY: RESULTS FROM EXPEDITIONS BETWEEN 1977 AND 1990

R. F. Weiss
F. A. Van Woy
P. K. Salameh

Scripps Institution of Oceanography
University of California, San Diego
La Jolla, California 92093-0220

Environmental Sciences Division Publication No. 3987

Scripps Institution of Oceanography Reference 92-11

Date Published: December 1992

Prepared by R. J. Sepanski

Energy, Environment, and Resources Center
The University of Tennessee
Knoxville, Tennessee 37996

Prepared for the
Global Change Research Program
Environmental Sciences Division
Office of Health and Environmental Research
U.S. Department of Energy
Budget Activity Number KP 05 00 00 0

Prepared by the
Carbon Dioxide Information Analysis Center
Environmental Sciences Division
OAK RIDGE NATIONAL LABORATORY
Oak Ridge, Tennessee 37831-6335
managed by
MARTIN MARIETTA ENERGY SYSTEMS, INC.
for the
U.S. DEPARTMENT OF ENERGY
under contract DE-AC05-84OR21400

CONTENTS

CONTENTS (continued)

LIST OF FIGURES

LIST OF FIGURES (continued)

LIST OF FIGURES (continued)

LIST OF FIGURES (continued)

LIST OF TABLES

ACKNOWLEDGMENTS

This report contains the results of many years of work which could not have been completed without the help of many colleagues. We are especially grateful to J. Bullister, E. Dlugokencky, K. Harrison, E. Hoopes, P. Murphy, M. Warner, and the officers and crews of the many research vessels upon which we have worked for their assistance with the shipboard operations. This work was supported by grants from the Marine Chemistry and Physical Oceanography programs of the National Science Foundation and from the Department of Energy, often as an ancillary part of our seagoing chlorofluorocarbon tracer measurement efforts.

ABSTRACT

R. F. WEISS, F. A. VAN WOY, AND P. K. SALAMEH. 1992. Surface water and atmospheric carbon dioxide and nitrous oxide observations by shipboard automated gas chromatography: Results from expeditions between 1977 and 1990. Scripps Institution of Oceanography Reference 92-11. ORNL/CDIAC-59, NDP-044. Carbon Dioxide Information Analysis Center, Oak Ridge National Laboratory, Oak Ridge, Tennessee. 144 pp.
doi: 10.3334/CDIAC/otg.ndp044

This document presents the results of surface water and atmospheric carbon dioxide (CO_2) and nitrous oxide (N_2O) measurements carried out by shipboard gas chromatography over the period 1977–1990. These data include results from 11 different oceanic surveys for a total of 41 expedition legs. Collectively, they represent a globally distributed sampling that includes locations in the Atlantic, Pacific, Indian, and Southern Oceans, as well as the Mediterranean and Red Seas.

The measurements were made by an automated high-precision shipboard gas chromatographic system developed during the late 1970s and used extensively over the intervening years. This instrument measures CO_2 by flame ionization after quantitative reaction to methane in a stream of hydrogen. Nitrous oxide is measured by a separate electron capture detector. The chromatographic system measures 196 dry-gas samples a day, divided equally among the atmosphere, gas equilibrated with surface water, a low-range gas standard, and a high-range gas standard.

These data constitute one of the most extensive records available of CO_2 and, particularly, N_2O in marine air and surface seawater. The data will be valuable in modeling applications dealing with the ocean's role in the global cycles of carbon and nitrogen, in studies of ocean–atmosphere dynamics, and in studies evaluating other methodologies for determining pCO_2.

All data have been assessed for quality and consistency and have been edited to remove serious outliers and contaminated samples and to correct gross numerical errors.

These data are available free of charge as a numeric data package (NDP) from the Carbon Dioxide Information Analysis Center (CDIAC). The NDP consists of this document and a magnetic tape (or set of floppy diskettes) containing machine-readable files.[a] This document provides sample listings of the surface water and atmospheric CO_2 and N_2O data, offers retrieval program listings (in FORTRAN and SAS[b] languages), furnishes graphical and tabular information on each of the contributing oceanic expeditions, defines limitations and restrictions of the data, and reprints pertinent literature.

[a] Files are also available through Internet using the File Transfer Protocol (FTP) from CDIAC's anonymous FTP area.

[b] SAS is the registered trademark of SAS Institute, Inc., Cary, NC 27511-8000.

PART 1

INFORMATION ABOUT THE NUMERIC DATA PACKAGE

1. NAME OF THE NUMERIC DATA PACKAGE

Surface Water and Atmospheric Carbon Dioxide and Nitrous Oxide Observations by Shipboard Automated Gas Chromatography: Results from Expeditions between 1977 and 1990

2. CONTRIBUTORS

R. F. Weiss F. A. Van Woy P. K. Salameh

Scripps Institution of Oceanography
University of California, San Diego
La Jolla, California

3. KEYWORDS

Carbon dioxide (CO_2); gas chromatography; marine atmospheric concentrations; nitrous oxide (N_2O); oceanography; surface seawater dissolved gases.

4. SOURCE INFORMATION

The surface water and atmospheric carbon dioxide (CO_2) and nitrous oxide (N_2O) data reported here were obtained by direct shipboard gas chromatographic measurement. These data include results from 11 different oceanic surveys for a total of 41 expedition legs. The represented oceanic surveys include the following: (1) the Indomed expedition, 1977–1979 [Indomed legs 4 and 5 are also part of the Geochemical Ocean Sections (GEOSECS) Indian Ocean expedition]; (2) the North Pacific Experiment (NORPAX) Hawaii–Tahiti Shuttle Experiment, 1979–1980; (3) and (4) the Transient Tracers in the Ocean, North Atlantic and Tropical Atlantic Studies (TTO/NAS, TTO/TAS), 1981–1983; (5) the Hudson 82-001 expedition, 1982; (6) the Ajax expedition, 1983–1984; (7) and (8) the Trans-Pacific Sections expeditions along 24 degrees North and 47 degrees North (TPS24 and TPS47), 1985; (9) the fifth "Antarktis" expedition (Ant V) of the R/V Polarstern, as part of the Winter Weddell Sea Experiment, 1986; (10) the South Atlantic Ventilation Experiment (SAVE), 1987–1989 (SAVE legs 4–6 are also designated as legs 2–4 of R/V Melville's Hydros expedition); and (11) the 1990 expedition of the National Oceanic and Atmospheric Administration's Climate and Global Change series (CGC-90). Table 1 presents a track list showing the dates, ports of departure and arrival, regions surveyed, and cruise ship names for each of the 41 expedition legs that contributed data. In addition, a series of maps showing the tracks of the expeditions and the N_2O and CO_2 results for each expedition leg is presented in Figs. 1–83.

Table 1. Track list of expeditions that contributed measurements to the surface water and atmospheric CO_2 and N_2O data set

No.	Cruise	Date/Port		Date/Port		Region	Ship
	Indomed						
1	* Leg 2	7 Nov 77	Panama	1 Dec 77	Cadiz	Carib./Atl.	Melville
2	* Leg 3	4 Dec 77	Cadiz	12 Dec 77	Alexandria	Med.	Melville
3	* Leg 4	16 Dec 77	Alexandria	22 Jan 78	Mauritius	Red S./Ind.	Melville
4	* Leg 5	28 Jan 78	Mauritius	25 Feb 78	Fremantle	S. Ind.	Melville
5	Leg 11A	21 Sep 78	Bermuda	25 Sep 78	San Juan	Atl.	Melville
6	Leg 12	28 Sep 78	San Juan	1 Nov 78	Montevideo	Atl.	Melville
7	Leg 15	10 Feb 79	Punta Arenas	5 Mar 79	Panama	S. Pac.	Melville
8	Leg 15A	7 Mar 79	Panama	15 Mar 79	Manzanillo	Trop. Pac.	Melville
	NORPAX Shuttle						
9	Transit	6 Jul 79	Newport OR	14 Jul 79	Honolulu	N. Pac.	Wecoma
10	Leg 7	19 Aug 79	Papeete	11 Sep 79	Honolulu	Trop. Pac.	Wecoma
11	Leg 9	31 Oct 79	Papeete	24 Nov 79	Honolulu	Trop. Pac.	Wecoma
12	Leg 13	18 Mar 80	Papeete	10 Apr 80	Honolulu	Trop. Pac.	Wecoma
13	Leg 15	18 May 80	Papeete	15 Jun 80	Honolulu	Trop. Pac.	Wecoma
	TTO/NAS						
14	Leg 1	1 Apr 81	Woods Hole	13 Apr 81	Bahamas	N. Atl.	Knorr
15	Leg 2	15 Apr 81	Bahamas	12 May 81	Bermuda	N. Atl.	Knorr
16	Leg 3	16 May 81	Bermuda	14 Jun 81	Azores	N. Atl.	Knorr
17	Leg 4	19 Jun 81	Azores	15 Jul 81	Glasgow	N. Atl.	Knorr
18	Leg 5	21 Jul 81	Glasgow	16 Aug 81	Reykjavik	Gnlnd. Sea	Knorr
19	Leg 6	21 Aug 81	Reykjavik	17 Sep 81	St. John's	N. Atl.	Knorr
20	Leg 7	23 Sep 81	St. John's	19 Oct 81	Woods Hole	N. Atl.	Knorr
	Hudson 82-001						
21	Leg 1	14 Feb 82	Halifax	23 Mar 82	Tromso	Gnlnd. Sea	Hudson
22	Leg 2	25 Mar 82	Tromso	6 Apr 82	Reykjavik	Gnlnd. Sea	Hudson
	TTO/TAS						
23	Leg 1	1 Dec 82	San Juan	22 Dec 82	Belem	Trop. Atl.	Knorr
24	Leg 2	29 Dec 82	Belem	24 Jan 83	Dakar	Trop. Atl.	Knorr
25	Leg 3	30 Jan 83	Dakar	18 Feb 83	Recife	Trop. Atl.	Knorr
26	Ajax 1	7 Oct 83	Abidjan	6 Nov 83	Cape Town	S. Atl.	Knorr
27	Ajax 2	11 Jan 84	Cape Town	18 Feb 84	Punta Arenas	S. Atl.	Knorr
28	TPS24 1	29 Mar 85	San Diego	1 May 85	Midway	N. Pac.	Thompson
29	TPS24 2	2 May 85	Midway	4 Jun 85	Nagasaki	N. Pac.	Thompson
30	TPS47 1	4 Aug 85	Hakodate	7 Sep 85	Seattle	N. Pac.	Thompson
31	Ant V/2	27 Jun 86	Bahia Blanca	17 Sep 86	Cape Town	Wedd. Sea	Plrstern
32	Ant V/3	28 Sep 86	Cape Town	13 Dec 86	Cape Town	Wedd. Sea	Plrstern
	SAVE						
33	Transit	31 Oct 87	Woods Hole	19 Nov 87	Recife	Atl.	Knorr
34	Leg 1	23 Nov 87	Recife	13 Dec 87	Abidjan	Trop. Atl.	Knorr
35	Leg 2	18 Dec 87	Abidjan	21 Jan 88	Rio	S. Atl.	Knorr
36	Leg 3	28 Jan 88	Rio	7 Mar 88	Abidjan	S. Atl.	Knorr
37	Leg 4	8 Dec 88	Punta Arenas	15 Jan 89	Cape Town	S. Atl.	Melville
38	Leg 5	23 Jan 89	Cape Town	8 Mar 89	Montevideo	S. Atl.	Melville
39	Leg 6	13 Mar 89	Montevideo	19 Apr 89	Barbados	S. Atl.	Melville
	CGC-90						
40	Leg 1	22 Feb 90	Pago Pago	22 Mar 90	Wellington	S. Pac.	Baldrige
41	Leg 2	27 Mar 90	Wellington	16 Apr 90	Honolulu	S. Pac.	Baldrige

* CO_2 not measured on these legs.

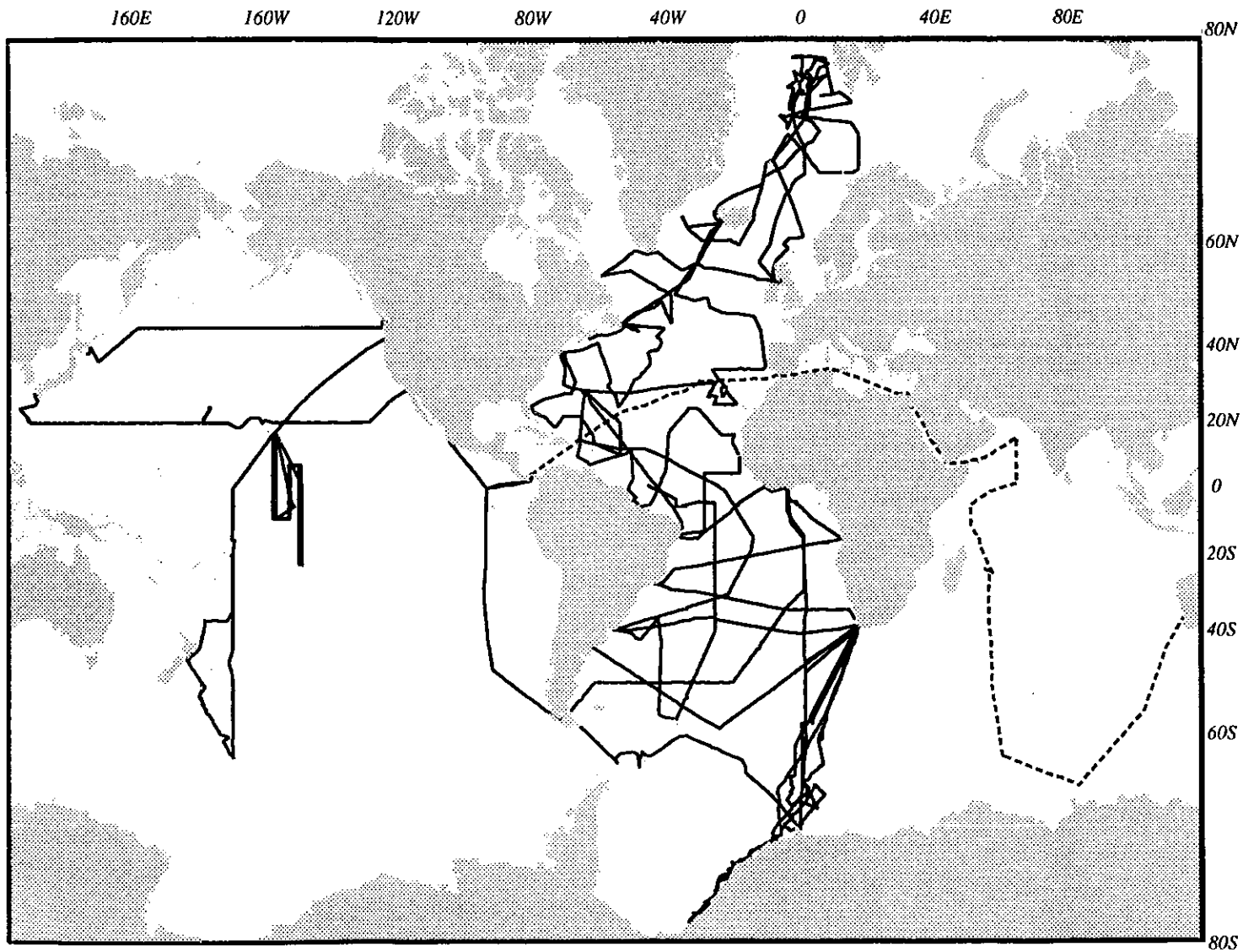

Figure 1. World map showing composite cruise track locations. Dashed lines denote expedition legs on which only N_2O was measured; on all other legs, both N_2O and CO_2 were measured.

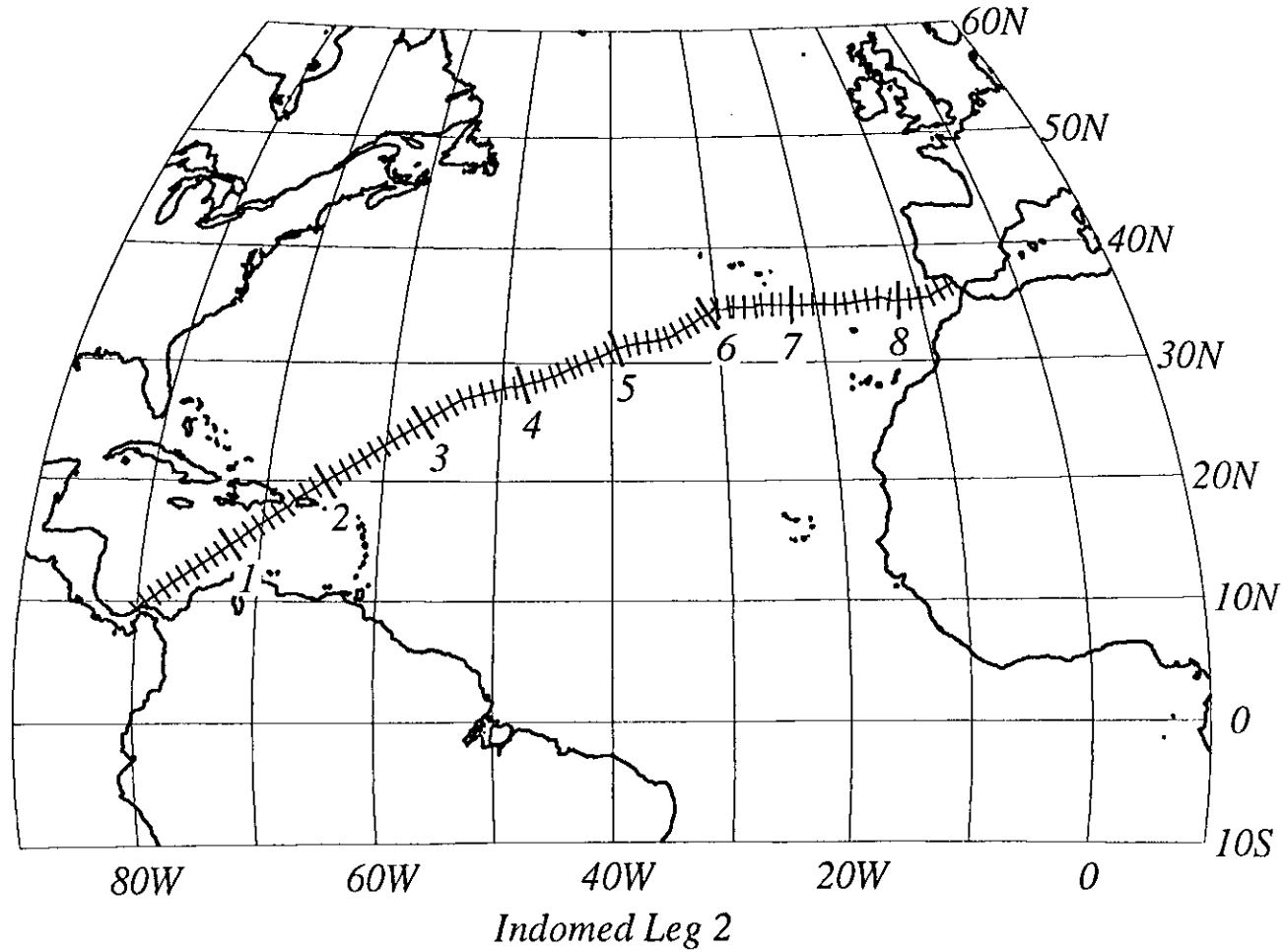

Figure 2. Cruise track plot, Indomed Leg 2. Track indicates cumulative distance in 1000 km intervals, with subdivisions of 100 km.

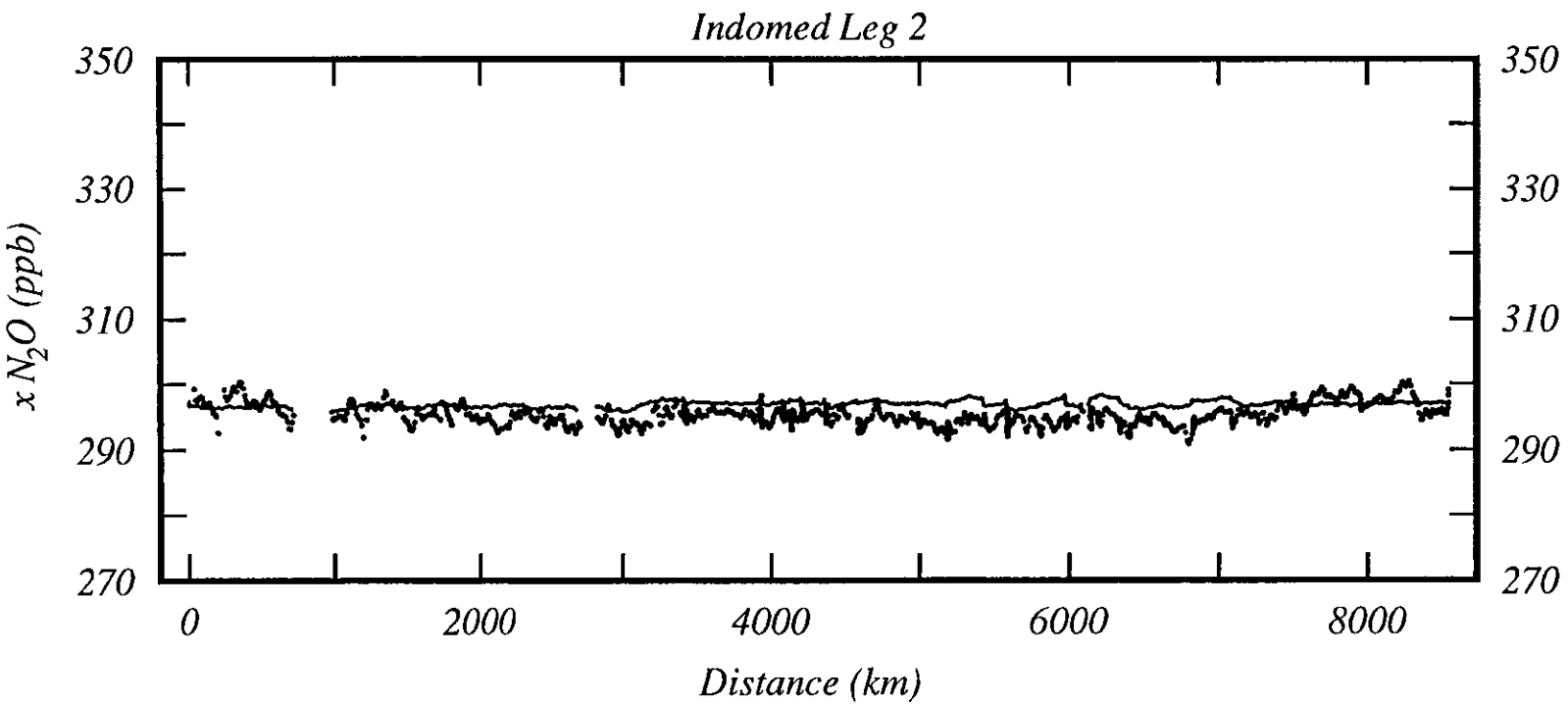

Figure 3. Data plot of xN_2O (dry gas mole fraction), Indomed Leg 2. Atmospheric measurements are plotted as a line (20 point running mean). Measurements of gas equilibrated with seawater are plotted as individual points after smoothing with a 5-point Gaussian smoother.

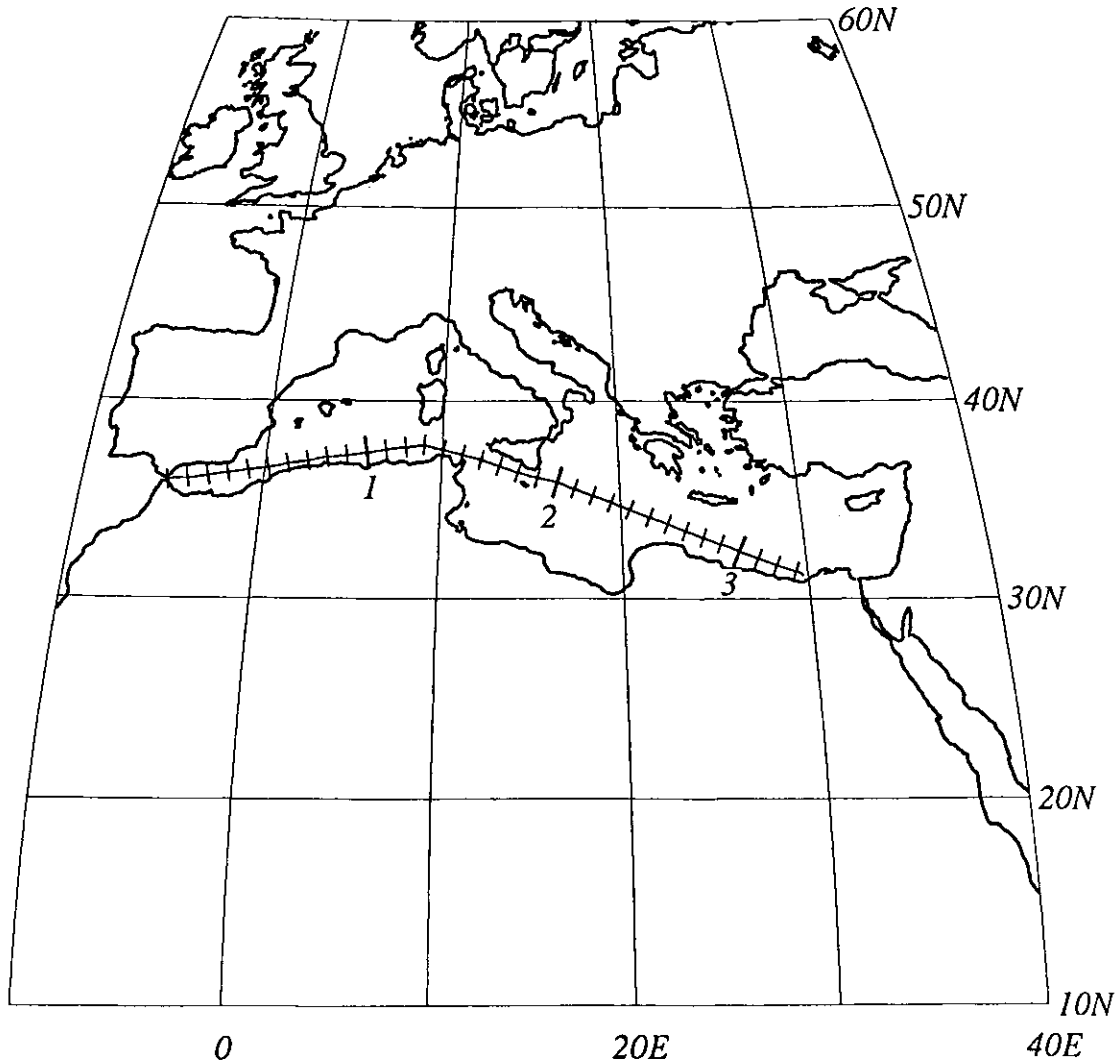

Figure 4. Cruise track plot, Indomed Leg 3. Track indicates cumulative distance in 1000 km intervals, with subdivisions of 100 km.

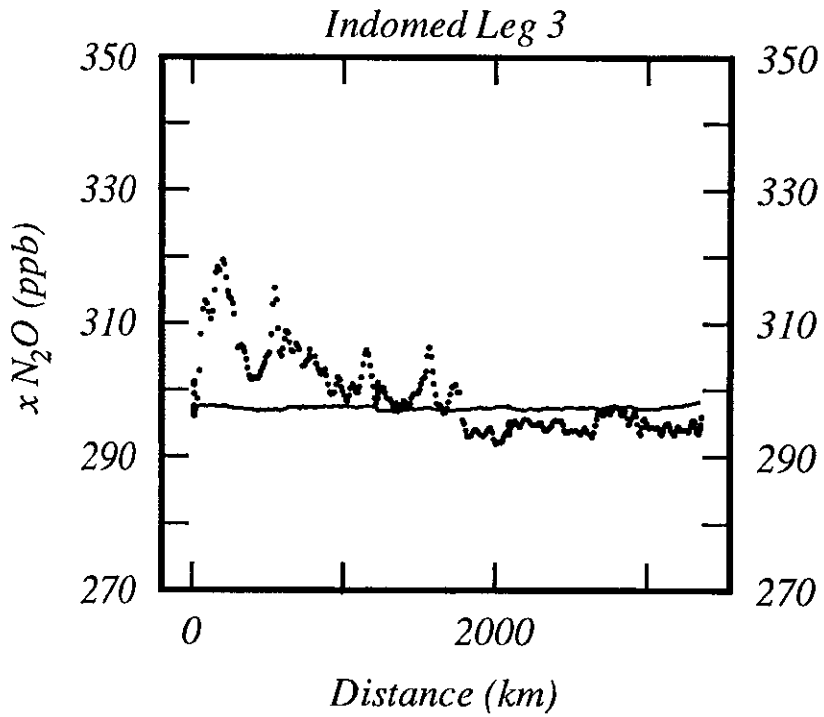

Figure 5. Data plot of xN_2O (dry gas mole fraction), Indomed Leg 3. Atmospheric measurements are plotted as a line (20 point running mean). Measurements of gas equilibrated with seawater are plotted as individual points after smoothing with a 5-point Gaussian smoother.

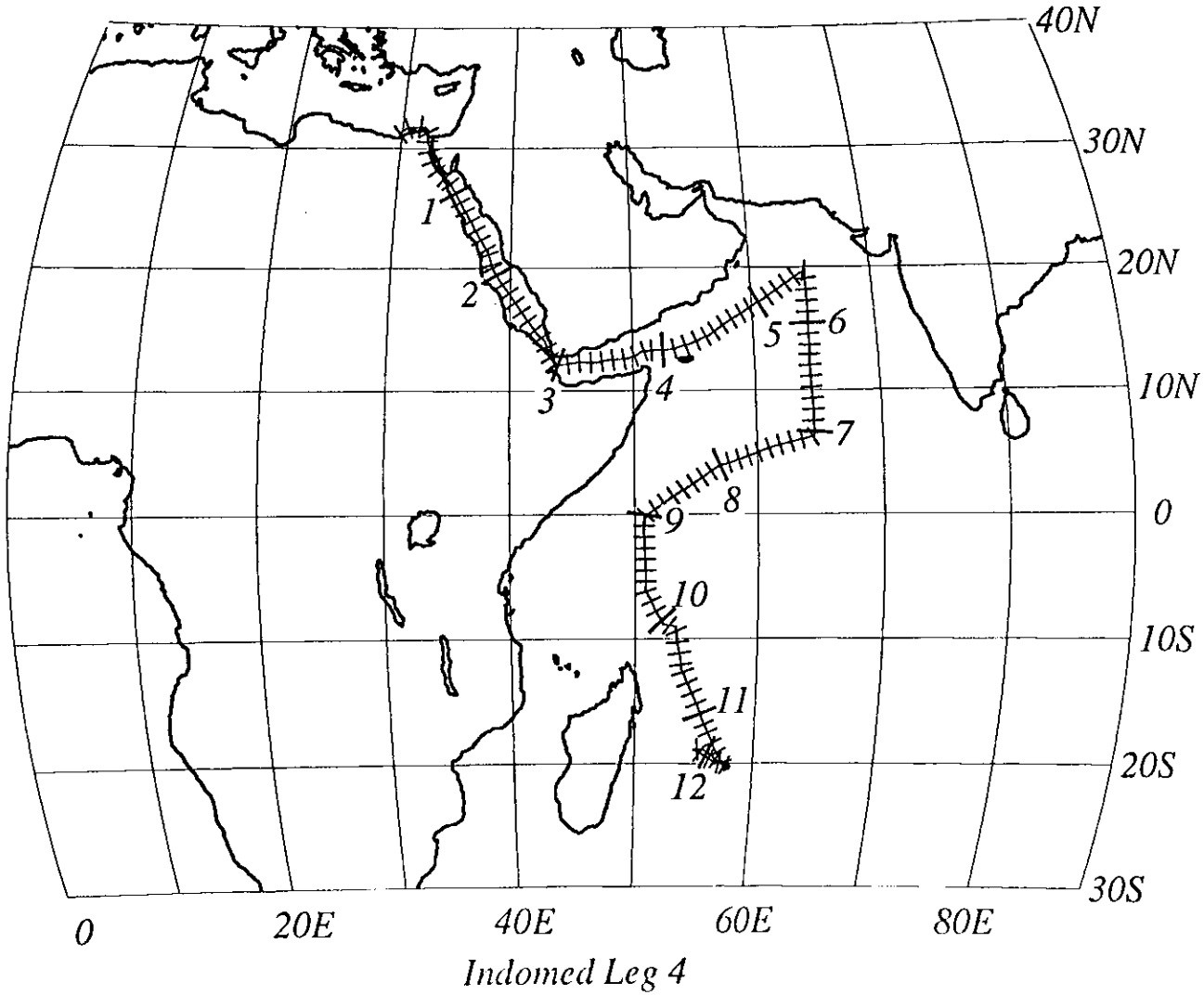

Figure 6. Cruise track plot, Indomed Leg 4. Track indicates cumulative distance in 1000 km intervals, with subdivisions of 100 km.

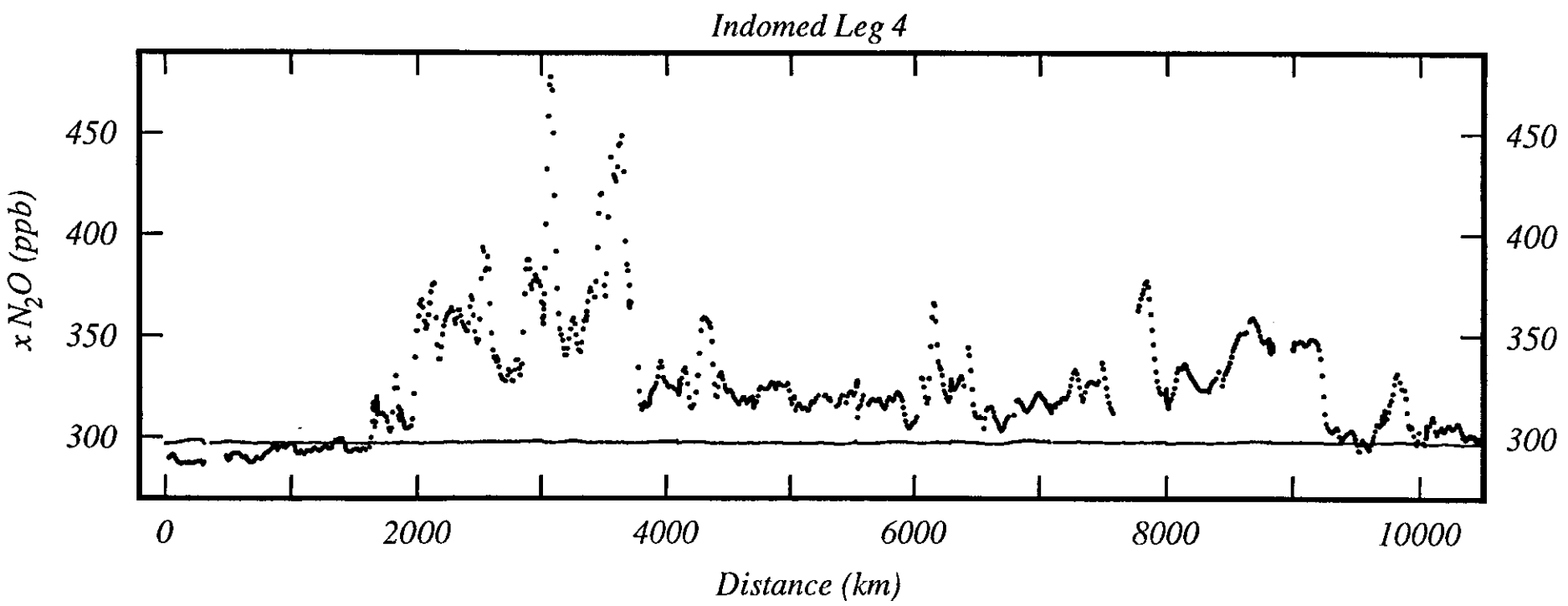

Figure 7. Data plot of xN_2O (dry gas mole fraction), Indomed Leg 4. Atmospheric measurements are plotted as a line (20 point running mean). Measurements of gas equilibrated with seawater are plotted as individual points after smoothing with a 5-point Gaussian smoother.

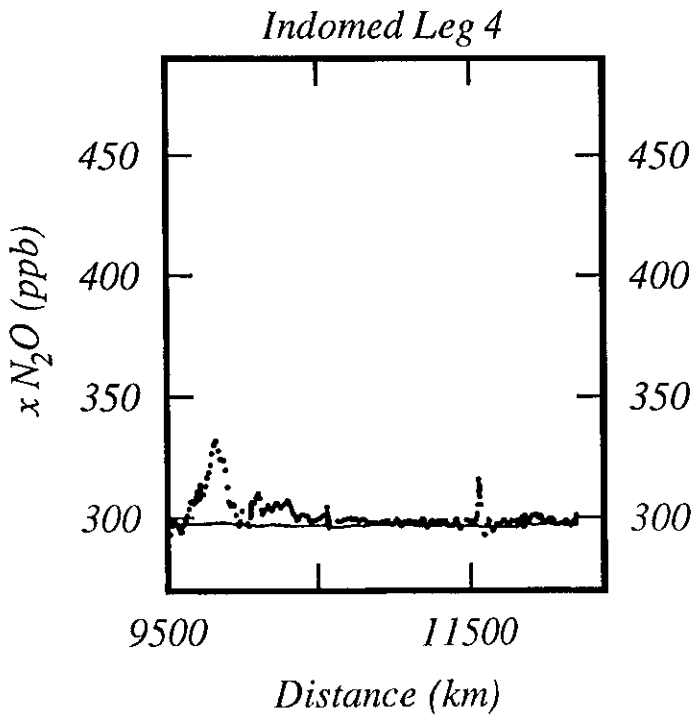

Figure 7. Continued

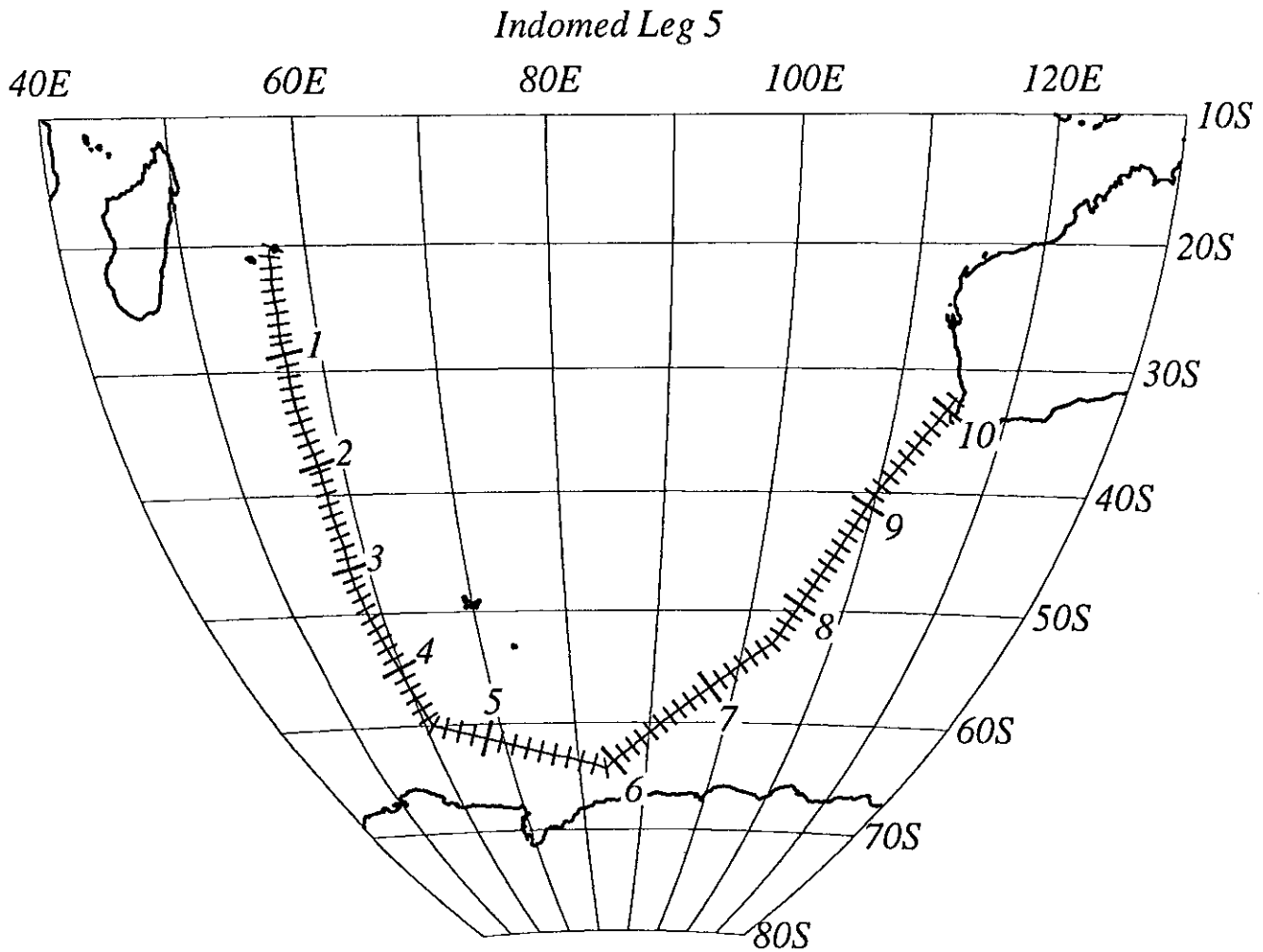

Figure 8. Cruise track plot, Indomed Leg 5. Track indicates cumulative distance in 1000 km intervals, with subdivisions of 100 km.

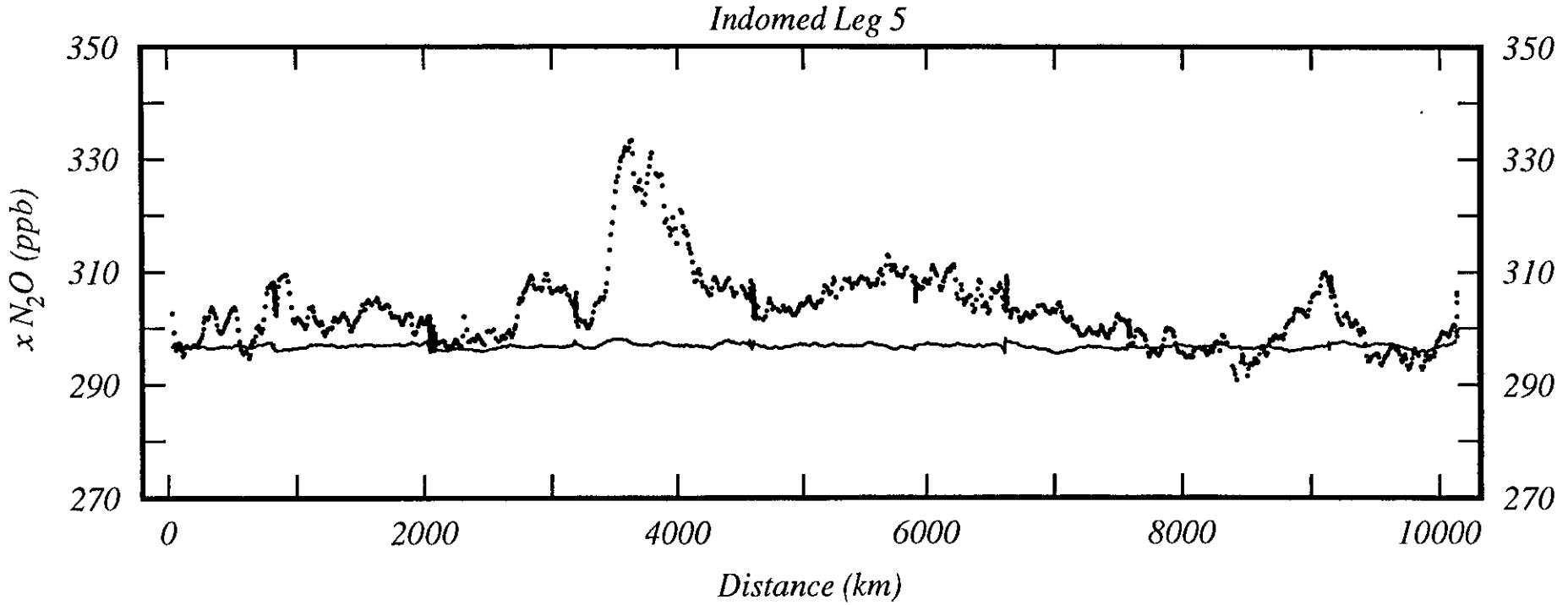

Figure 9. Data plot of xN_2O (dry gas mole fraction), Indomed Leg 5. Atmospheric measurements are plotted as a line (20 point running mean). Measurements of gas equilibrated with seawater are plotted as individual points after smoothing with a 5-point Gaussian smoother.

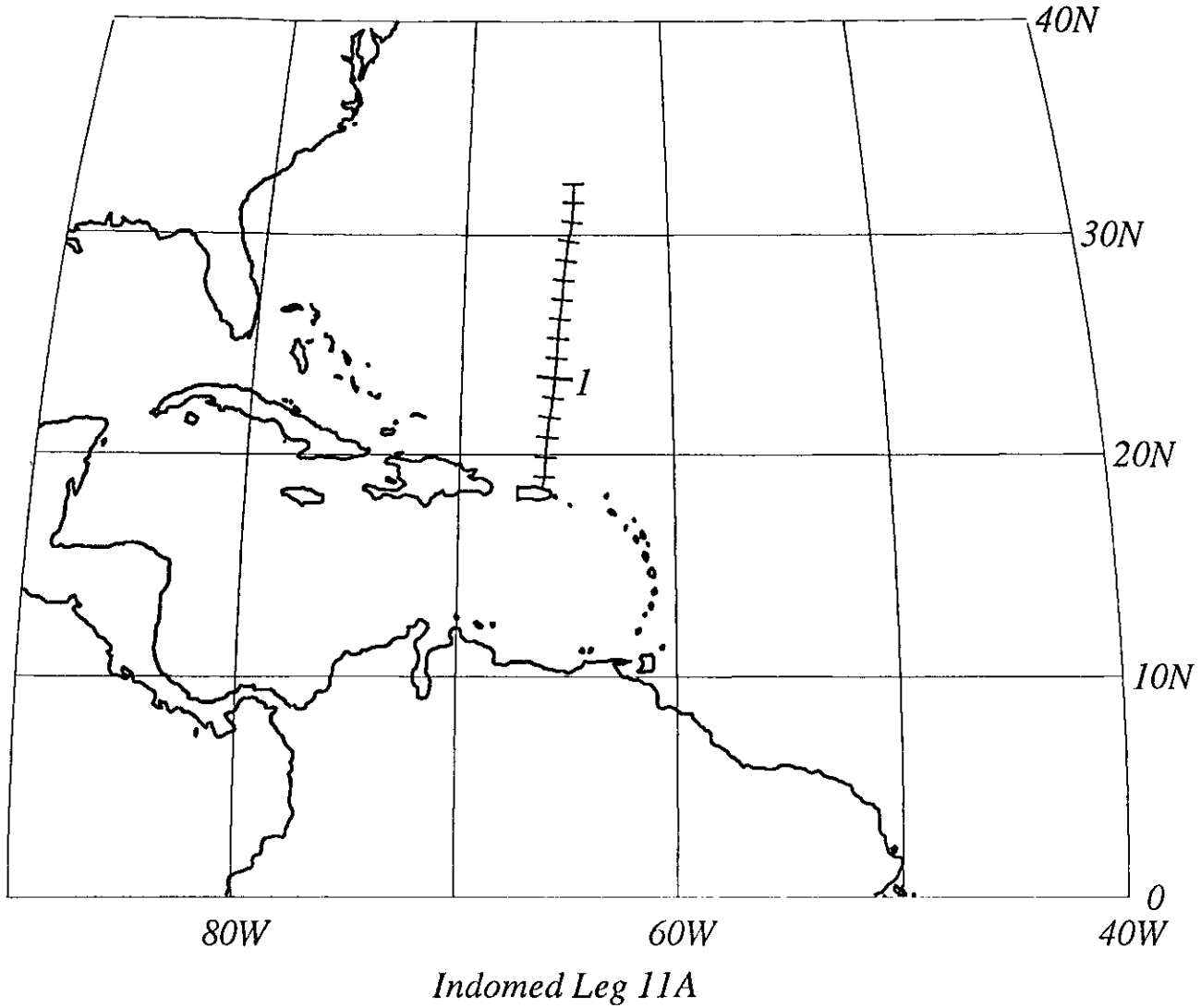

Figure 10. Cruise track plot, Indomed Leg 11A. Track indicates cumulative distance in 1000 km intervals, with subdivisions of 100 km.

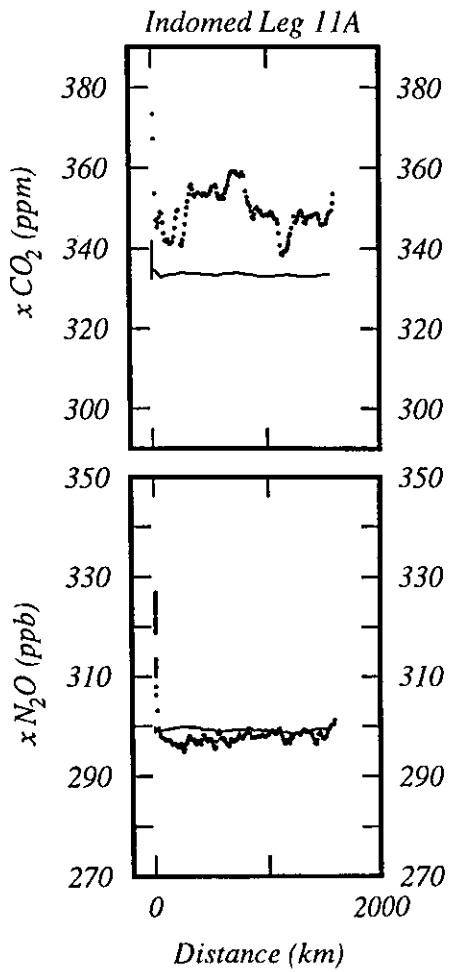

Figure 11. Data plot of xCO_2 and xN_2O (dry gas mole fractions), Indomed Leg 11A. Atmospheric measurements are plotted as a line (20 point running mean). Measurements of gas equilibrated with seawater are plotted as individual points after smoothing with a 5-point Gaussian smoother.

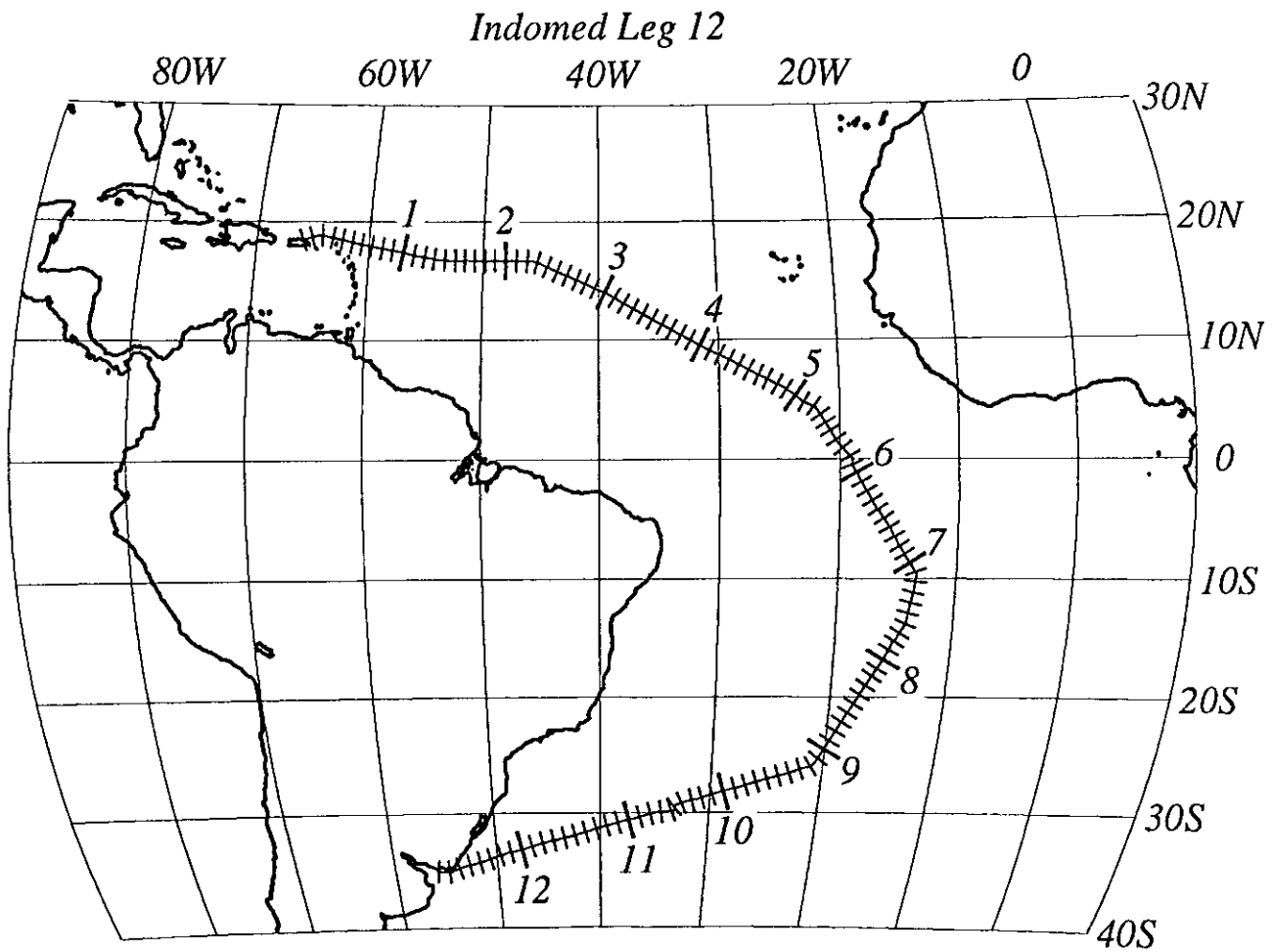

Figure 12. Cruise track plot, Indomed Leg 12. Track indicates cumulative distance in 1000 km intervals, with subdivisions of 100 km.

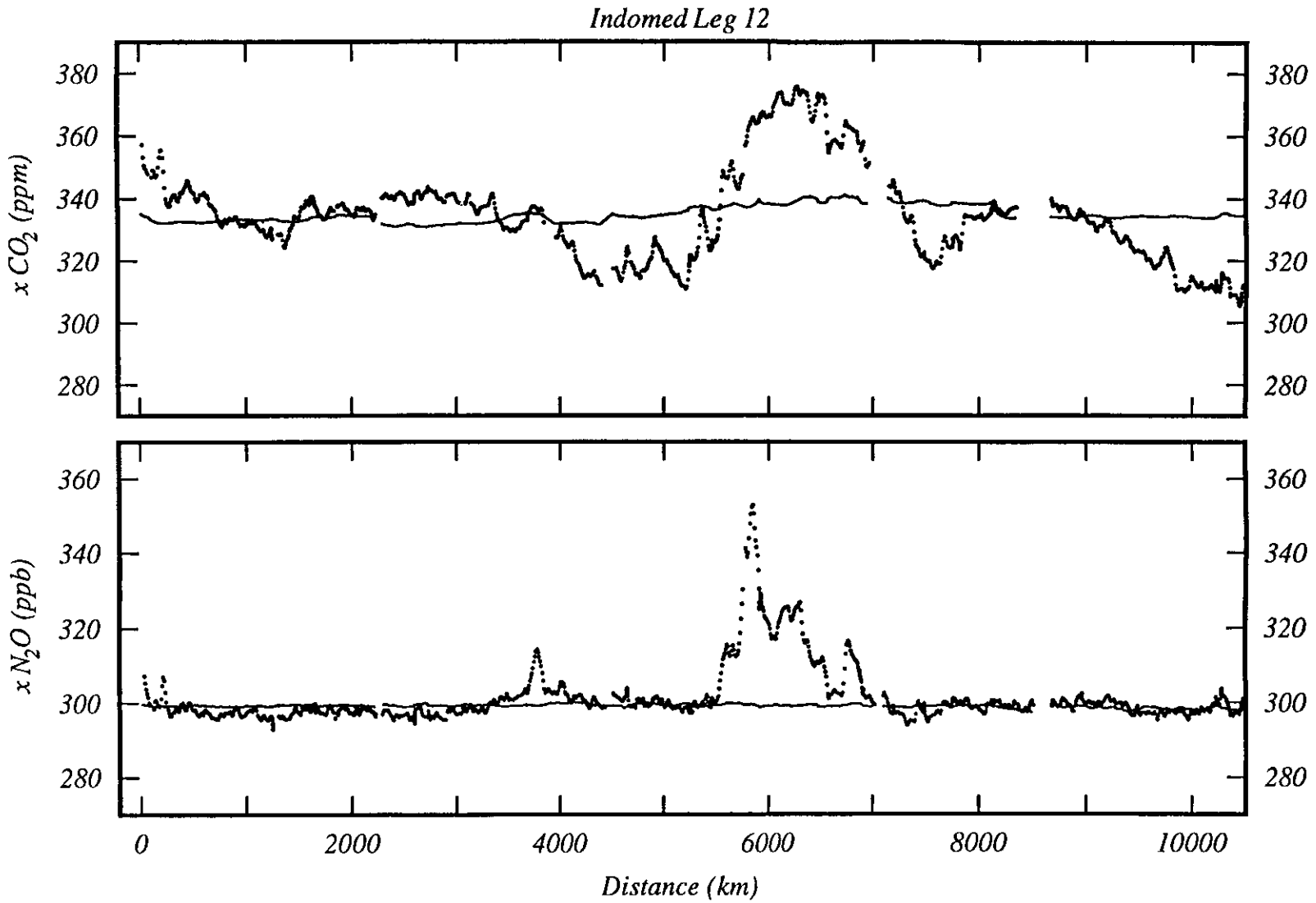

Figure 13. Data plot of xCO_2 and xN_2O (dry gas mole fractions), Indomed Leg 12. Atmospheric measurements are plotted as a line (20 point running mean). Measurements of gas equilibrated with seawater are plotted as individual points after smoothing with a 5-point Gaussian smoother.

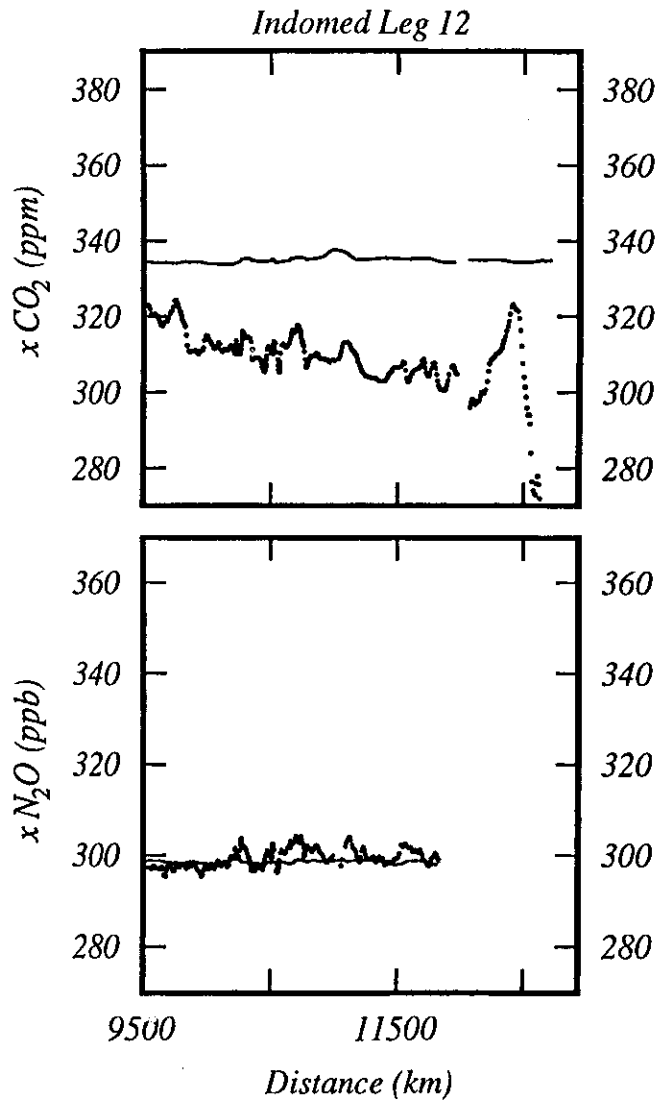

Figure 13. Continued

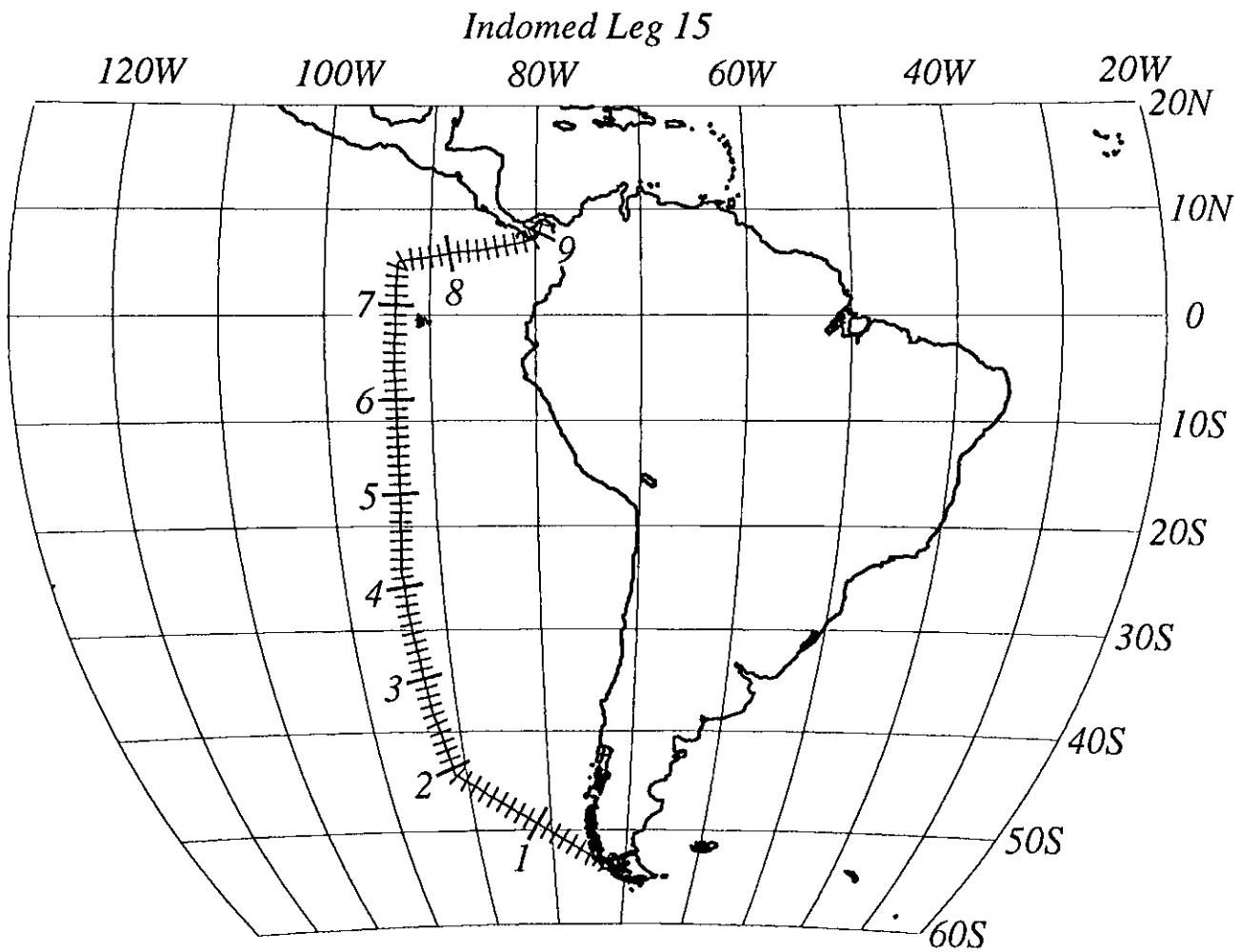

Figure 14. Cruise track plot, Indomed Leg 15. Track indicates cumulative distance in 1000 km intervals, with subdivisions of 100 km.

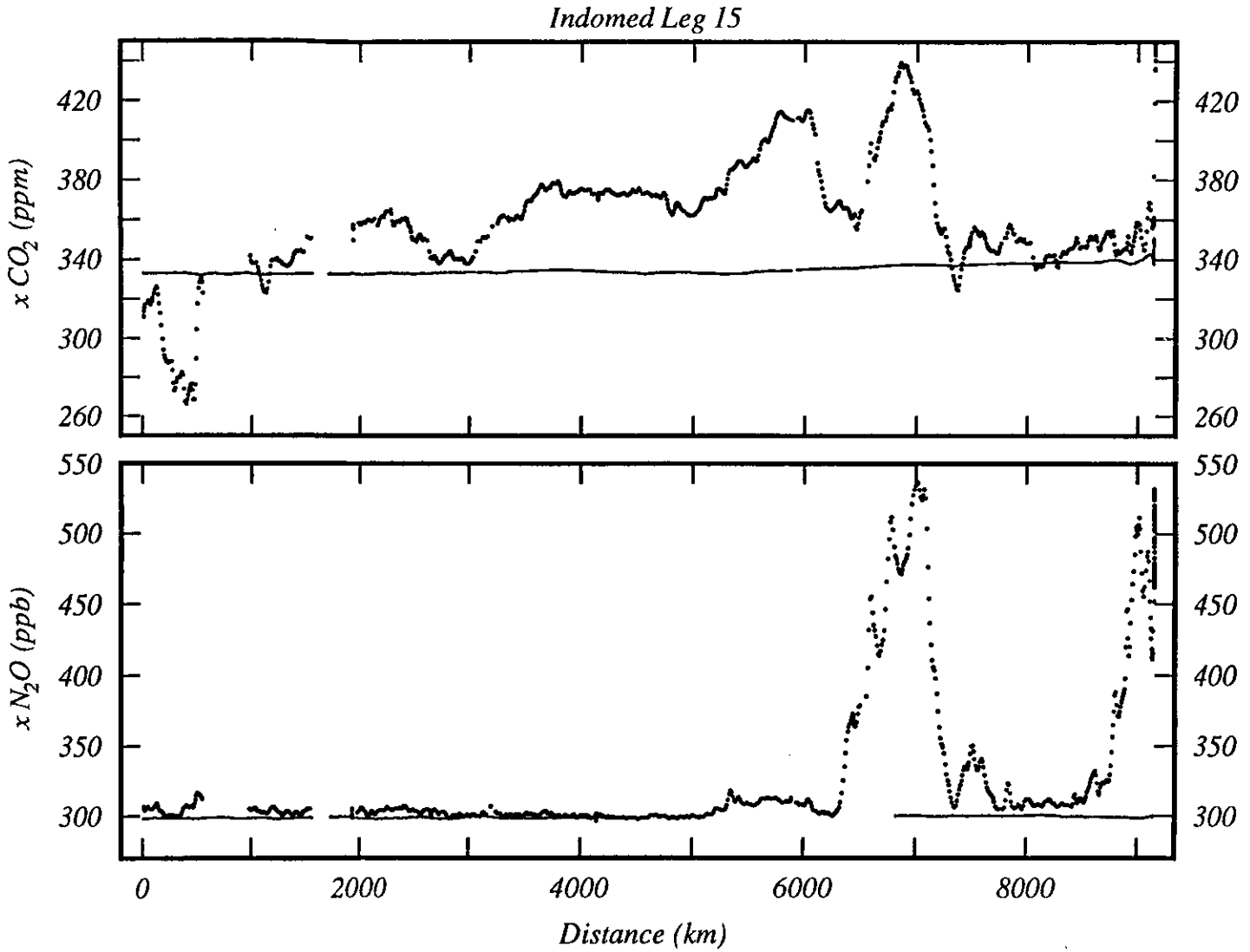

Figure 15. Data plot of xCO_2 and xN_2O (dry gas mole fractions), Indomed Leg 15. Atmospheric measurements are plotted as a line (20 point running mean). Measurements of gas equilibrated with seawater are plotted as individual points after smoothing with a 5-point Gaussian smoother.

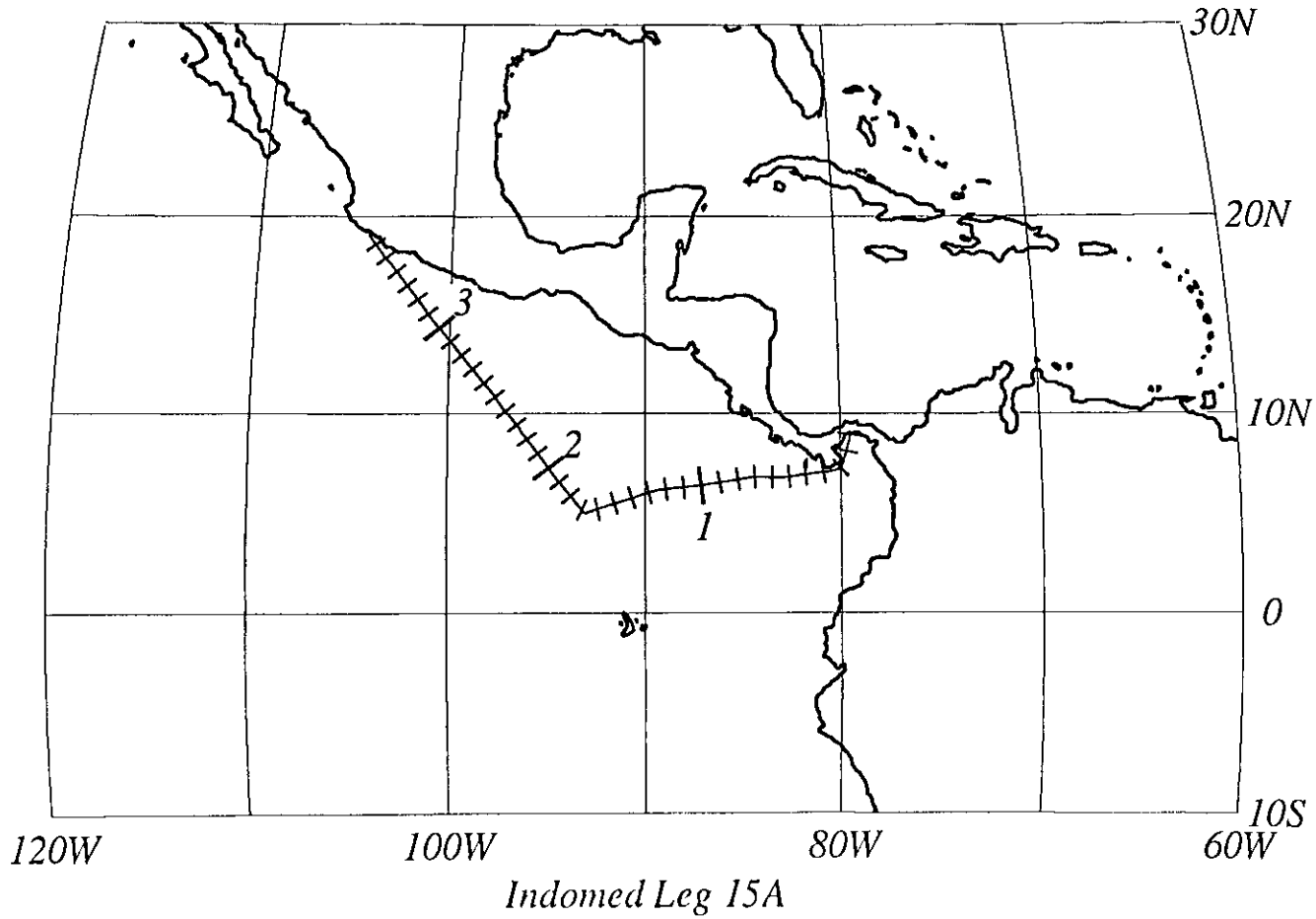

Figure 16. Cruise track plot, Indomed Leg 15A. Track indicates cumulative distance in 1000 km intervals, with subdivisions of 100 km.

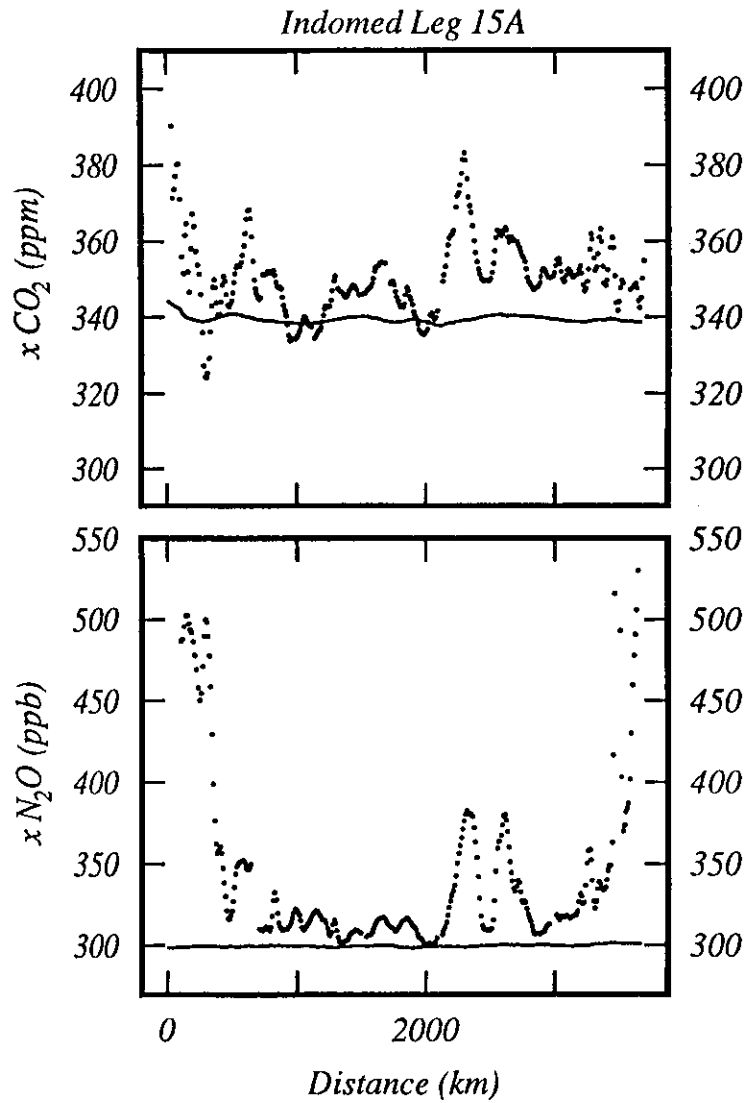

Figure 17. Data plot of xCO_2 and xN_2O (dry gas mole fractions), Indomed Leg 15A. Atmospheric measurements are plotted as a line (20 point running mean). Measurements of gas equilibrated with seawater are plotted as individual points after smoothing with a 5-point Gaussian smoother.

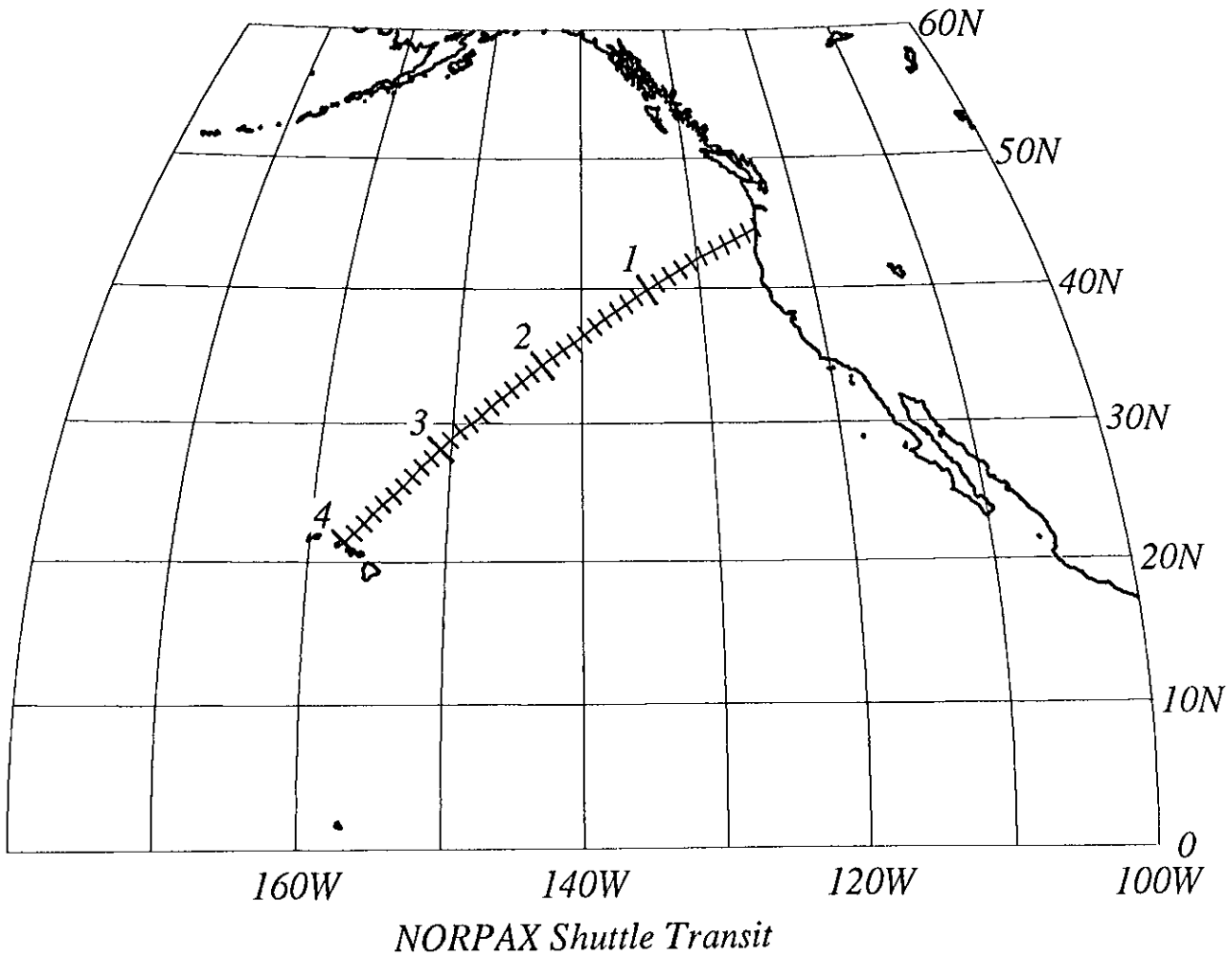

Figure 18. Cruise track plot, NORPAX Shuttle Transit. Track indicates cumulative distance in 1000 km intervals, with subdivisions of 100 km.

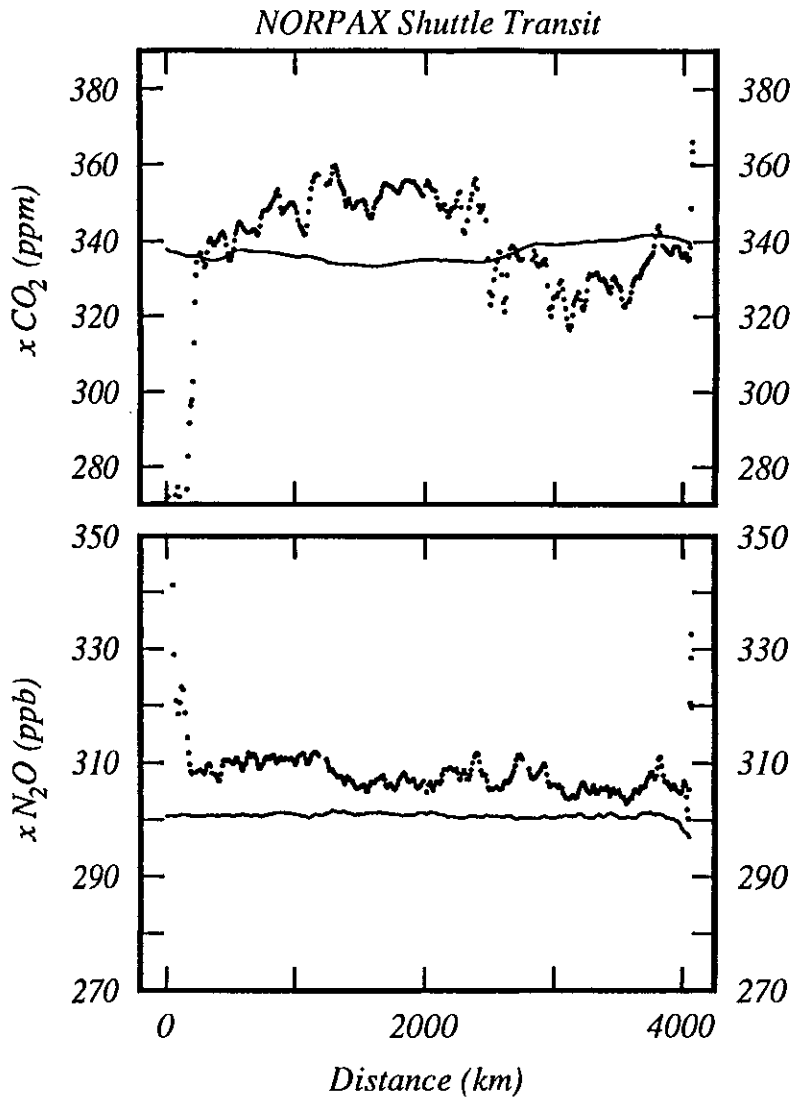

Figure 19. Data plot of xCO_2 and xN_2O (dry gas mole fractions), NORPAX Shuttle Transit. Atmospheric measurements are plotted as a line (20 point running mean). Measurements of gas equilibrated with seawater are plotted as individual points after smoothing with a 5-point Gaussian smoother.

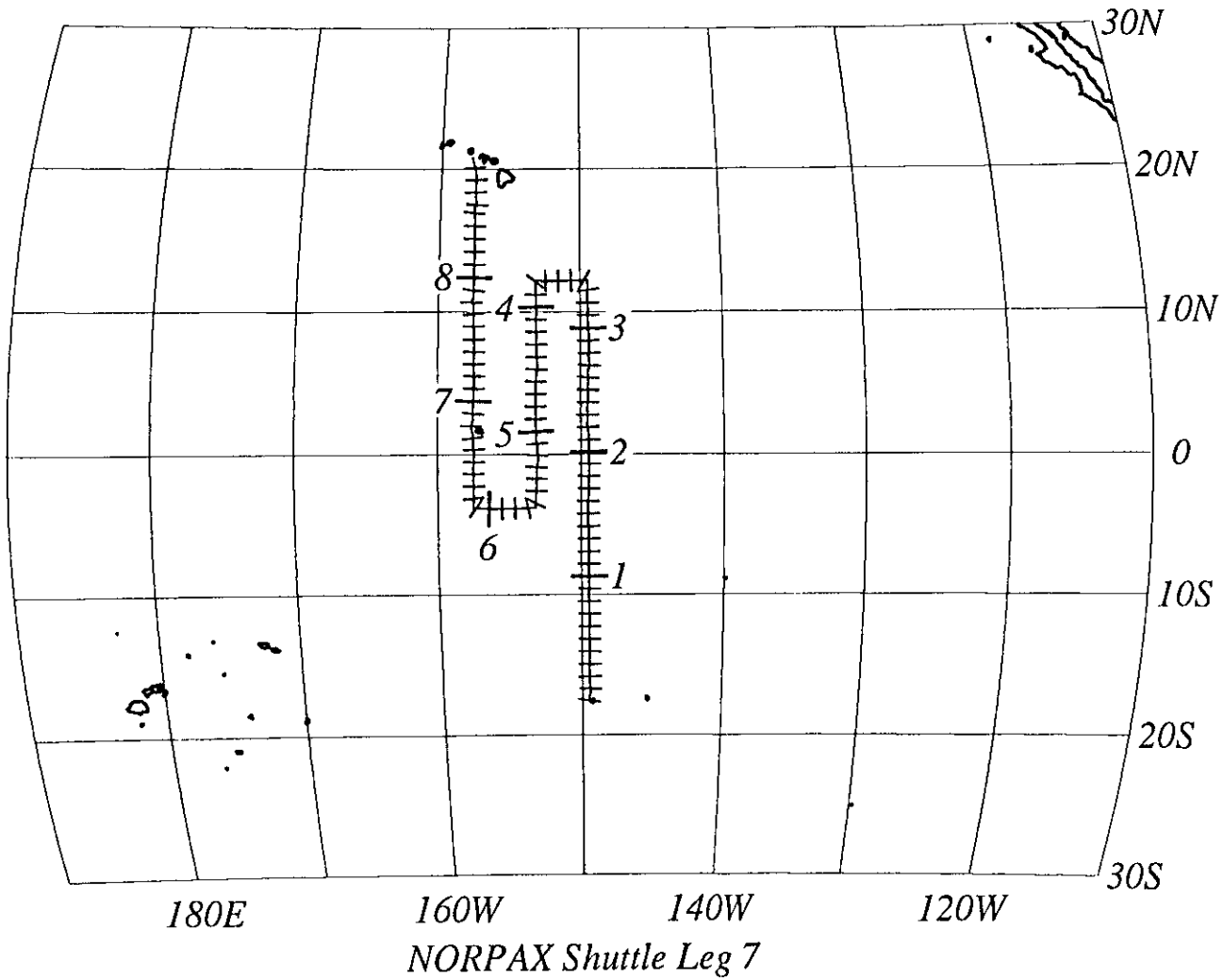

Figure 20. Cruise track plot, NORPAX Shuttle Leg 7. Track indicates cumulative distance in 1000 km intervals, with subdivisions of 100 km.

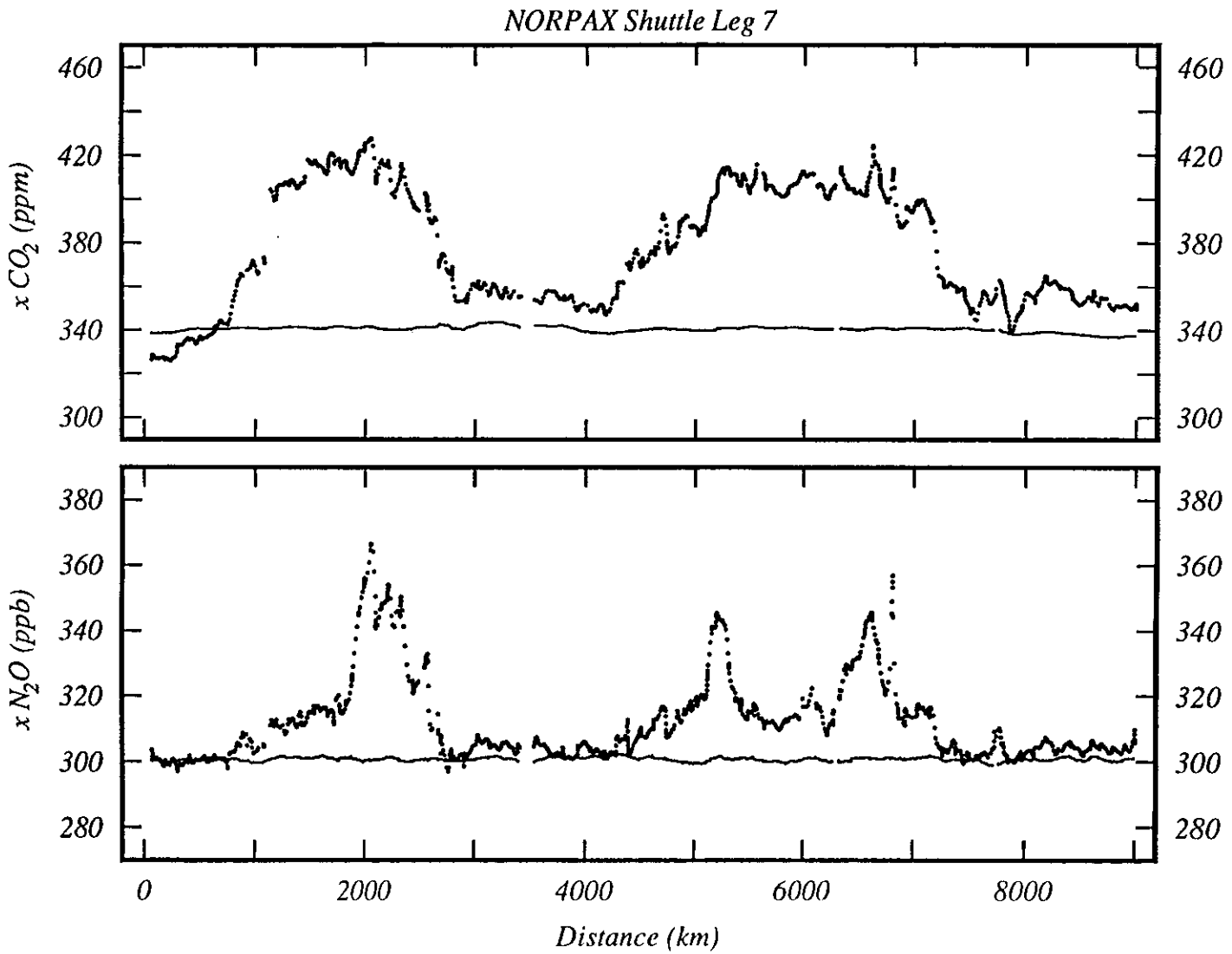

Figure 21. Data plot of xCO_2 and xN_2O (dry gas mole fractions), NORPAX Shuttle Leg 7. Atmospheric measurements are plotted as a line (20 point running mean). Measurements of gas equilibrated with seawater are plotted as individual points after smoothing with a 5-point Gaussian smoother.

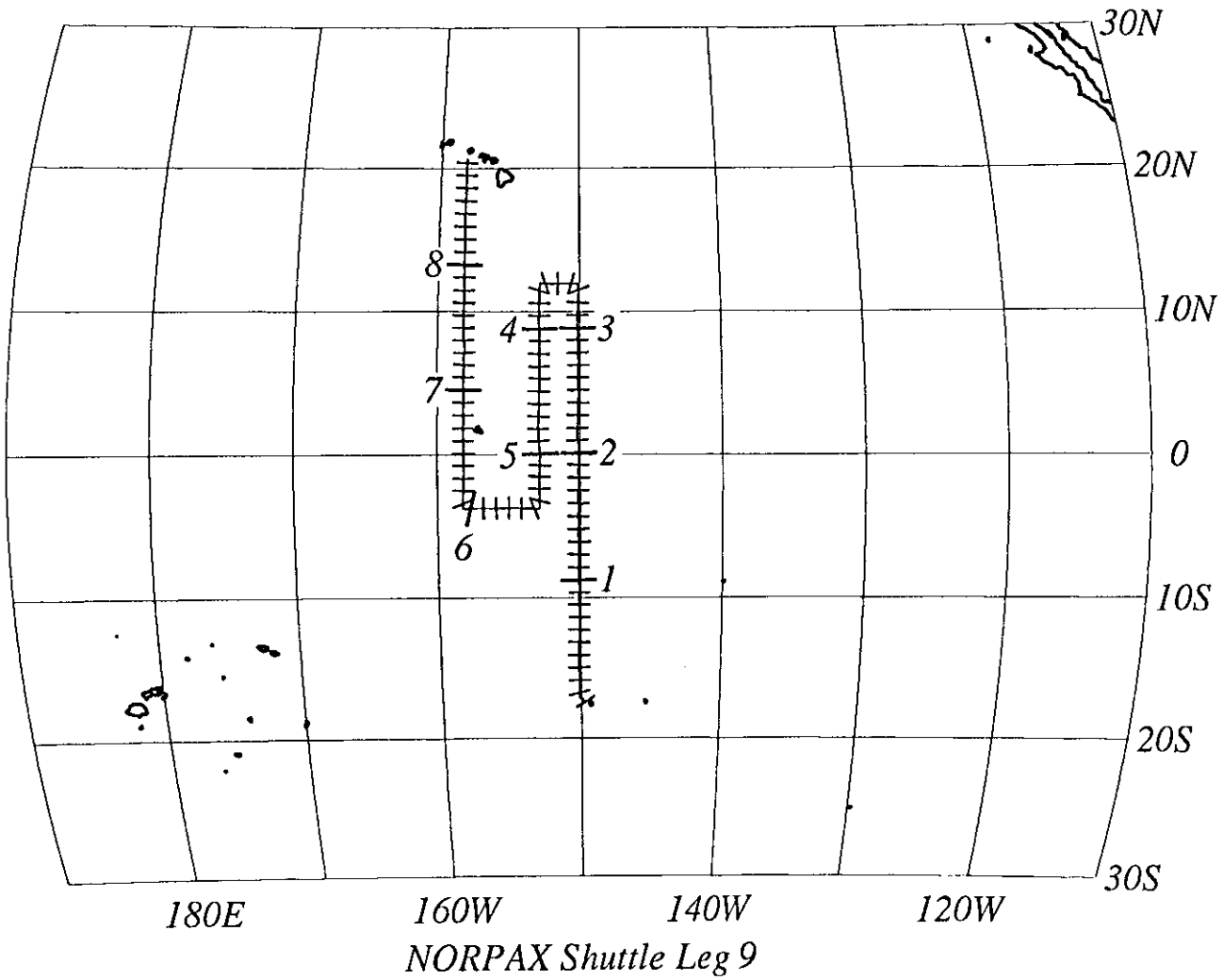

Figure 22. Cruise track plot, NORPAX Shuttle Leg 9. Track indicates cumulative distance in 1000 km intervals, with subdivisions of 100 km.

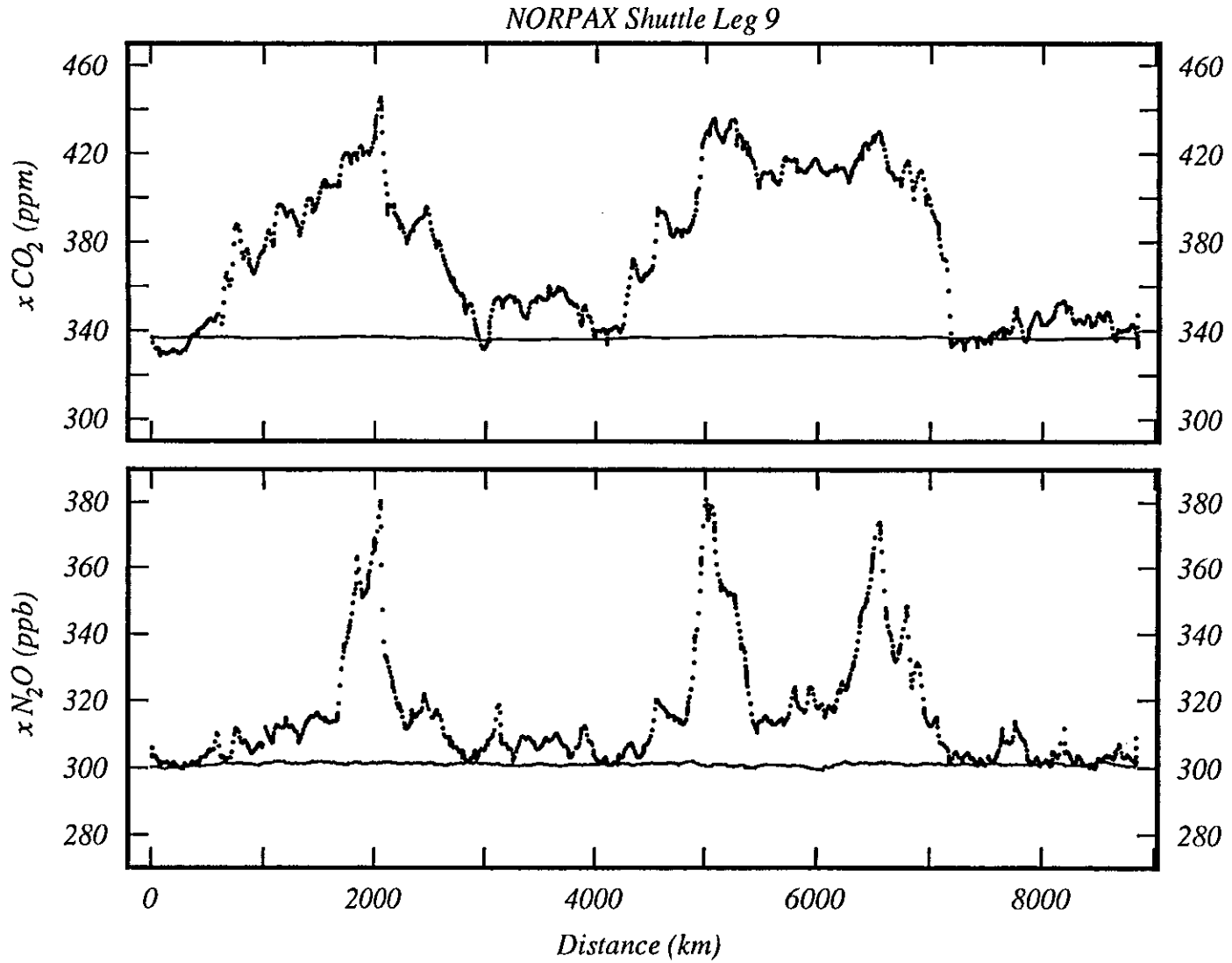

Figure 23. Data plot of xCO_2 and xN_2O (dry gas mole fractions), NORPAX Shuttle Leg 9. Atmospheric measurements are plotted as a line (20 point running mean). Measurements of gas equilibrated with seawater are plotted as individual points after smoothing with a 5-point Gaussian smoother.

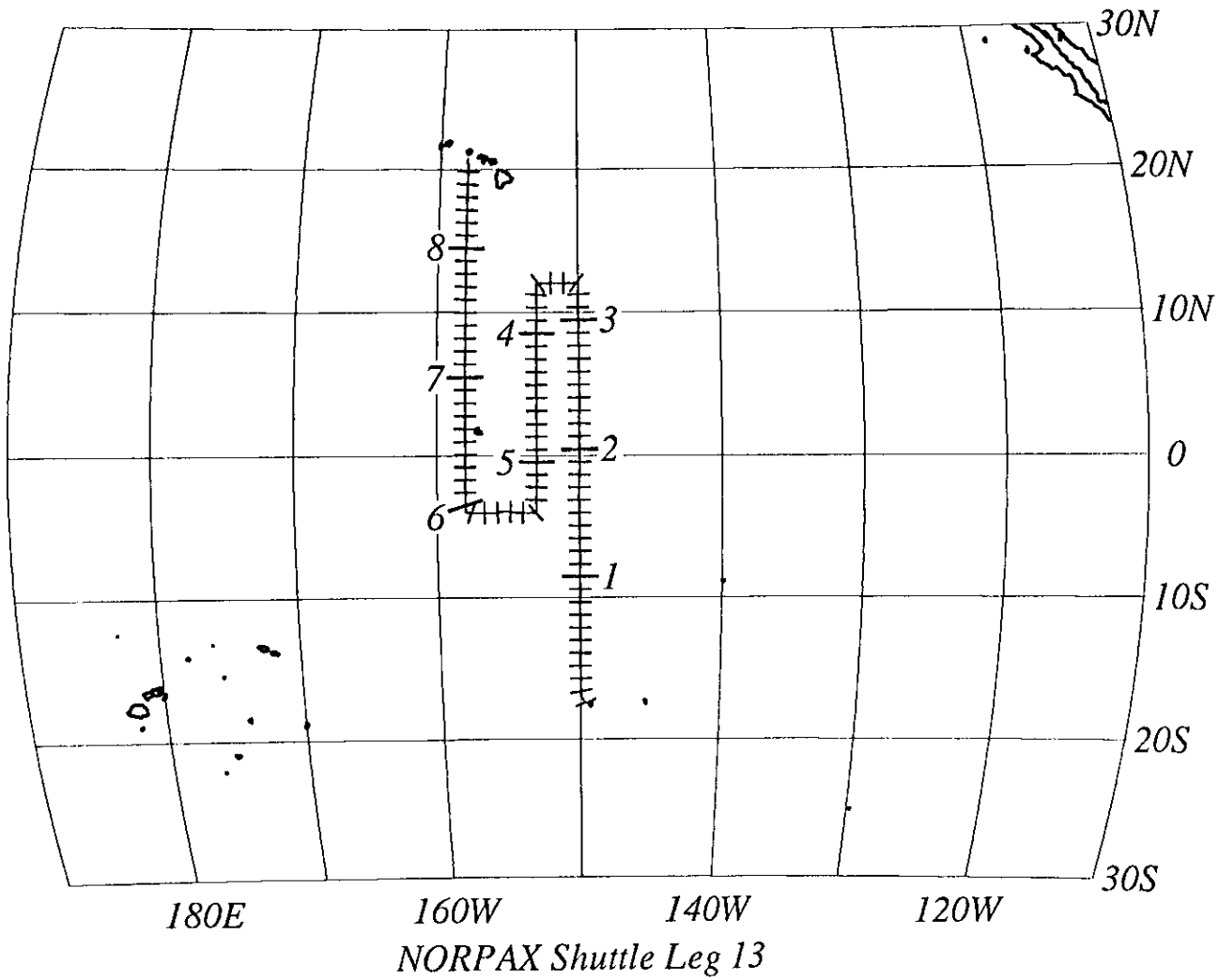

Figure 24. Cruise track plot, NORPAX Shuttle Leg 13. Track indicates cumulative distance in 1000 km intervals, with subdivisions of 100 km.

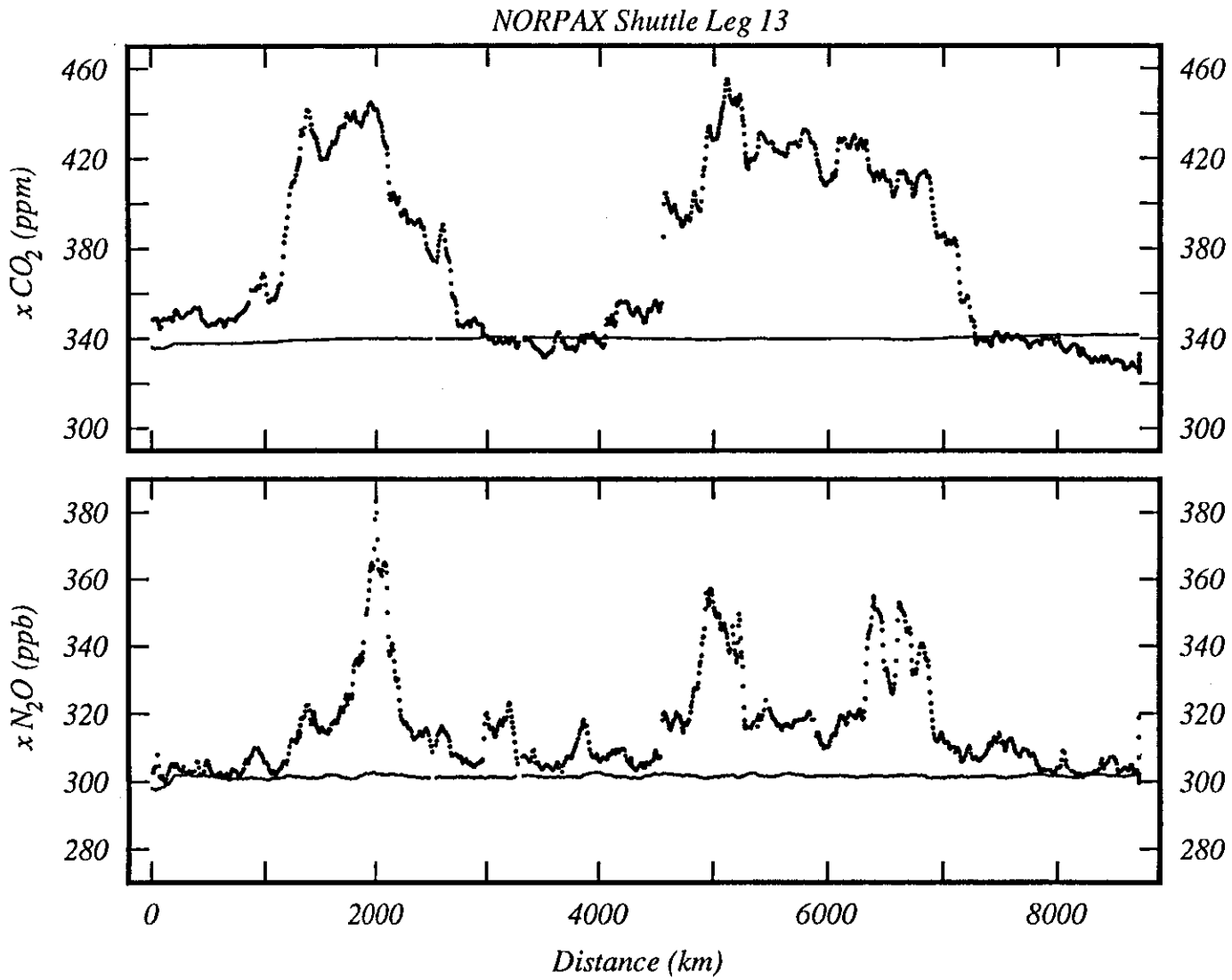

Figure 25. Data plot of xCO_2 and xN_2O (dry gas mole fractions), NORPAX Shuttle Leg 13. Atmospheric measurements are plotted as a line (20 point running mean). Measurements of gas equilibrated with seawater are plotted as individual points after smoothing with a 5-point Gaussian smoother.

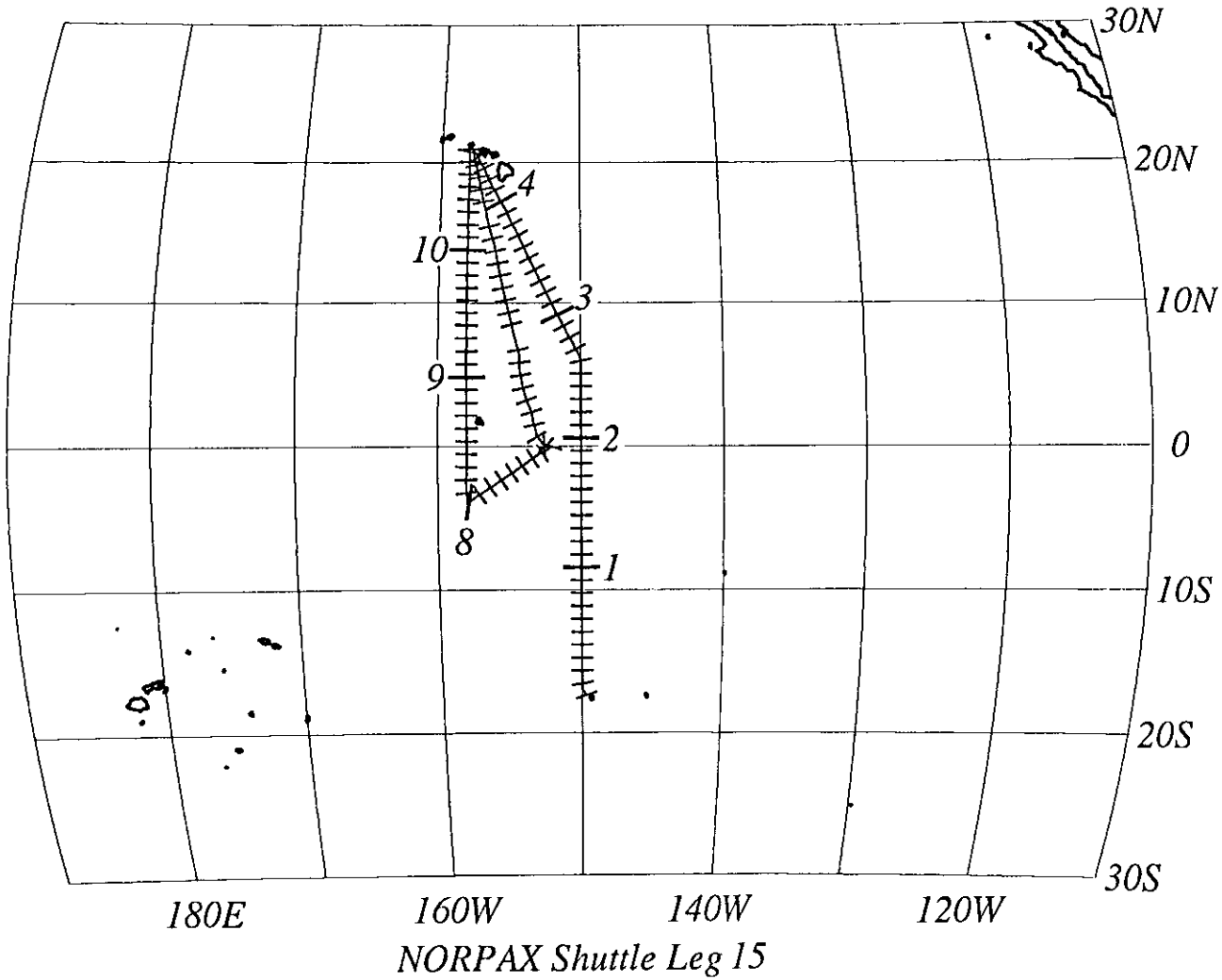

Figure 26. Cruise track plot, NORPAX Shuttle Leg 15. Track indicates cumulative distance in 1000 km intervals, with subdivisions of 100 km.

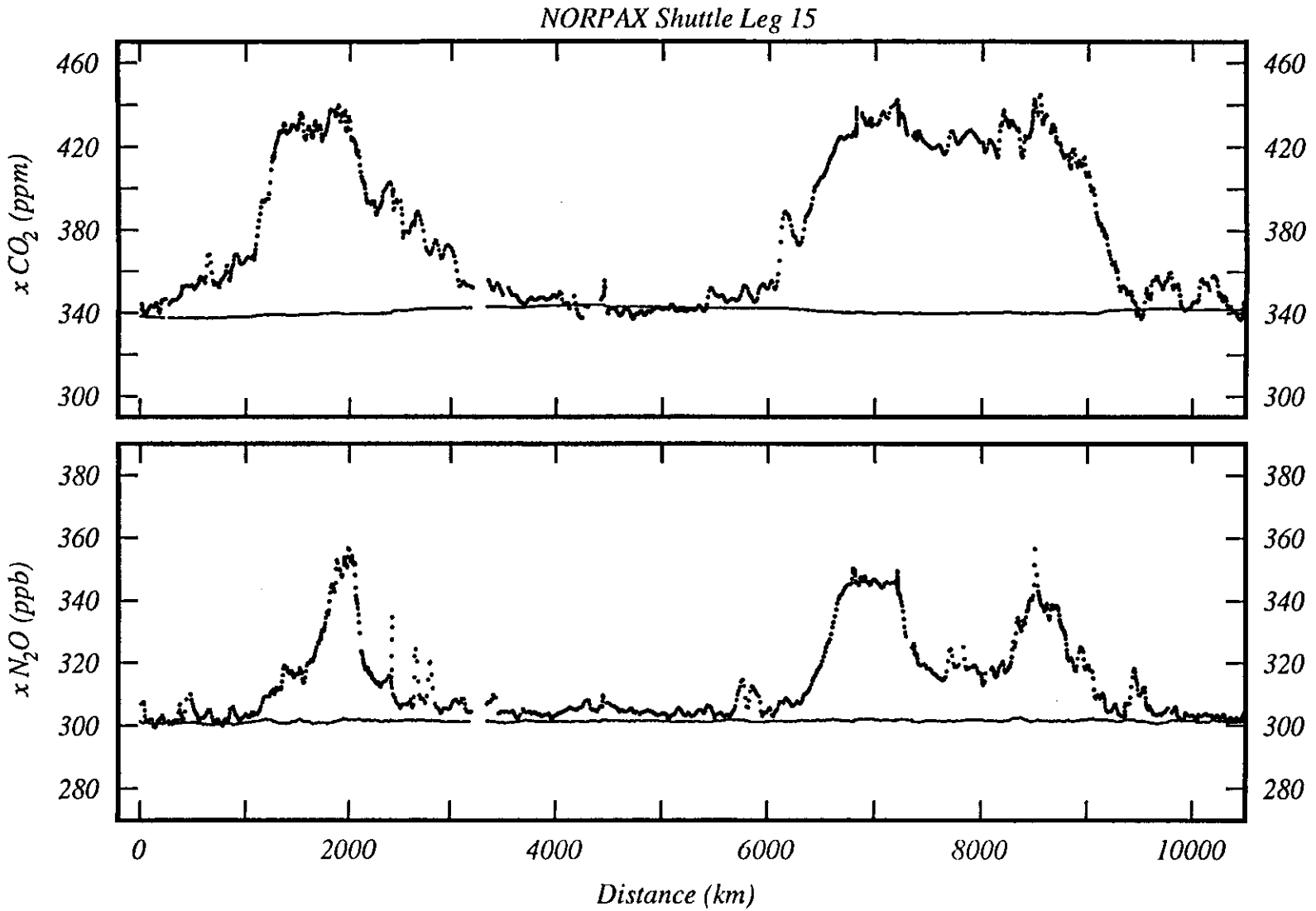

Figure 27. Data plot of xCO_2 and xN_2O (dry gas mole fractions), NORPAX Shuttle Leg 15. Atmospheric measurements are plotted as a line (20 point running mean). Measurements of gas equilibrated with seawater are plotted as individual points after smoothing with a 5-point Gaussian smoother.

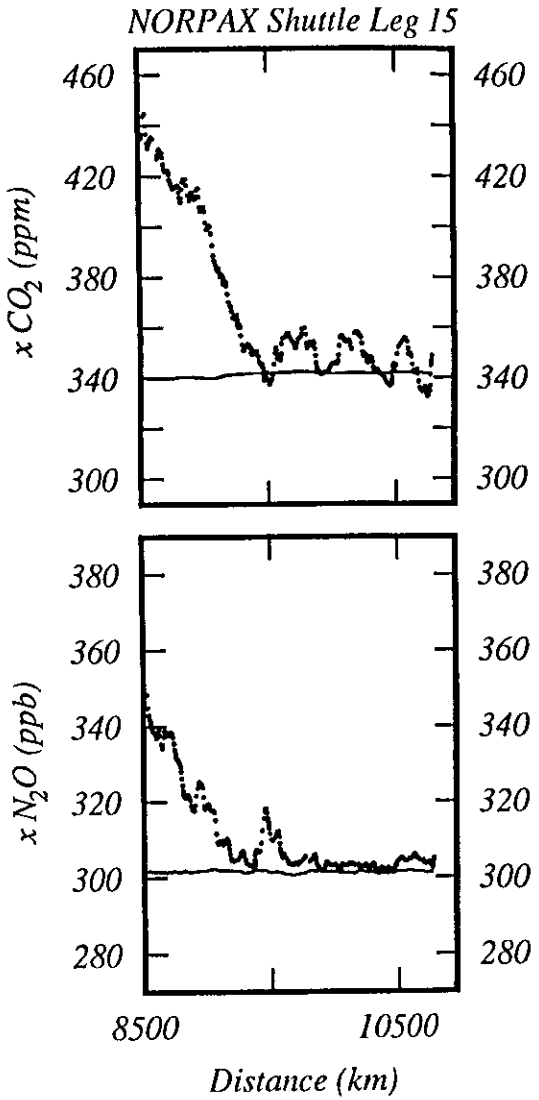

Figure 27. Continued

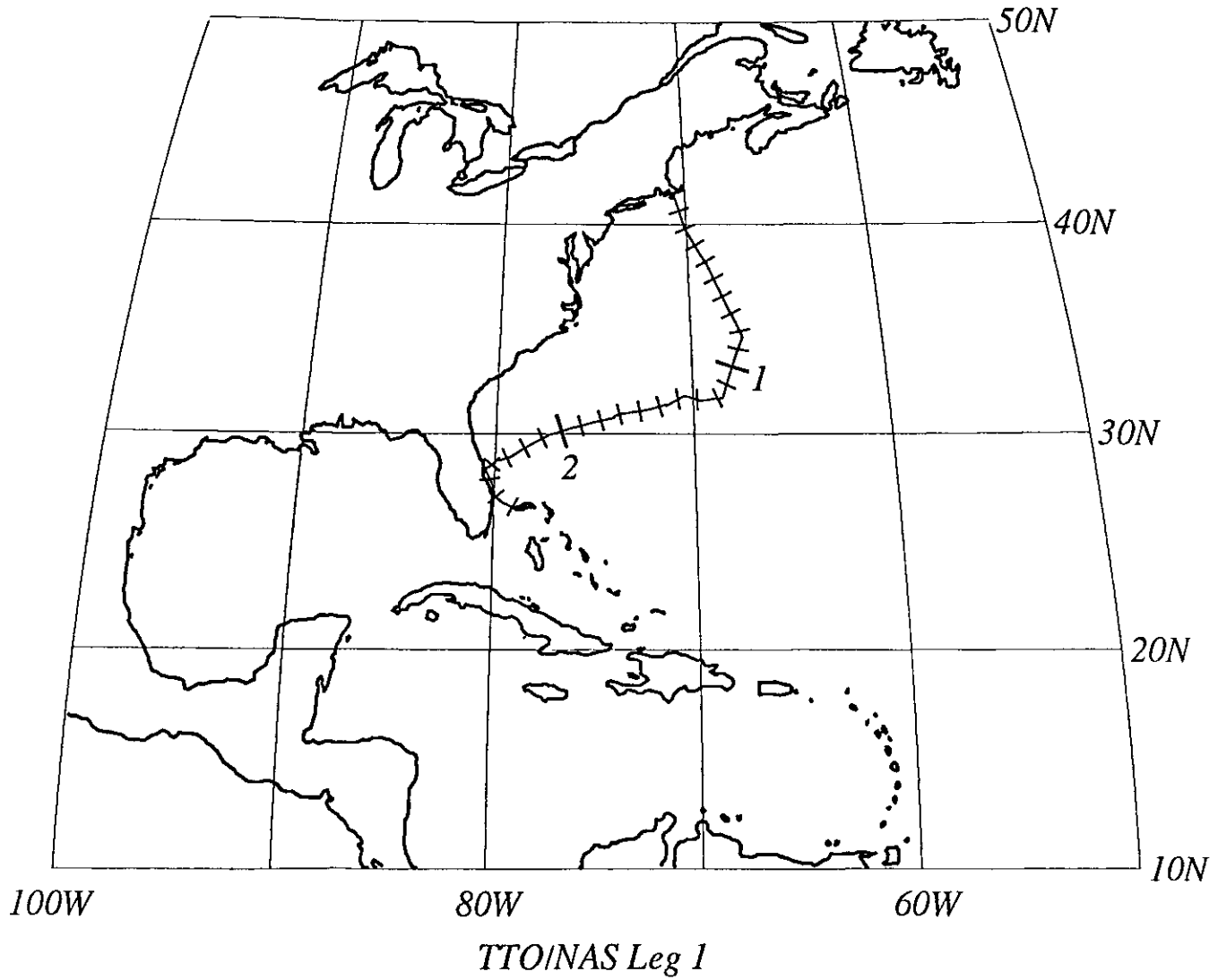

Figure 28. Cruise track plot, TTO/NAS Leg 1. Track indicates cumulative distance in 1000 km intervals, with subdivisions of 100 km.

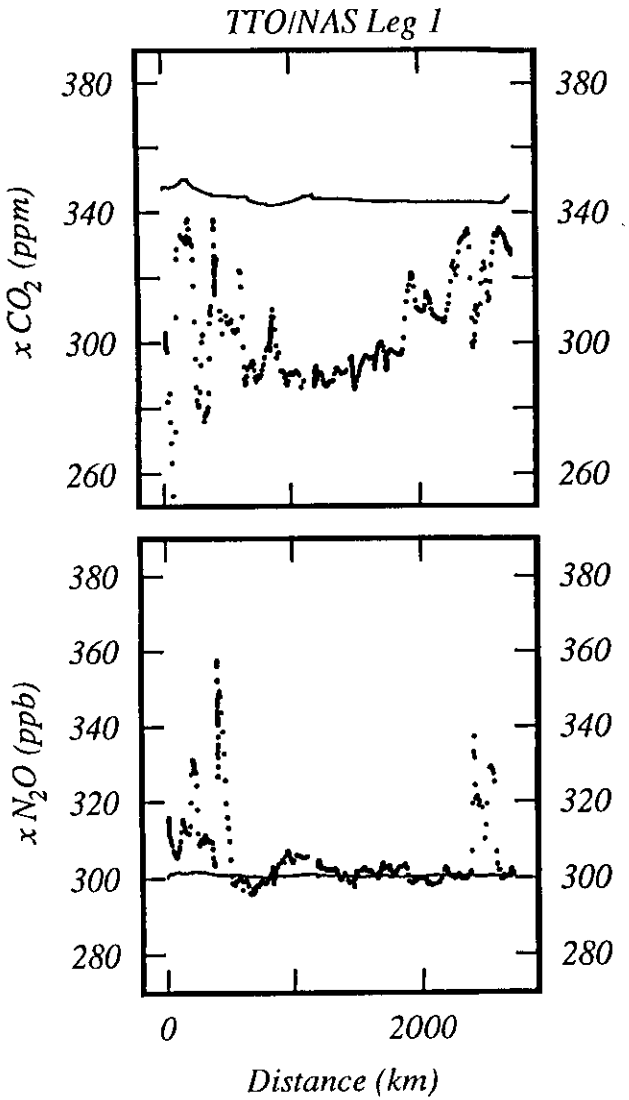

Figure 29. Data plot of xCO_2 and xN_2O (dry gas mole fractions), TTO/NAS Leg 1. Atmospheric measurements are plotted as a line (20 point running mean). Measurements of gas equilibrated with seawater are plotted as individual points after smoothing with a 5-point Gaussian smoother.

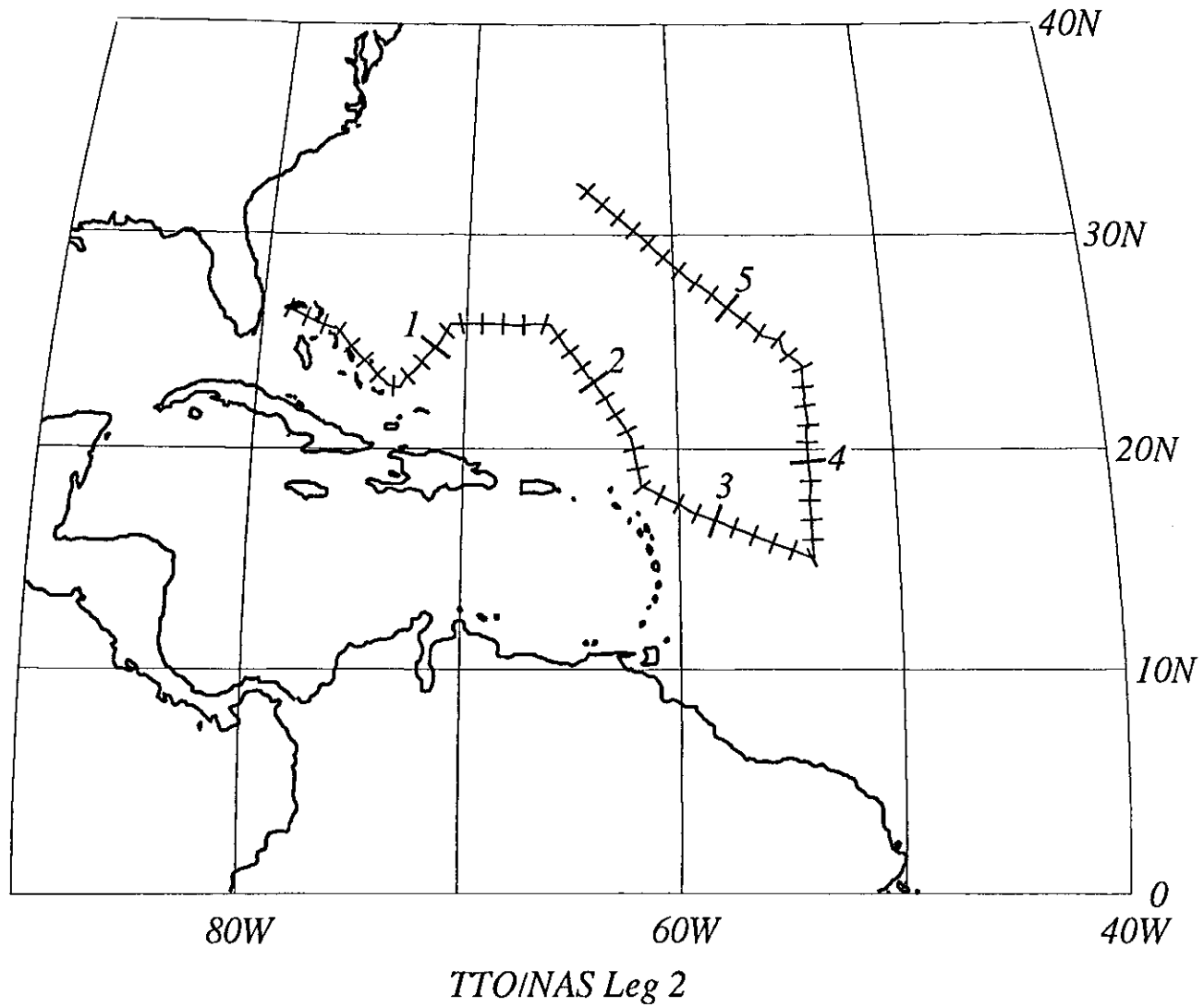

Figure 30. Cruise track plot, TTO/NAS Leg 2. Track indicates cumulative distance in 1000 km intervals, with subdivisions of 100 km.

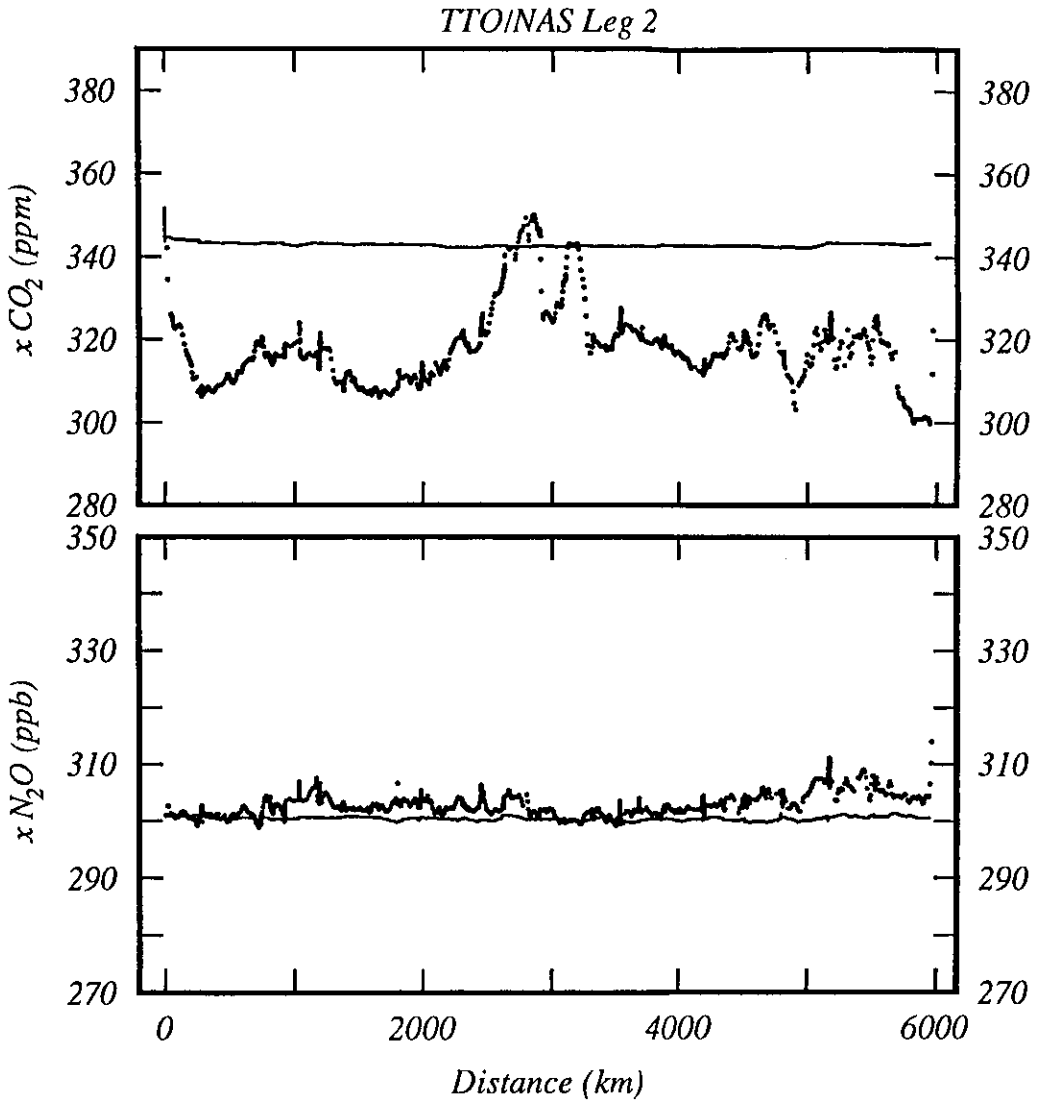

Figure 31. Data plot of xCO_2 and xN_2O (dry gas mole fractions), TTO/NAS Leg 2. Atmospheric measurements are plotted as a line (20 point running mean). Measurements of gas equilibrated with seawater are plotted as individual points after smoothing with a 5-point Gaussian smoother.

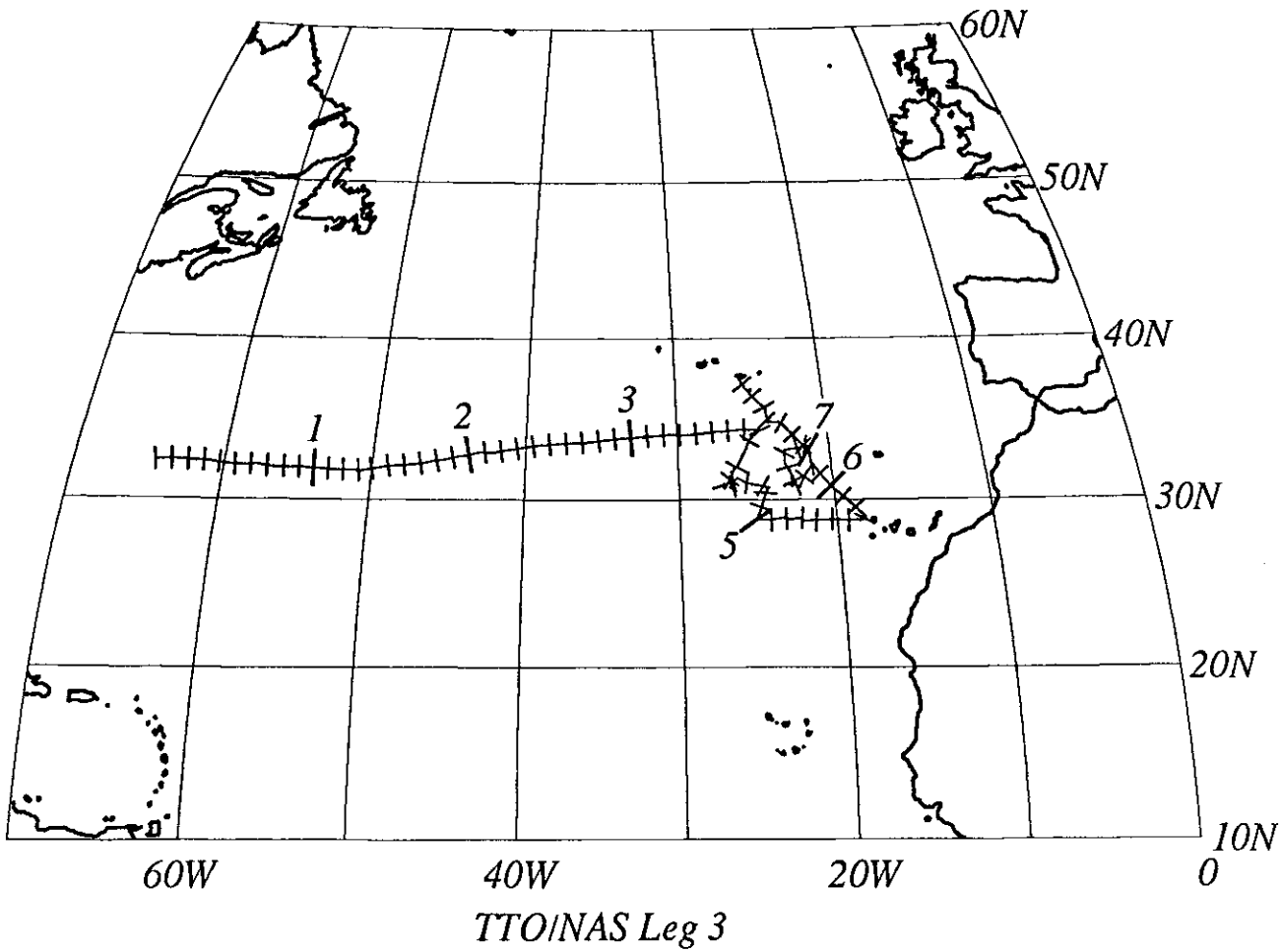

Figure 32. Cruise track plot, TTO/NAS Leg 3. Track indicates cumulative distance in 1000 km intervals, with subdivisions of 100 km.

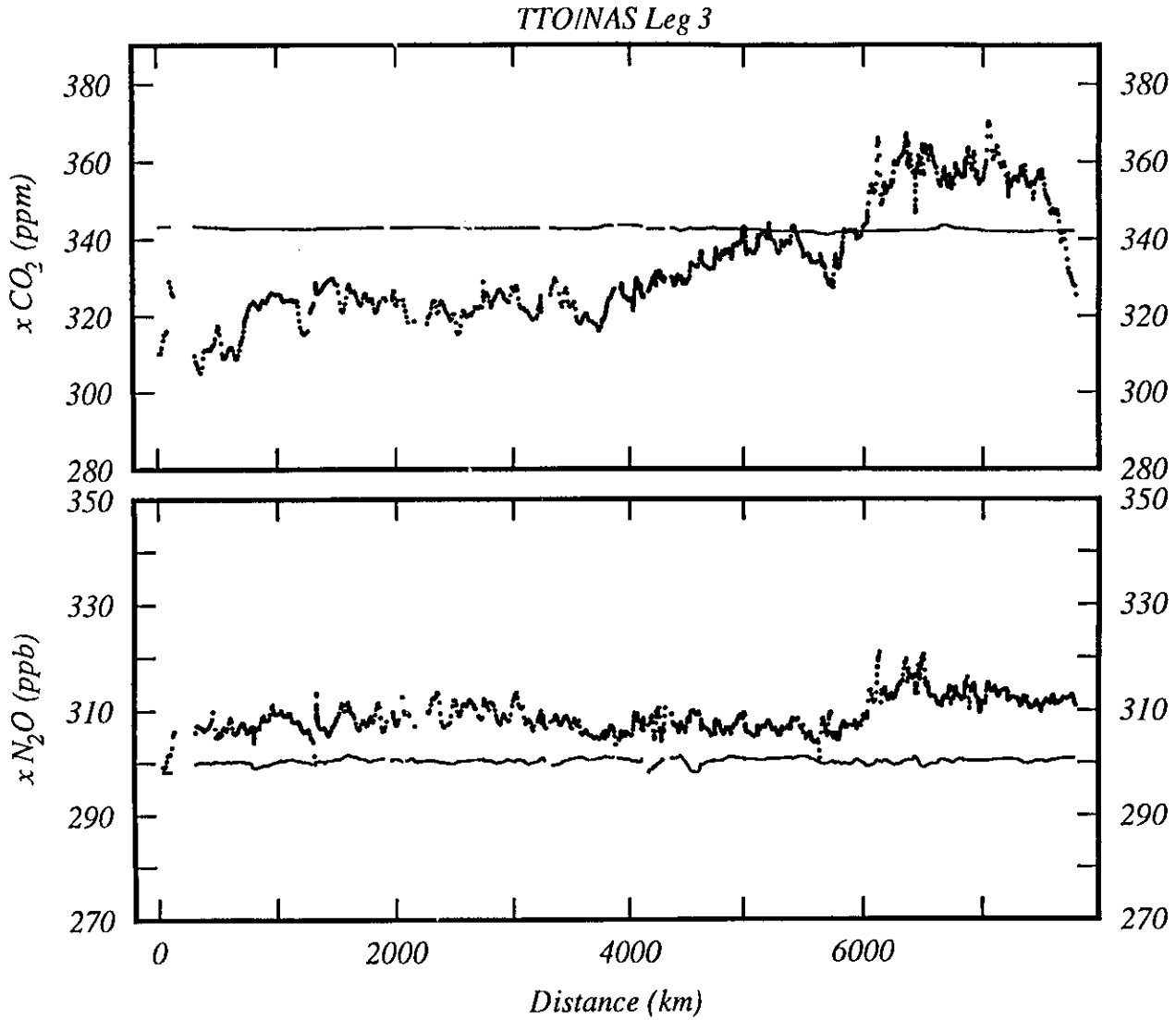

Figure 33. Data plot of xCO_2 and xN_2O (dry gas mole fractions), TTO/NAS Leg 3. Atmospheric measurements are plotted as a line (20 point running mean). Measurements of gas equilibrated with seawater are plotted as individual points after smoothing with a 5-point Gaussian smoother.

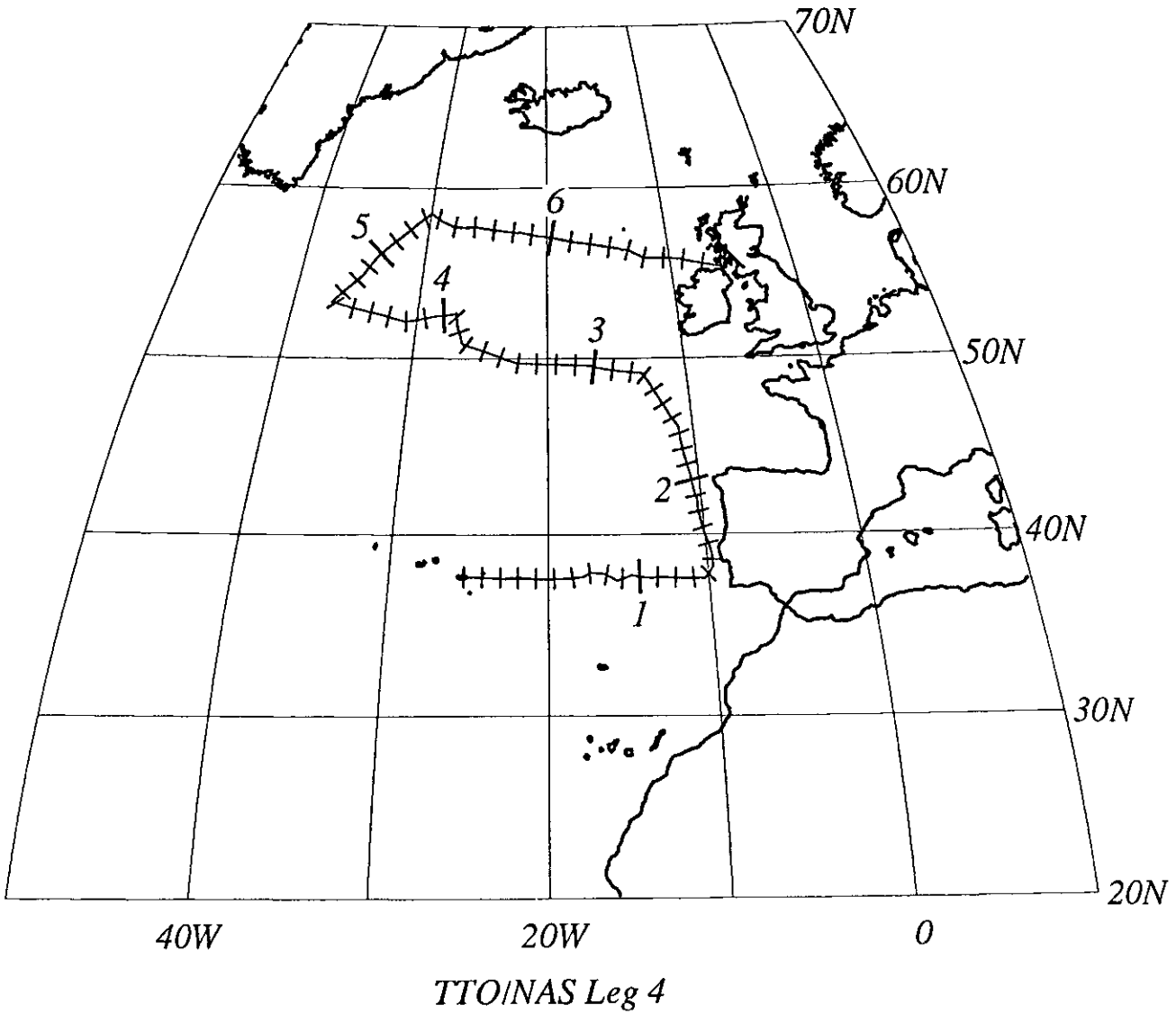

Figure 34. Cruise track plot, TTO/NAS Leg 4. Track indicates cumulative distance in 1000 km intervals, with subdivisions of 100 km.

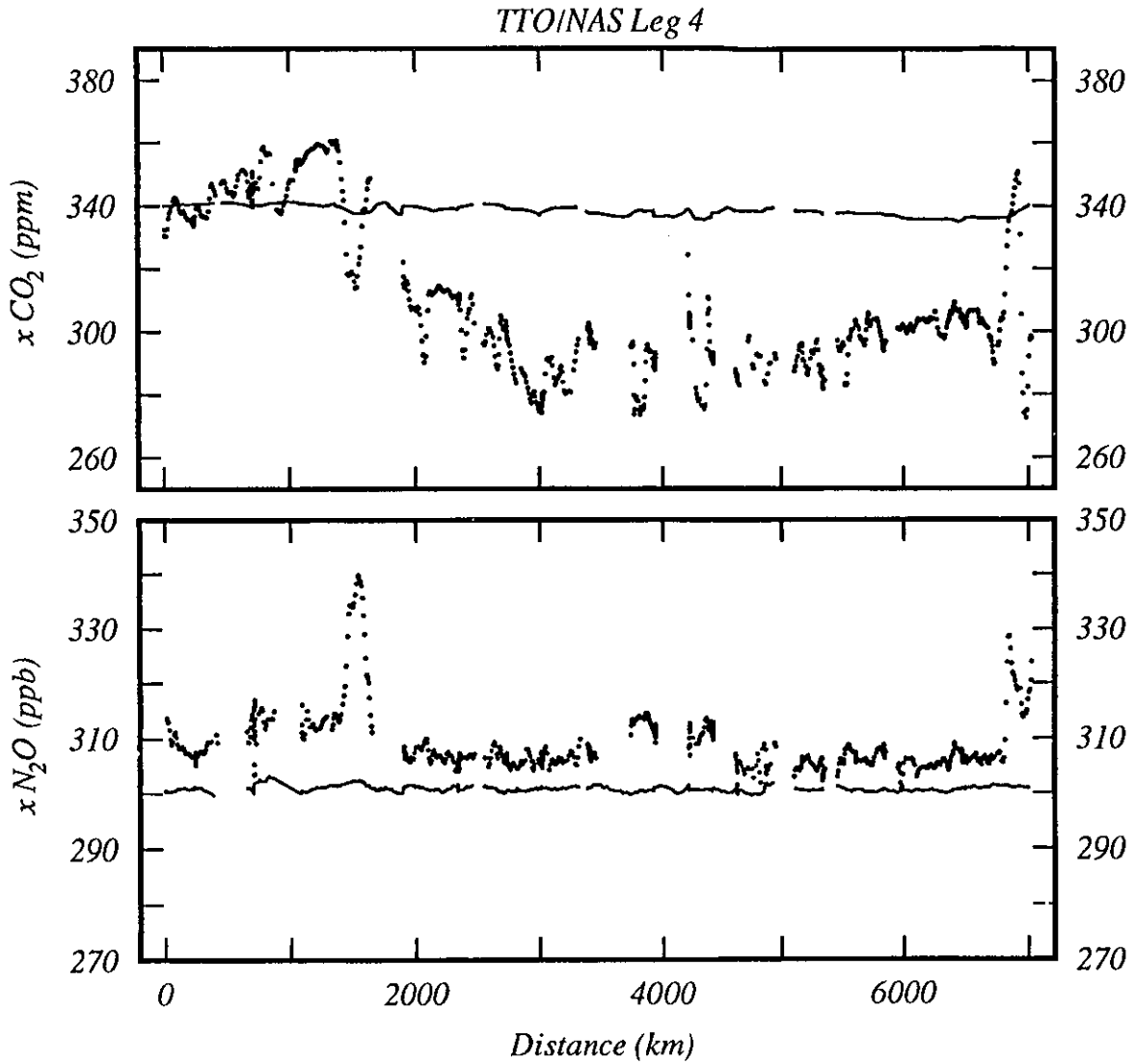

Figure 35. Data plot of xCO_2 and xN_2O (dry gas mole fractions), TTO/NAS Leg 4. Atmospheric measurements are plotted as a line (20 point running mean). Measurements of gas equilibrated with seawater are plotted as individual points after smoothing with a 5-point Gaussian smoother.

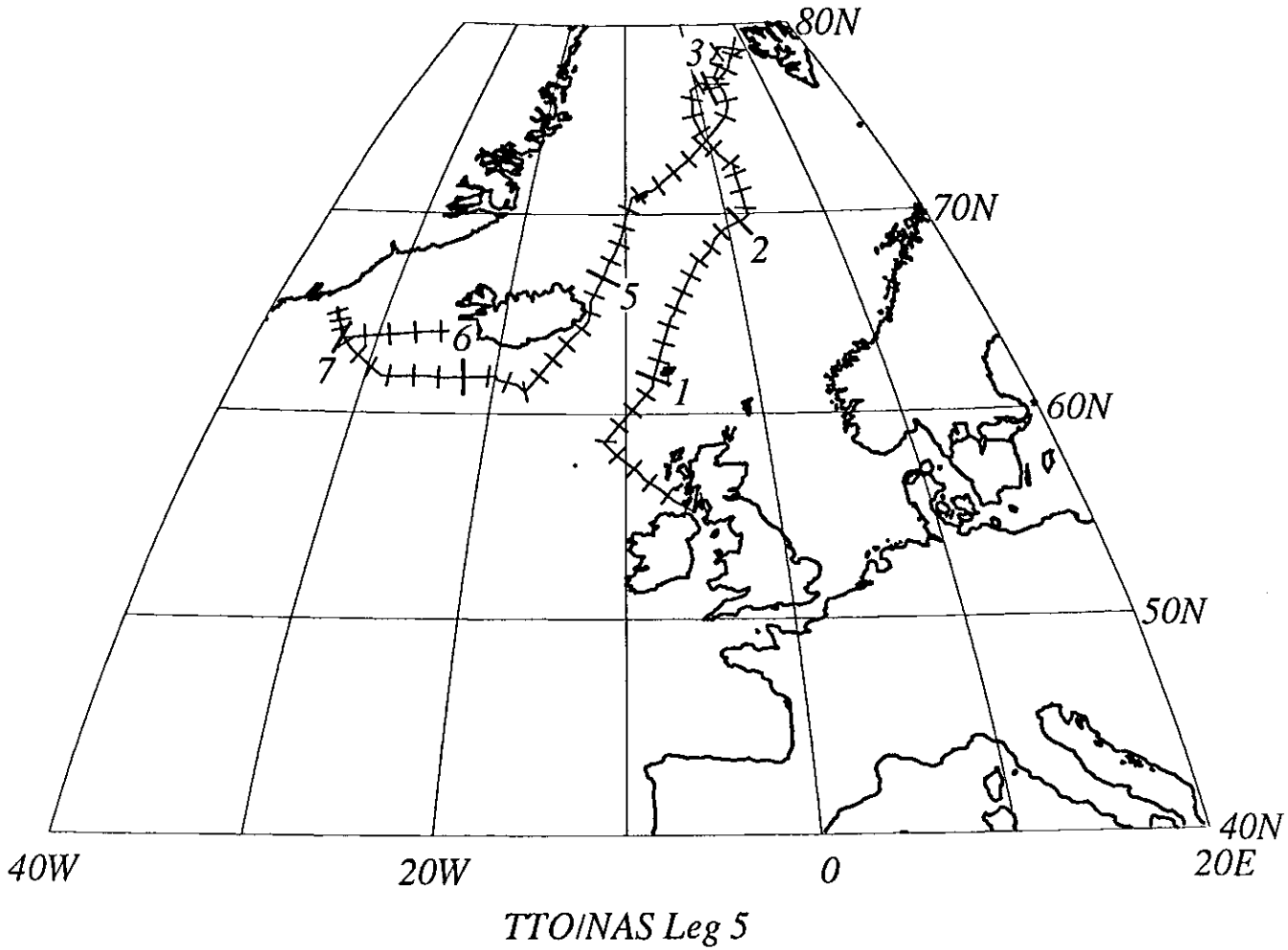

Figure 36. Cruise track plot, TTO/NAS Leg 5. Track indicates cumulative distance in 1000 km intervals, with subdivisions of 100 km.

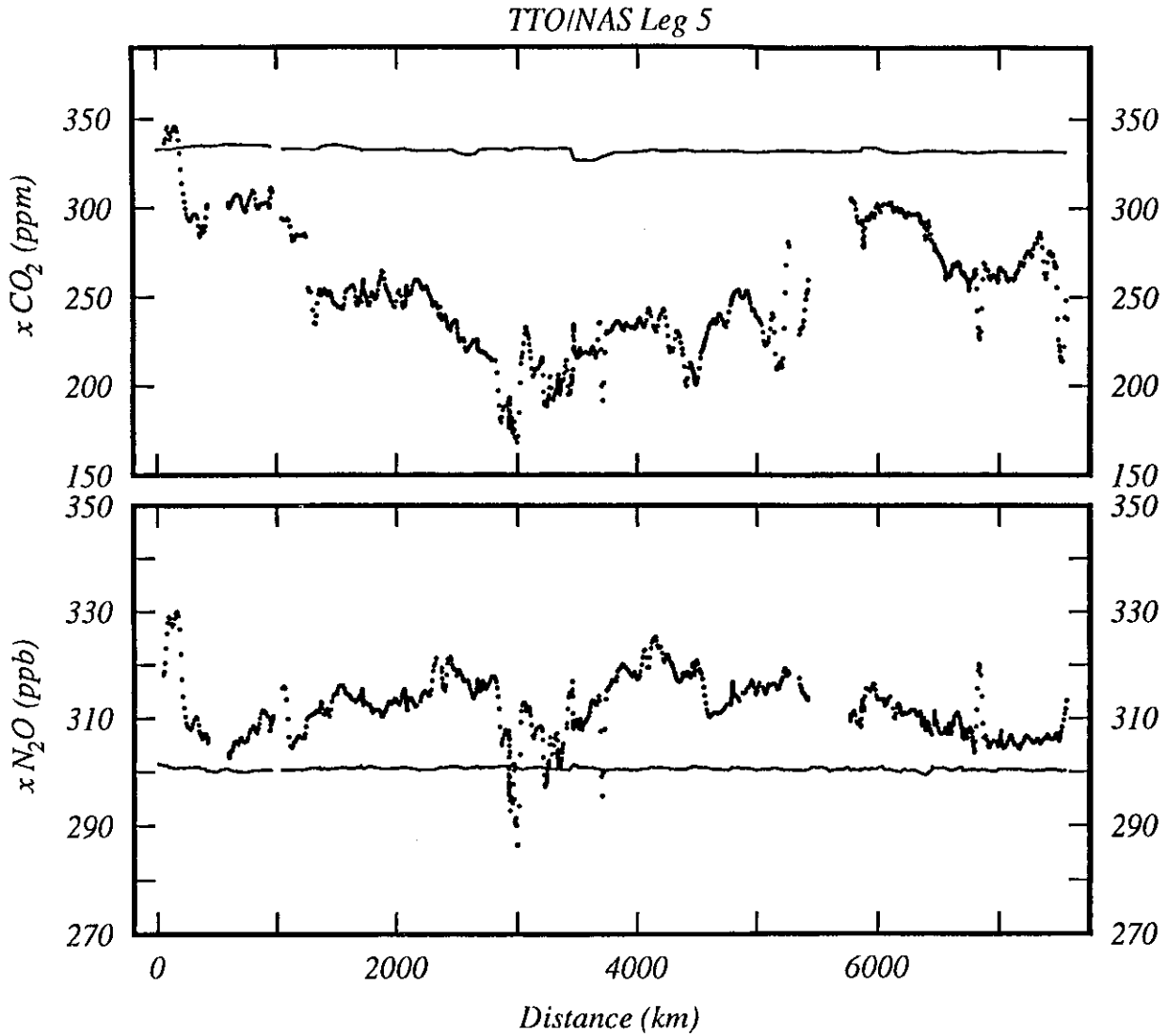

Figure 37. Data plot of xCO_2 and xN_2O (dry gas mole fractions), TTO/NAS Leg 5. Atmospheric measurements are plotted as a line (20 point running mean). Measurements of gas equilibrated with seawater are plotted as individual points after smoothing with a 5-point Gaussian smoother.

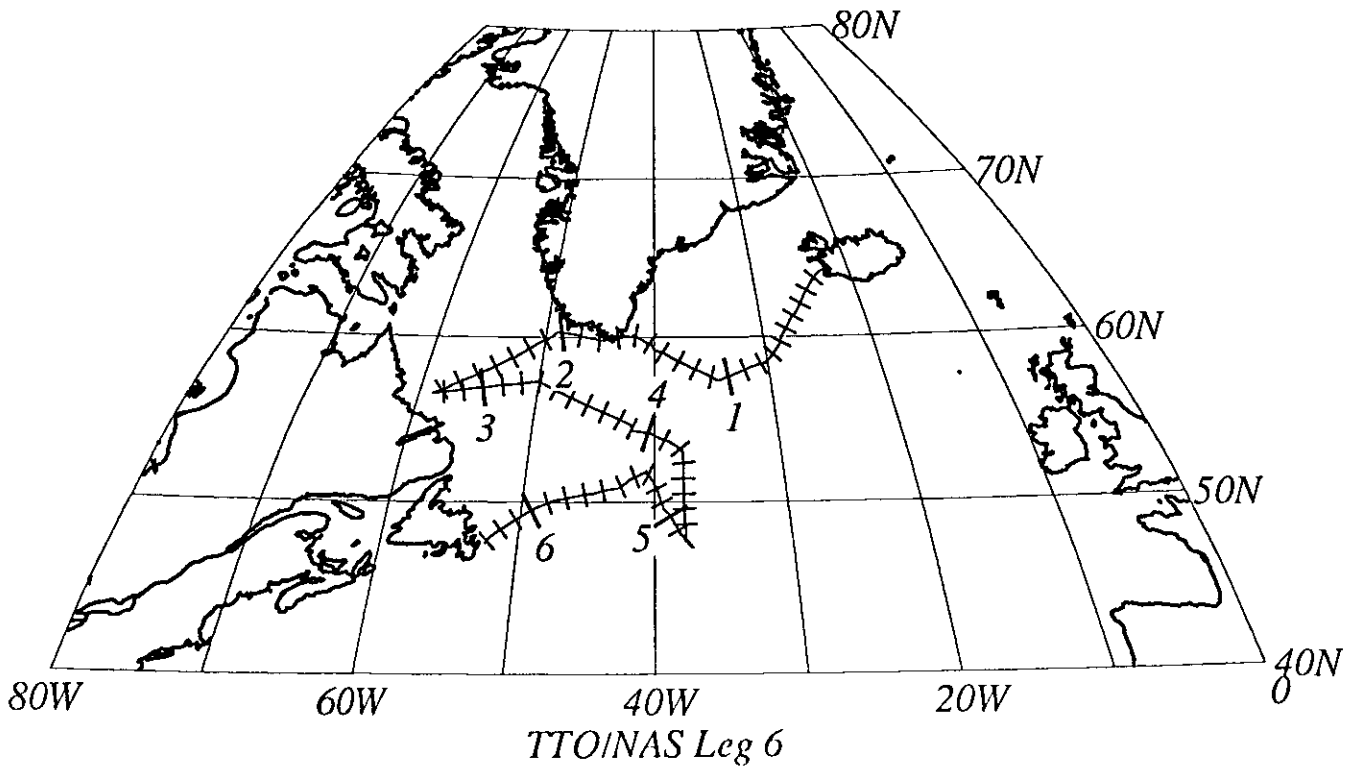

Figure 38. Cruise track plot, TTO/NAS Leg 6. Track indicates cumulative distance in 1000 km intervals, with subdivisions of 100 km.

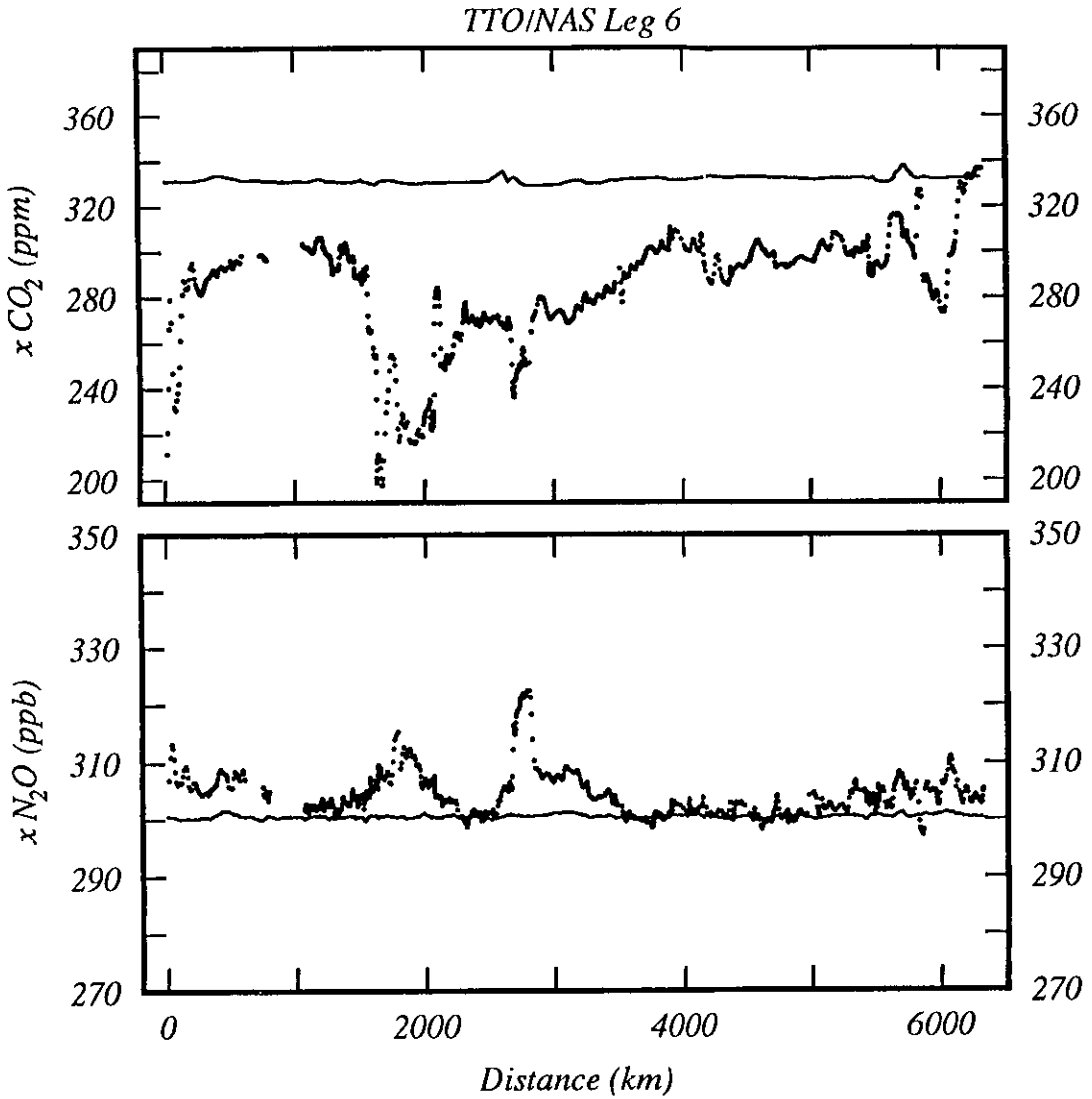

Figure 39. Data plot of xCO_2 and xN_2O (dry gas mole fractions), TTO/NAS Leg 6. Atmospheric measurements are plotted as a line (20 point running mean). Measurements of gas equilibrated with seawater are plotted as individual points after smoothing with a 5-point Gaussian smoother.

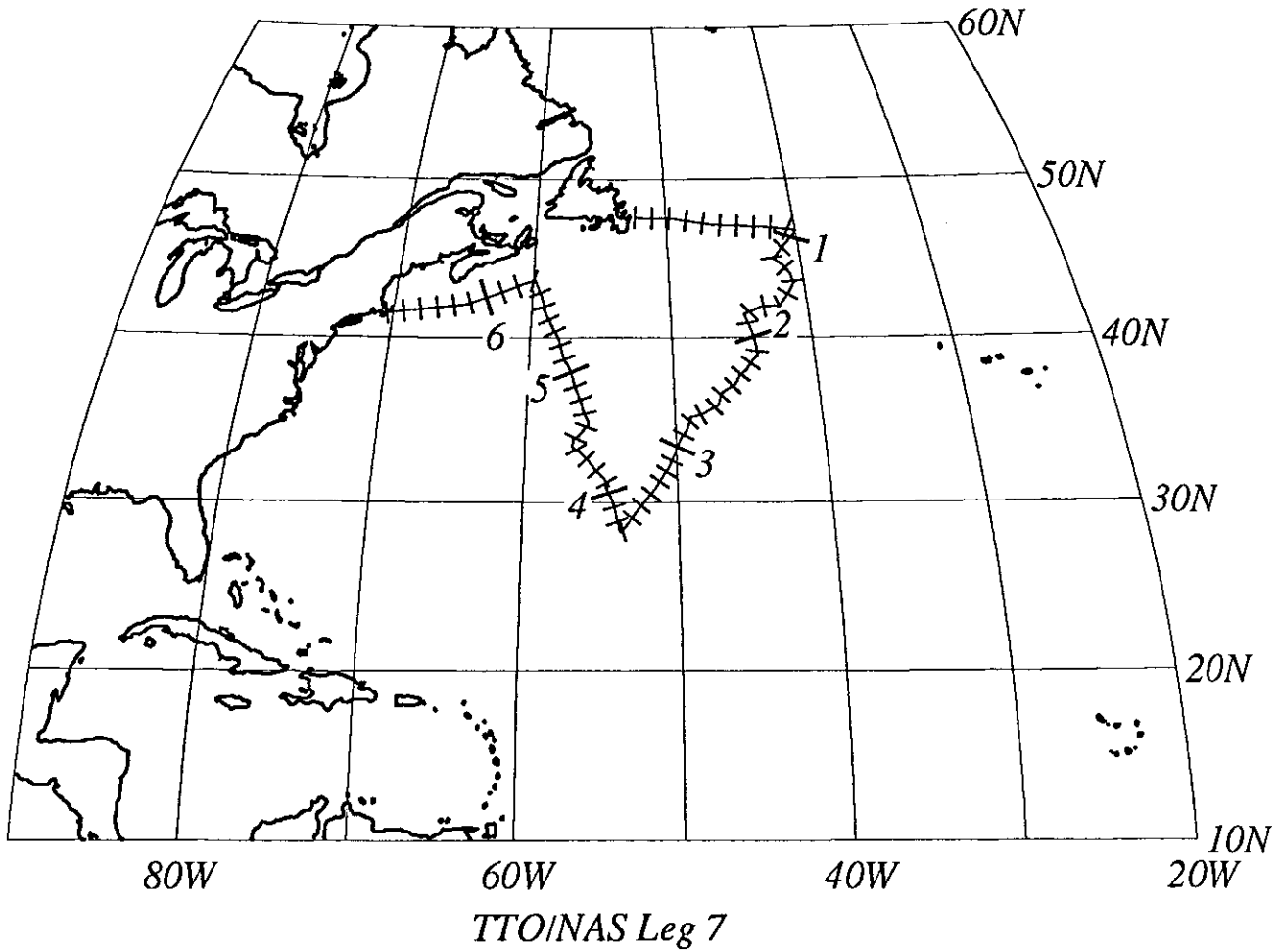

Figure 40. Cruise track plot, TTO/NAS Leg 7. Track indicates cumulative distance in 1000 km intervals, with subdivisions of 100 km.

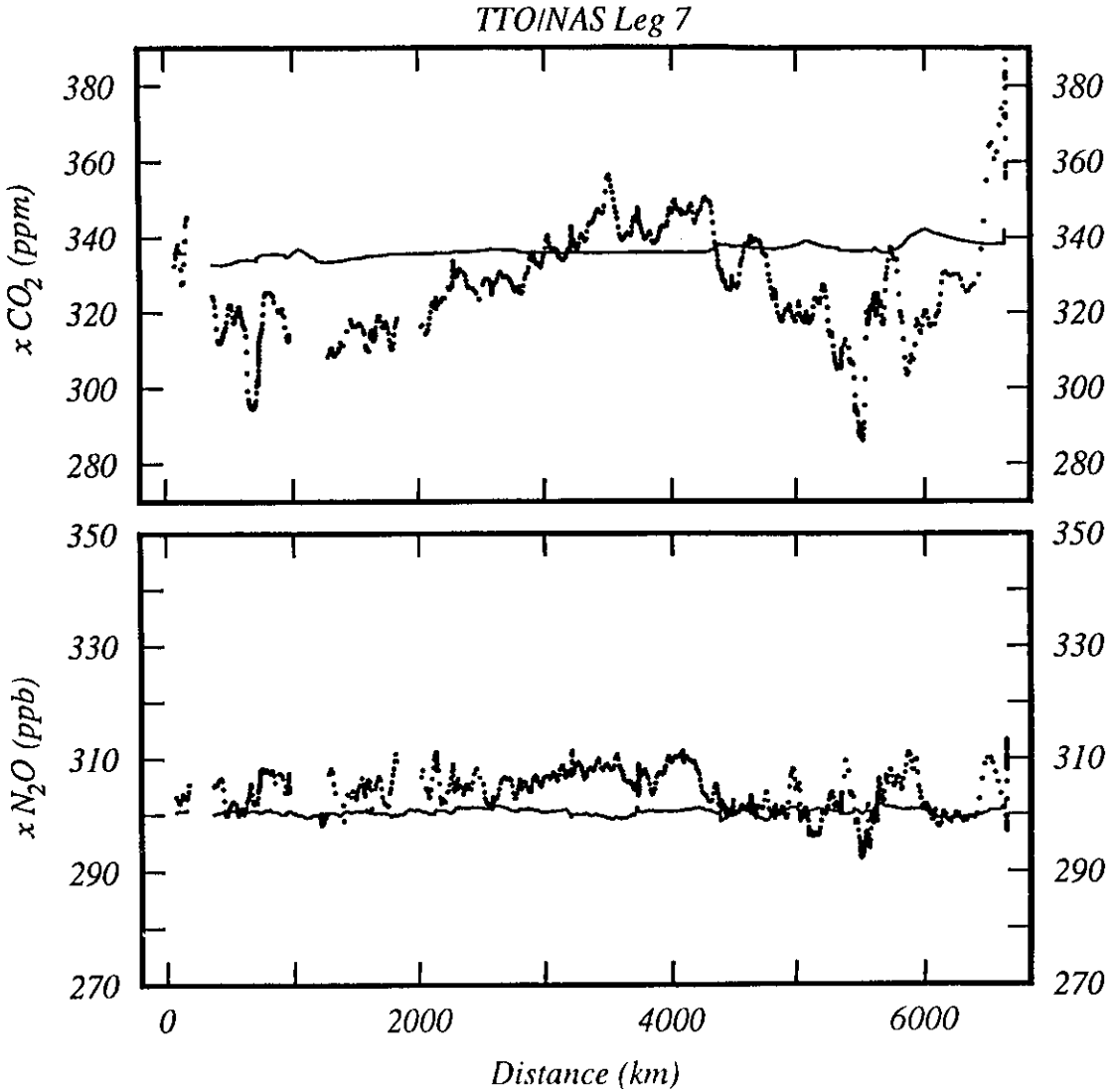

Figure 41. Data plot of xCO_2 and xN_2O (dry gas mole fractions), TTO/NAS Leg 7. Atmospheric measurements are plotted as a line (20 point running mean). Measurements of gas equilibrated with seawater are plotted as individual points after smoothing with a 5-point Gaussian smoother.

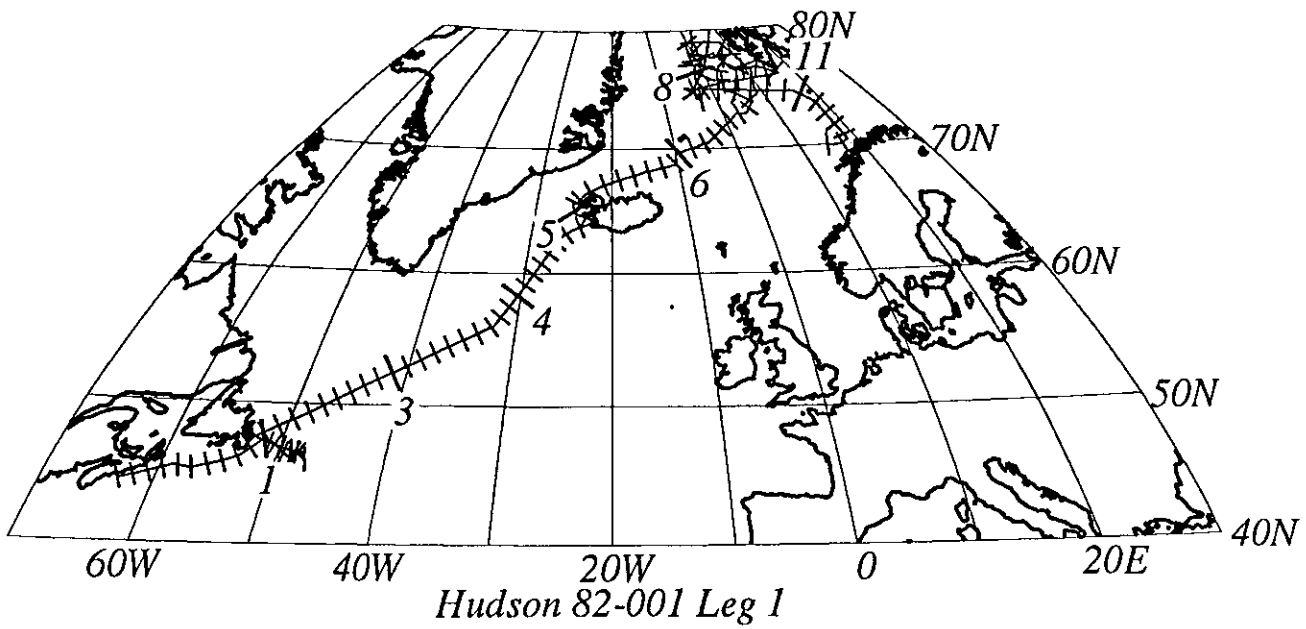

Figure 42. Cruise track plot, Hudson 82-001 Leg 1. Track indicates cumulative distance in 1000 km intervals, with subdivisions of 100 km.

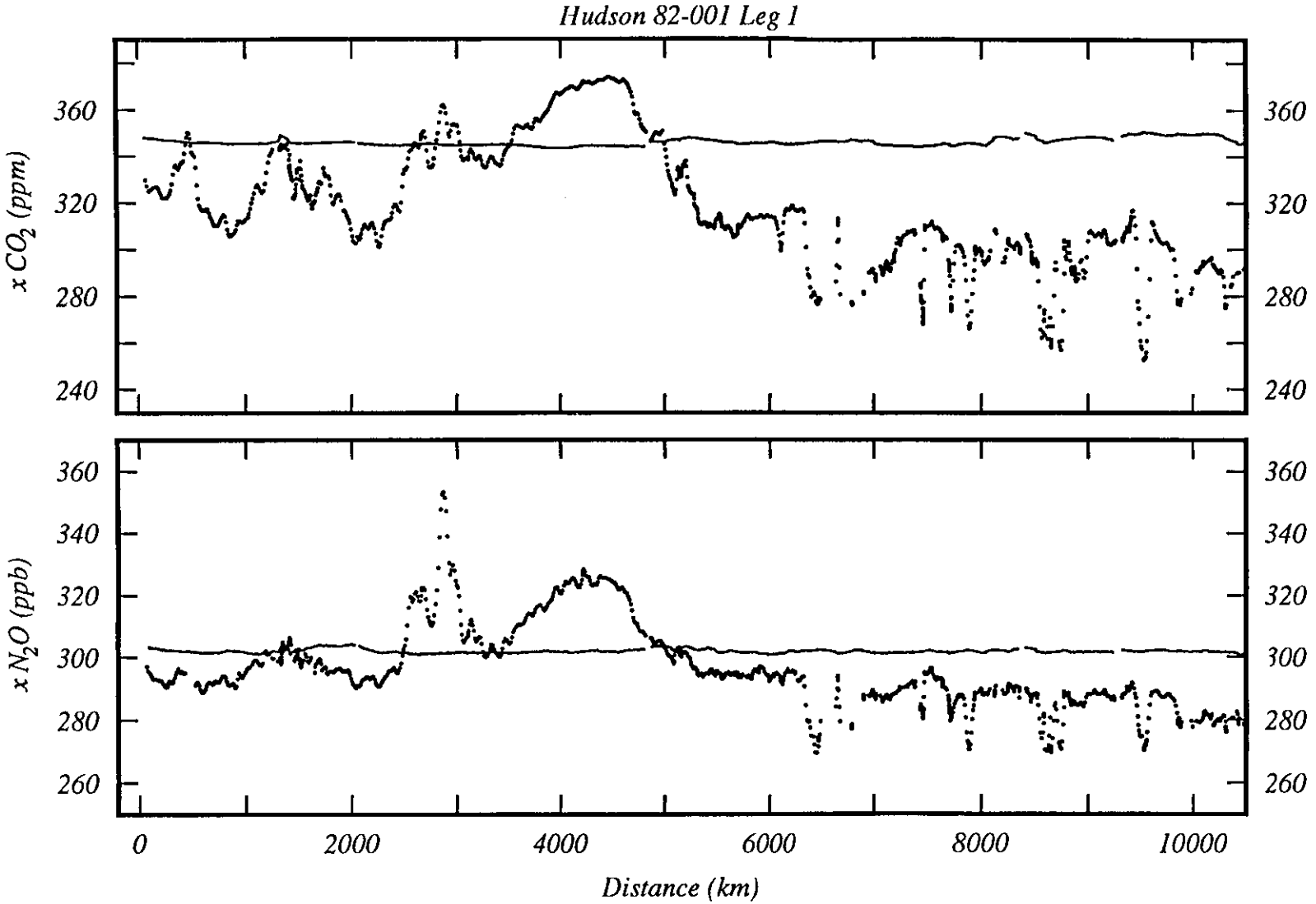

Figure 43. Data plot of xCO_2 and xN_2O (dry gas mole fractions), Hudson 82-001 Leg 1. Atmospheric measurements are plotted as a line (20 point running mean). Measurements of gas equilibrated with seawater are plotted as individual points after smoothing with a 5-point Gaussian smoother.

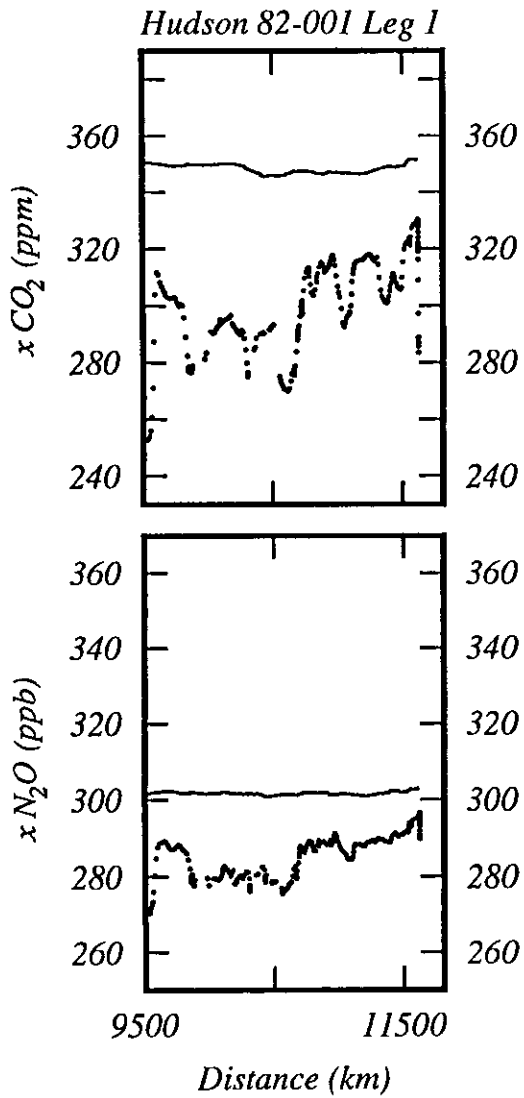

Figure 43. Continued

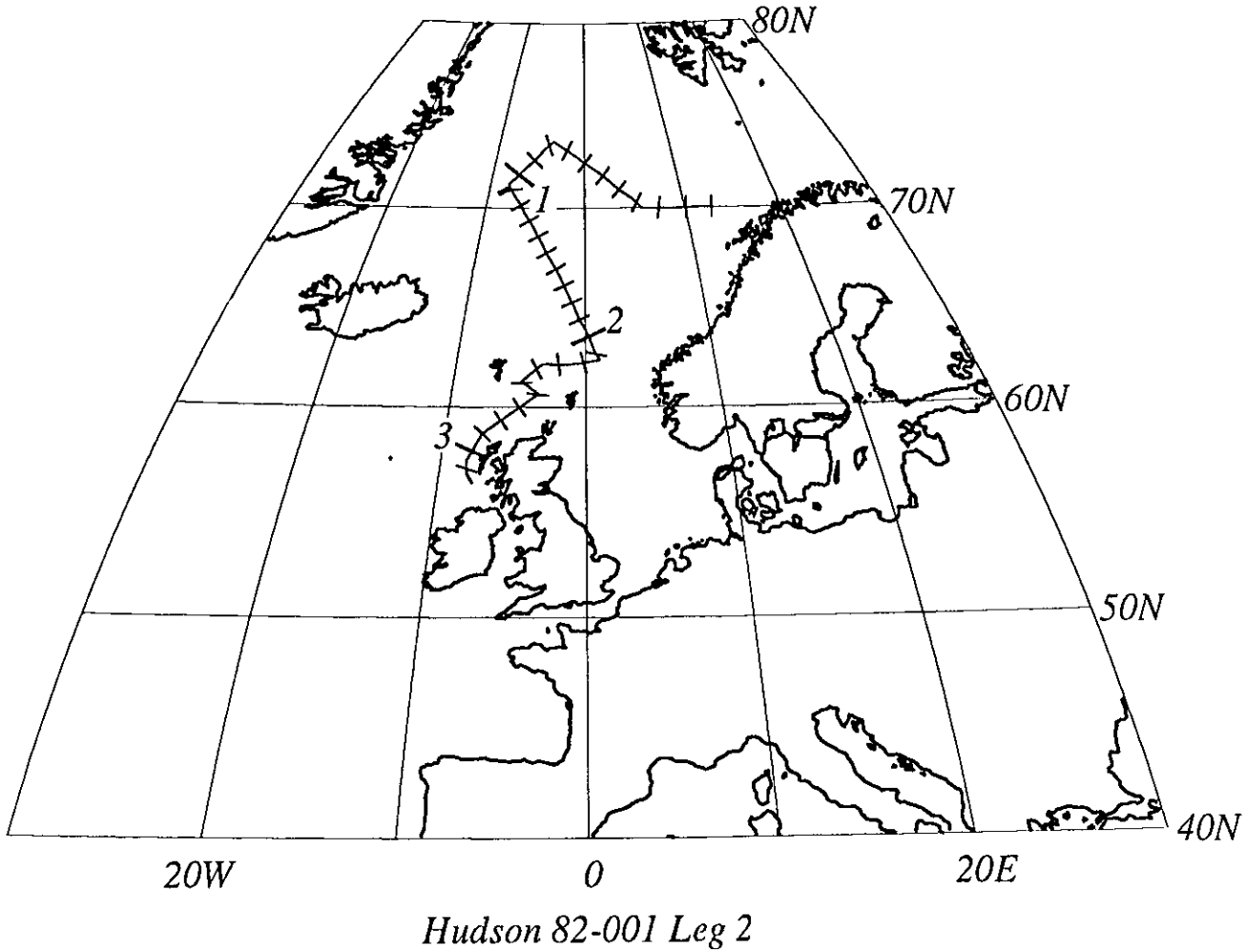

Figure 44. Cruise track plot, Hudson 82-001 Leg 2. Track indicates cumulative distance in 1000 km intervals, with subdivisions of 100 km.

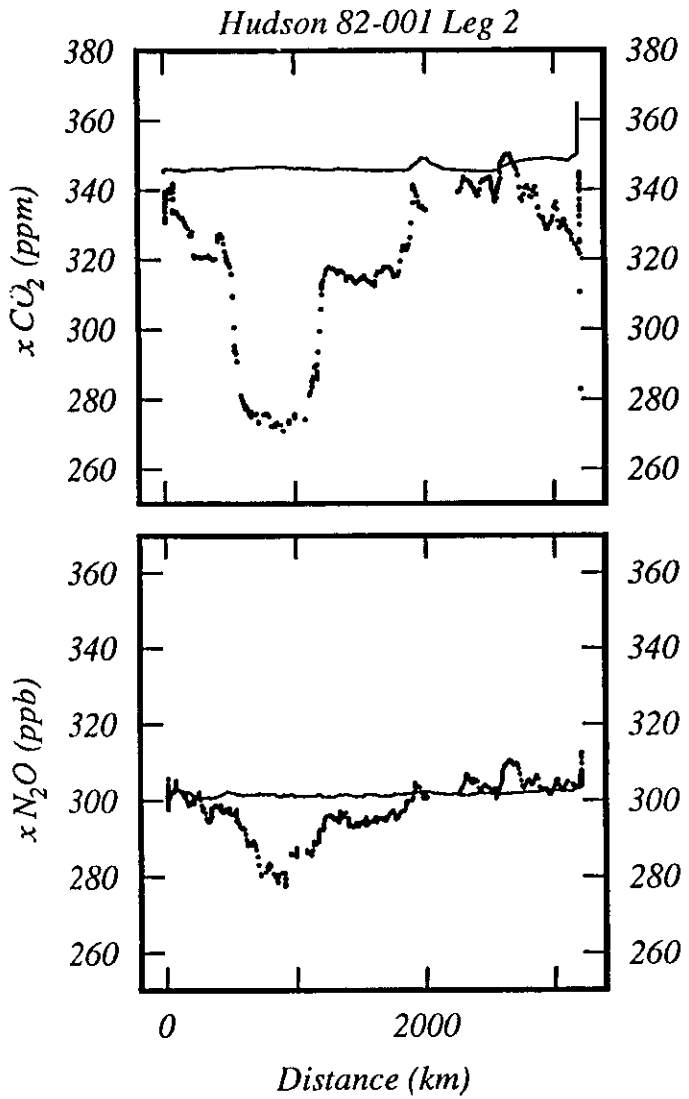

Figure 45. Data plot of xCO_2 and xN_2O (dry gas mole fractions), Hudson 82-001 Leg 2. Atmospheric measurements are plotted as a line (20 point running mean). Measurements of gas equilibrated with seawater are plotted as individual points after smoothing with a 5-point Gaussian smoother.

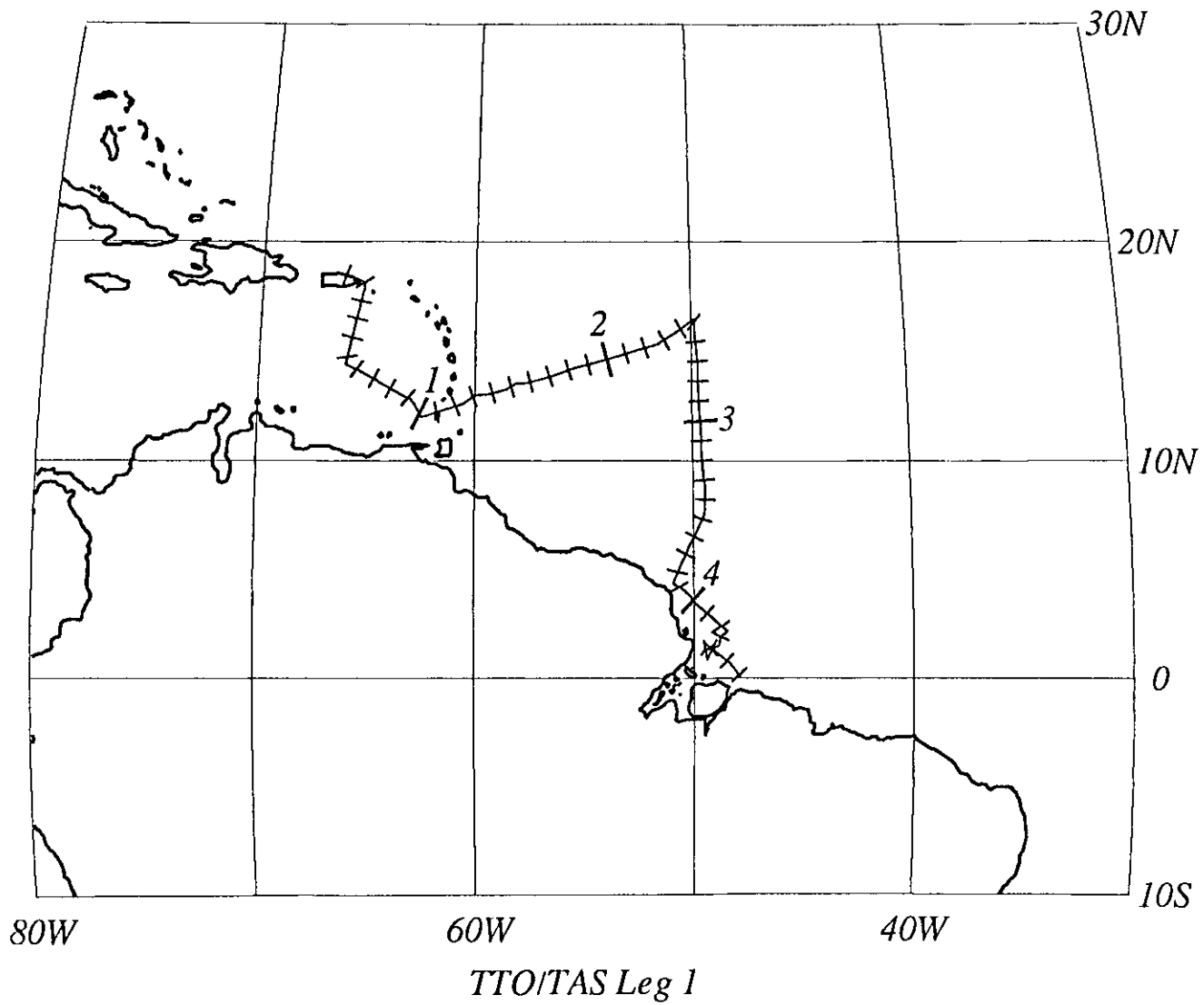

Figure 46. Cruise track plot, TTO/TAS Leg 1. Track indicates cumulative distance in 1000 km intervals, with subdivisions of 100 km.

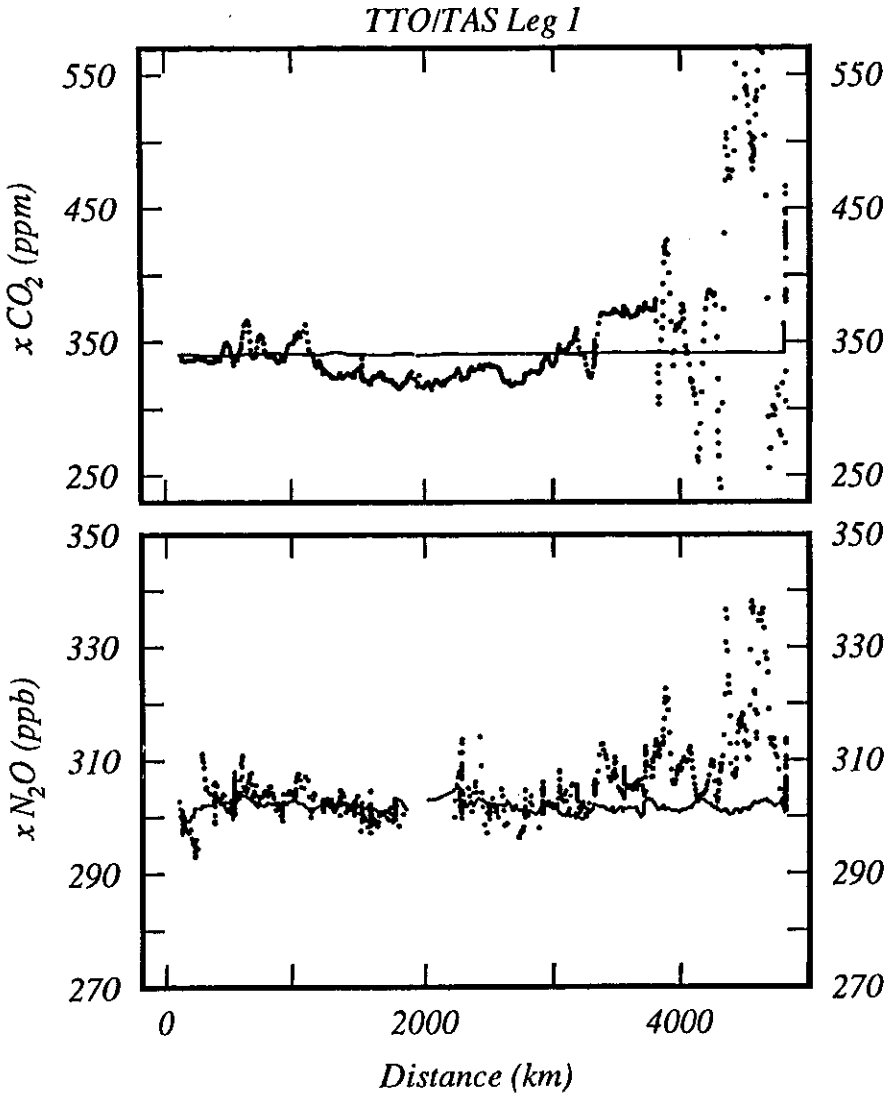

Figure 47. Data plot of xCO_2 and xN_2O (dry gas mole fractions), TTO/TAS Leg 1. Atmospheric measurements are plotted as a line (20 point running mean). Measurements of gas equilibrated with seawater are plotted as individual points after smoothing with a 5-point Gaussian smoother.

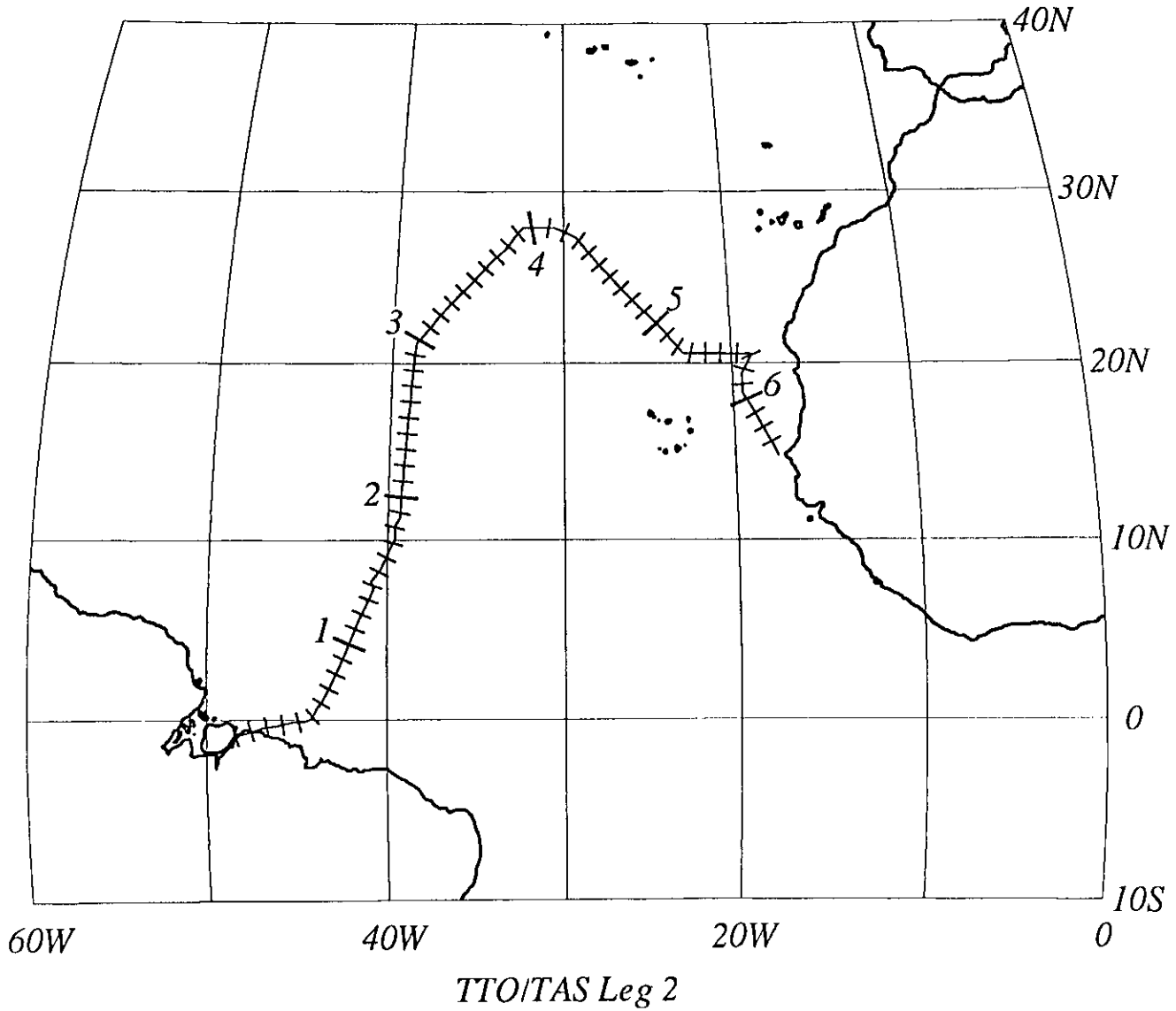

Figure 48. Cruise track plot, TTO/TAS Leg 2. Track indicates cumulative distance in 1000 km intervals, with subdivisions of 100 km.

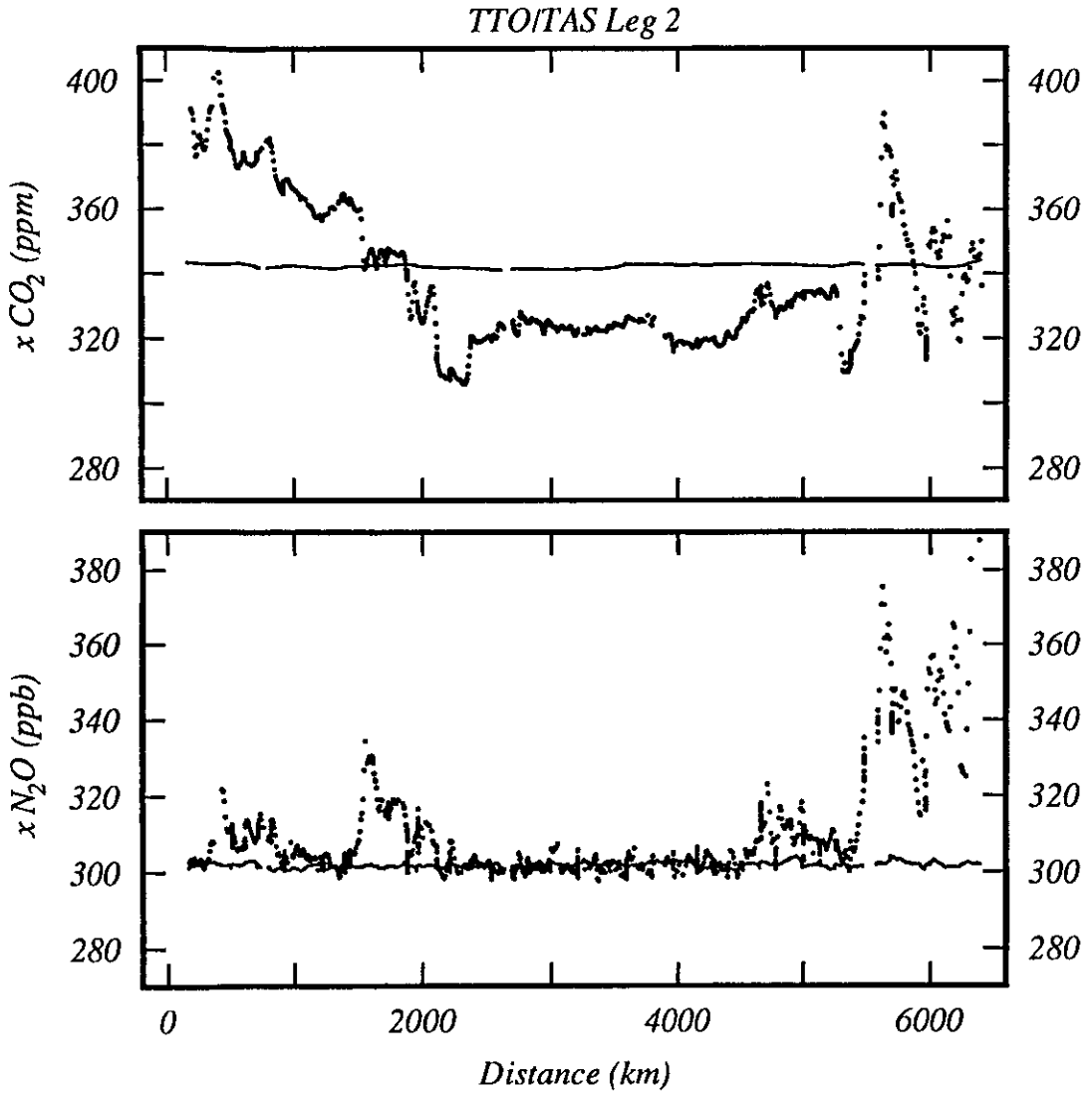

Figure 49. Data plot of xCO_2 and xN_2O (dry gas mole fractions), TTO/TAS Leg 2. Atmospheric measurements are plotted as a line (20 point running mean). Measurements of gas equilibrated with seawater are plotted as individual points after smoothing with a 5-point Gaussian smoother.

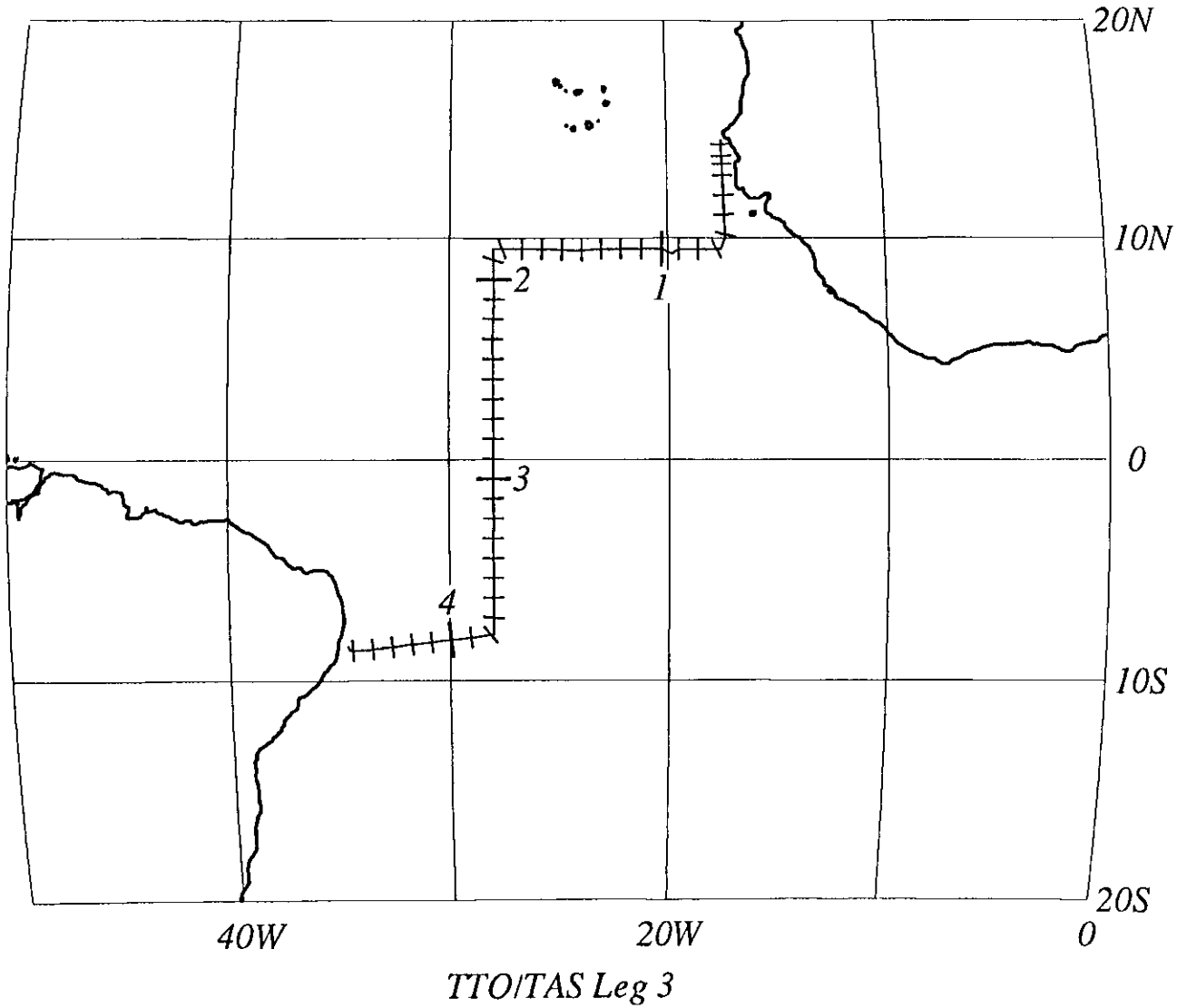

Figure 50. Cruise track plot, TTO/TAS Leg 3. Track indicates cumulative distance in 1000 km intervals, with subdivisions of 100 km.

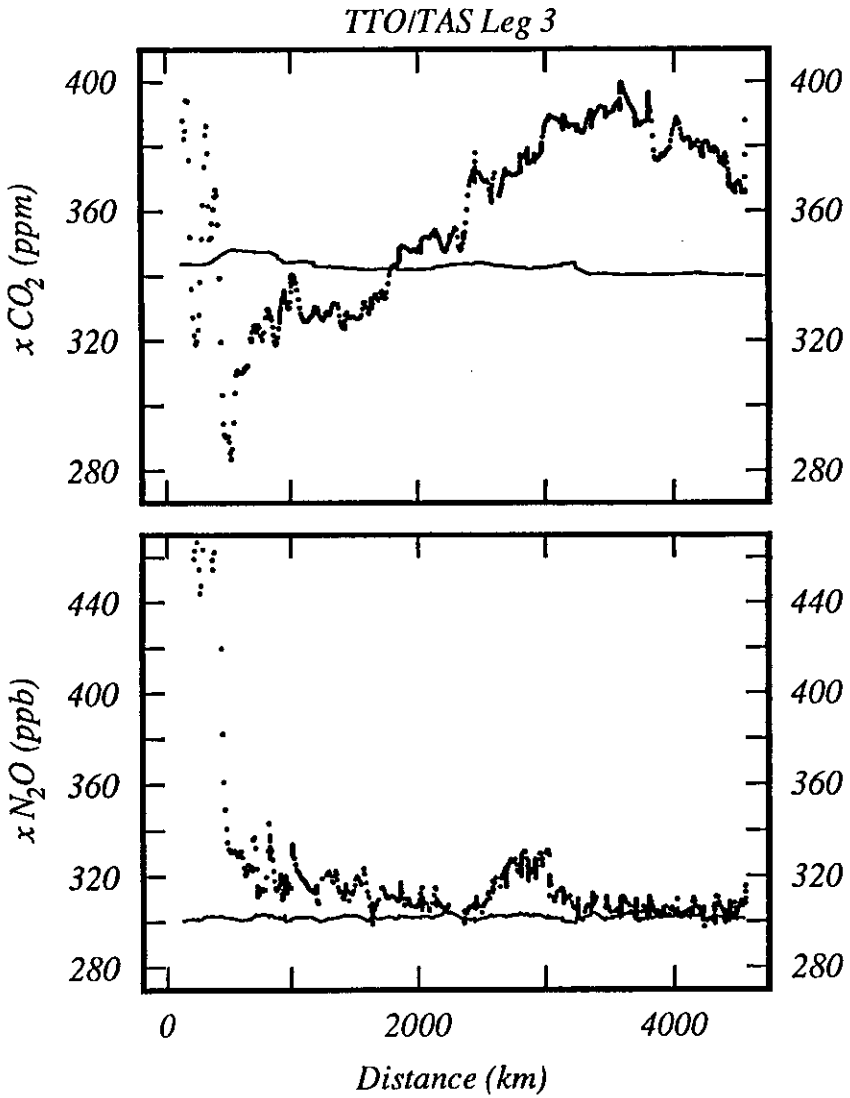

Figure 51. Data plot of xCO_2 and xN_2O (dry gas mole fractions), TTO/TAS Leg 3. Atmospheric measurements are plotted as a line (20 point running mean). Measurements of gas equilibrated with seawater are plotted as individual points after smoothing with a 5-point Gaussian smoother.

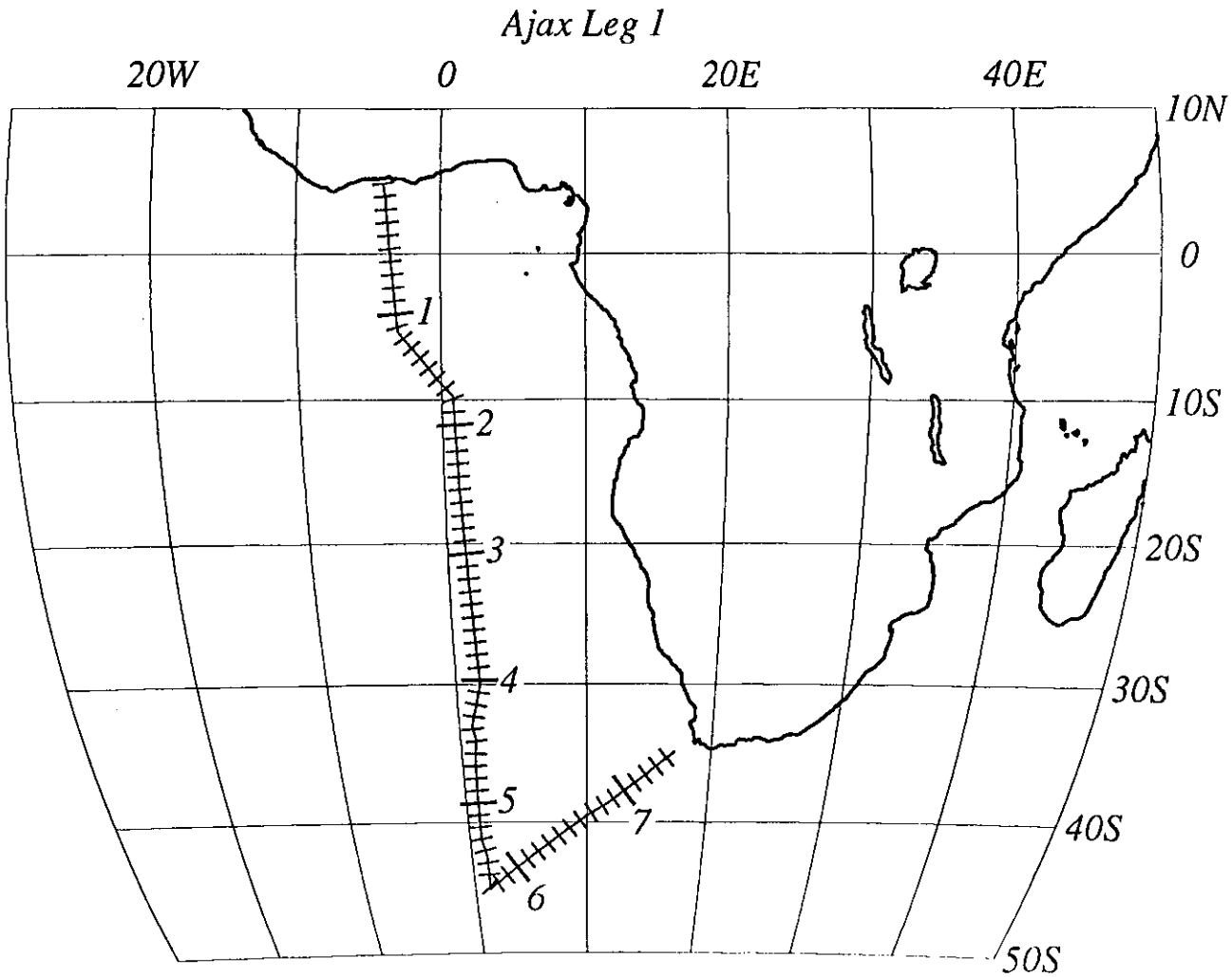

Figure 52. Cruise track plot, Ajax Leg 1. Track indicates cumulative distance in 1000 km intervals, with subdivisions of 100 km.

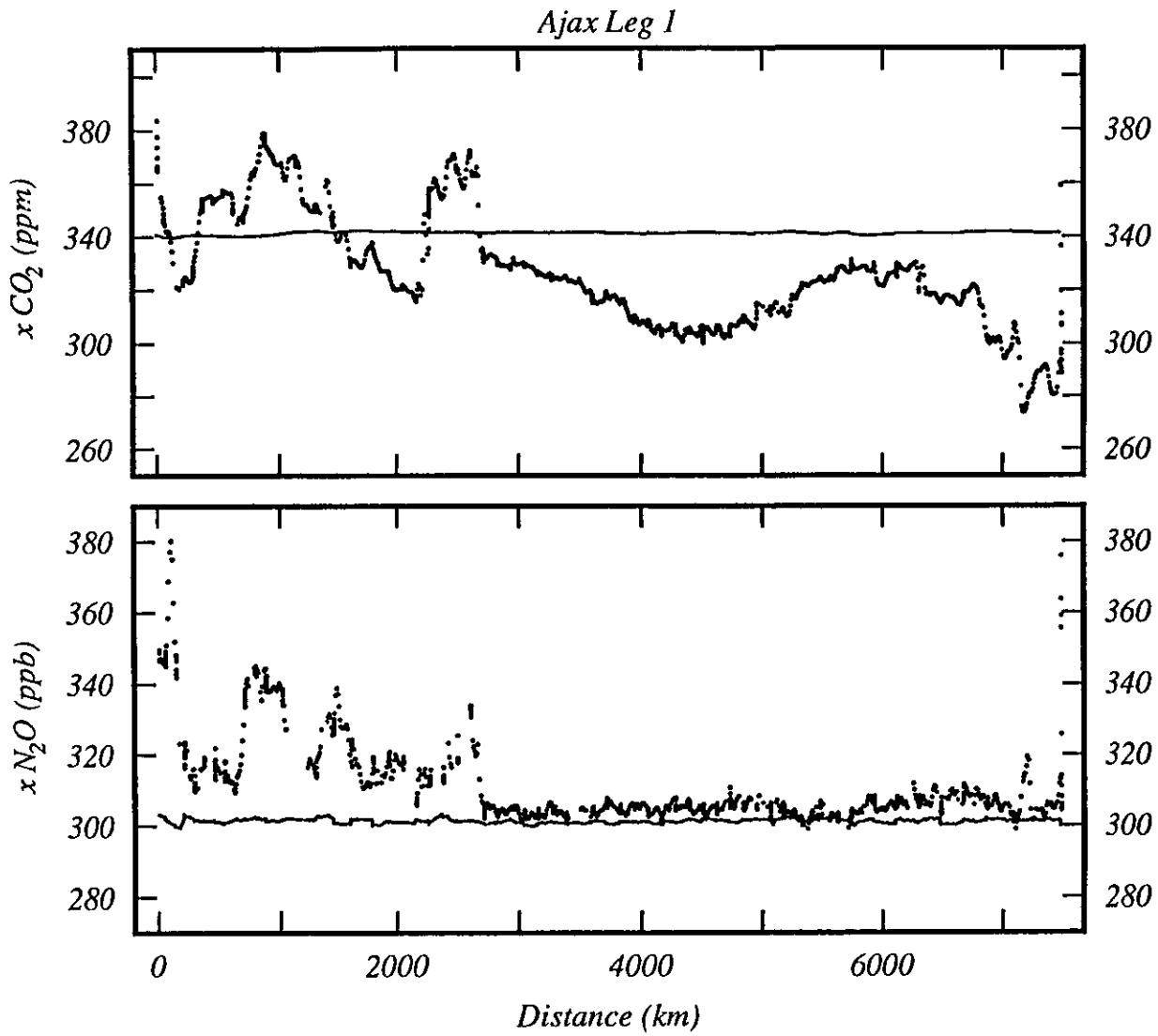

Figure 53. Data plot of xCO_2 and xN_2O (dry gas mole fractions), Ajax Leg 1. Atmospheric measurements are plotted as a line (20 point running mean). Measurements of gas equilibrated with seawater are plotted as individual points after smoothing with a 5-point Gaussian smoother.

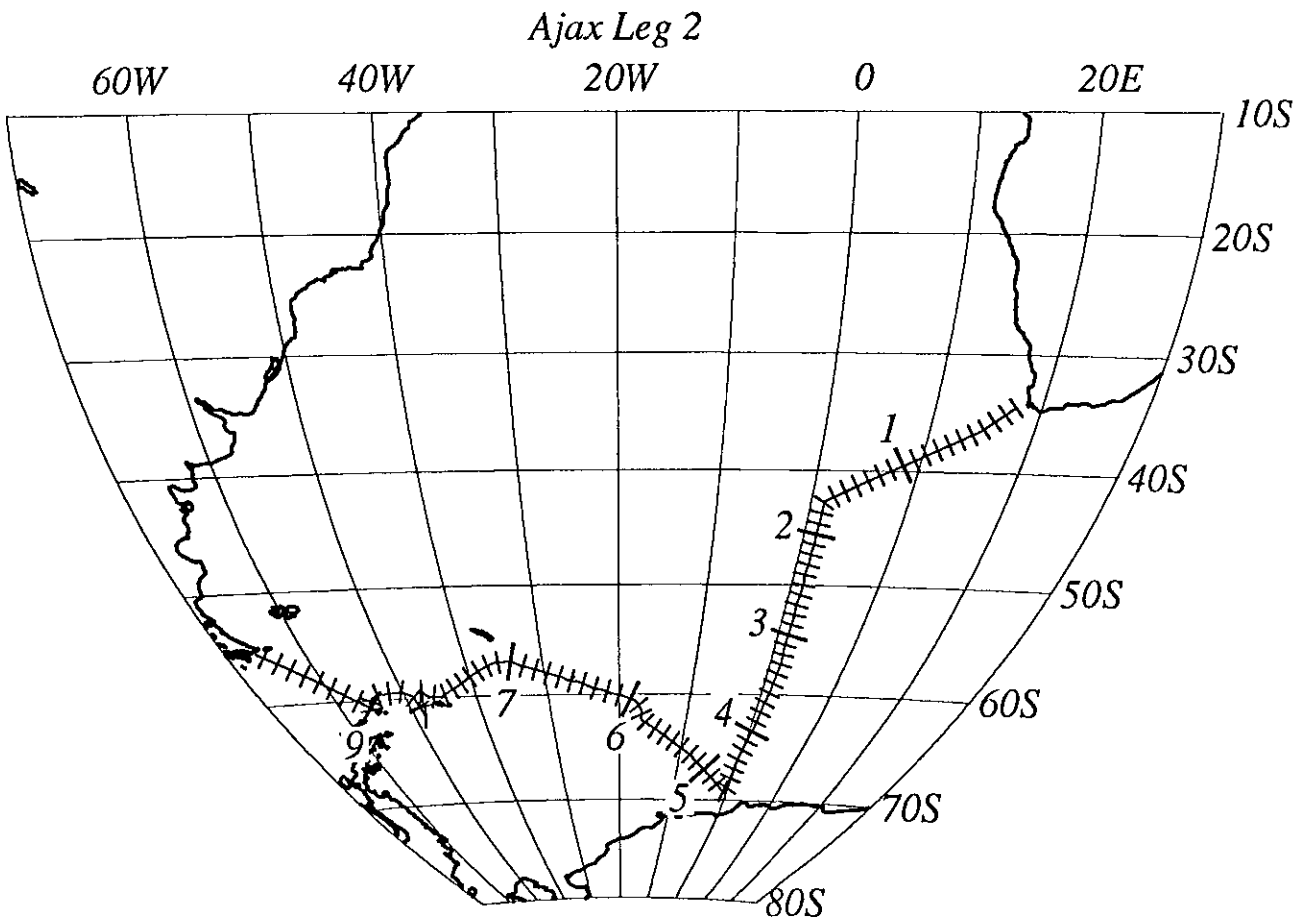

Figure 54. Cruise track plot, Ajax Leg 2. Track indicates cumulative distance in 1000 km intervals, with subdivisions of 100 km.

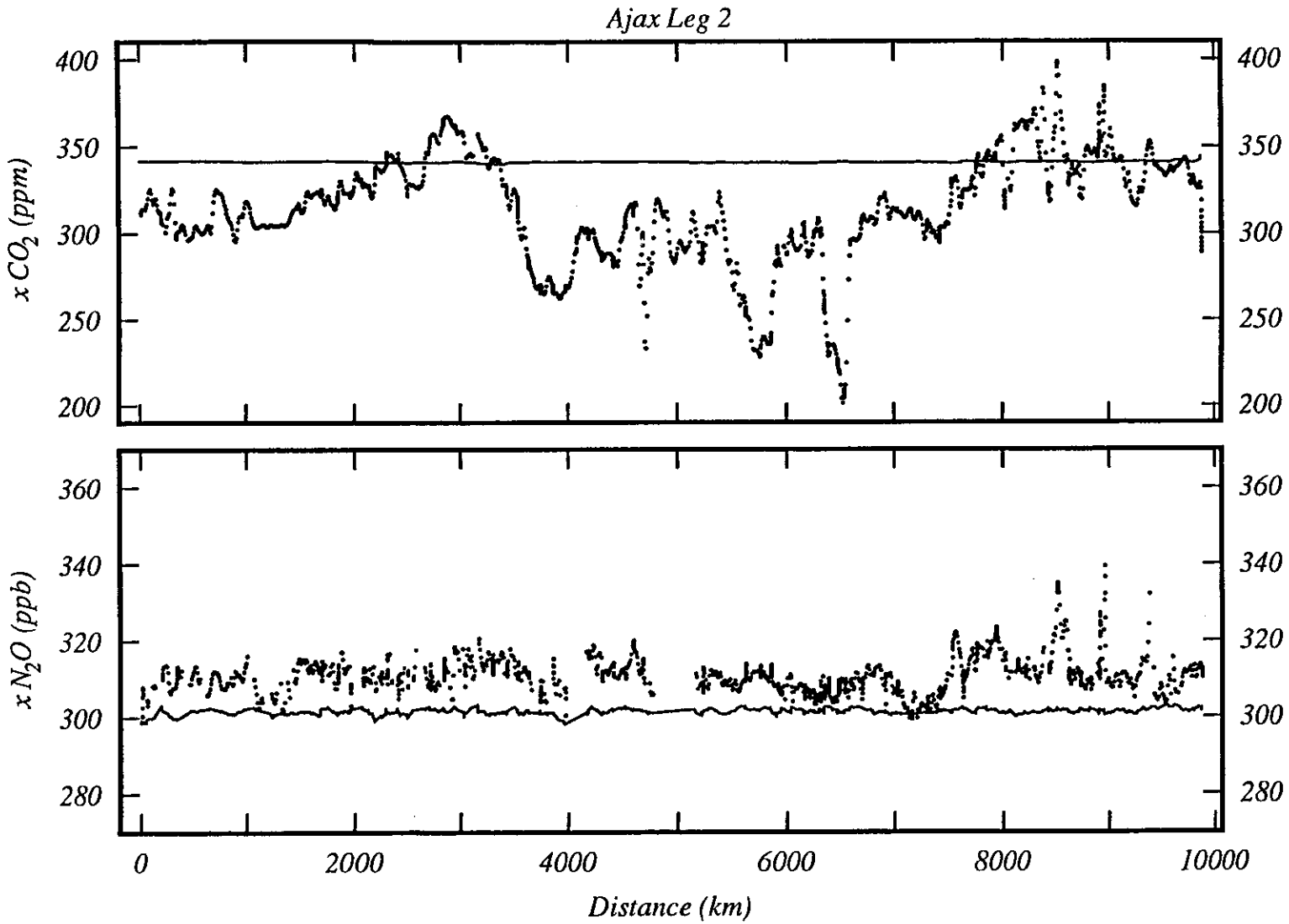

Figure 55. Data plot of xCO_2 and xN_2O (dry gas mole fractions), Ajax Leg 2. Atmospheric measurements are plotted as a line (20 point running mean). Measurements of gas equilibrated with seawater are plotted as individual points after smoothing with a 5-point Gaussian smoother.

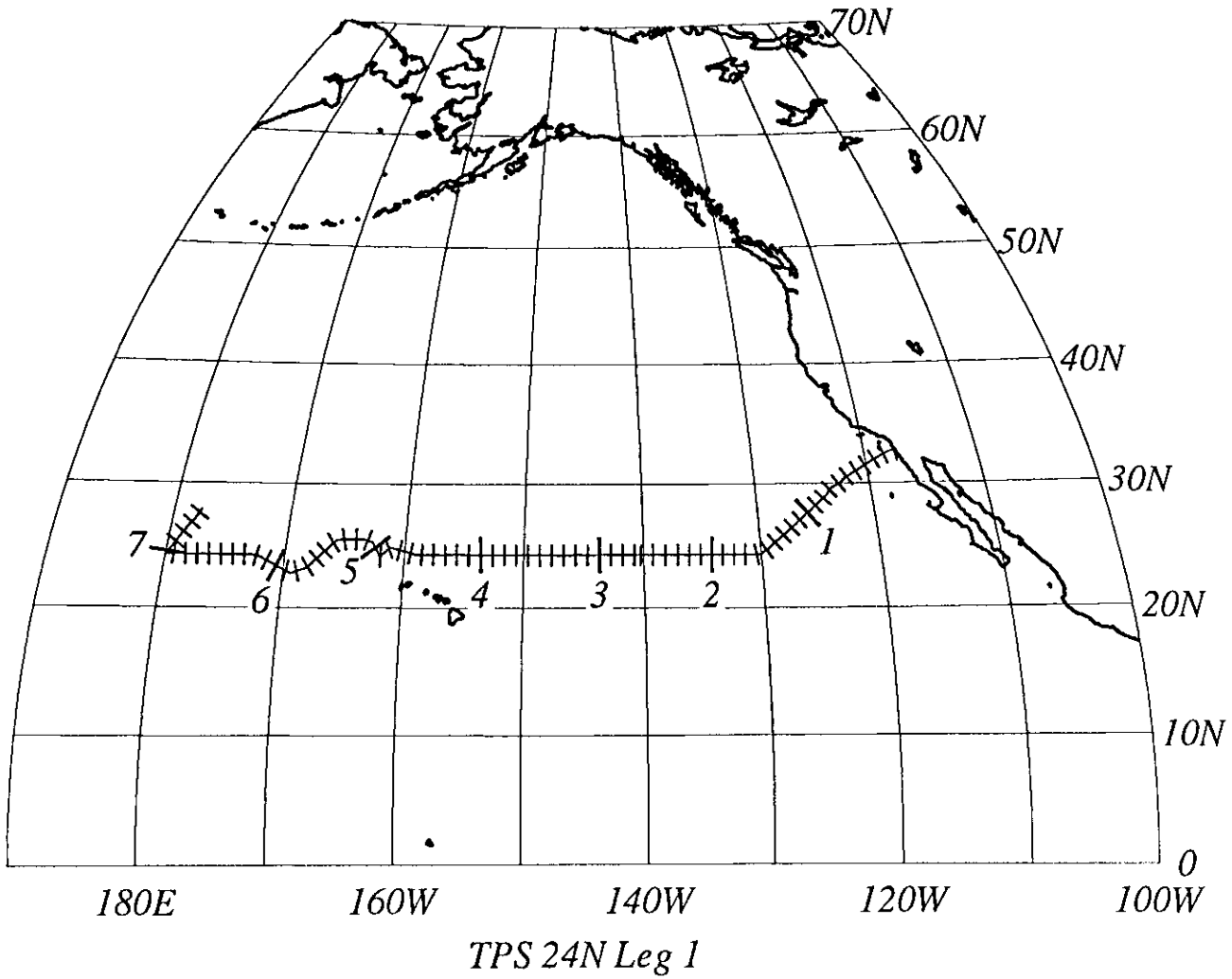

Figure 56. Cruise track plot, TPS24 Leg 1. Track indicates cumulative distance in 1000 km intervals, with subdivisions of 100 km.

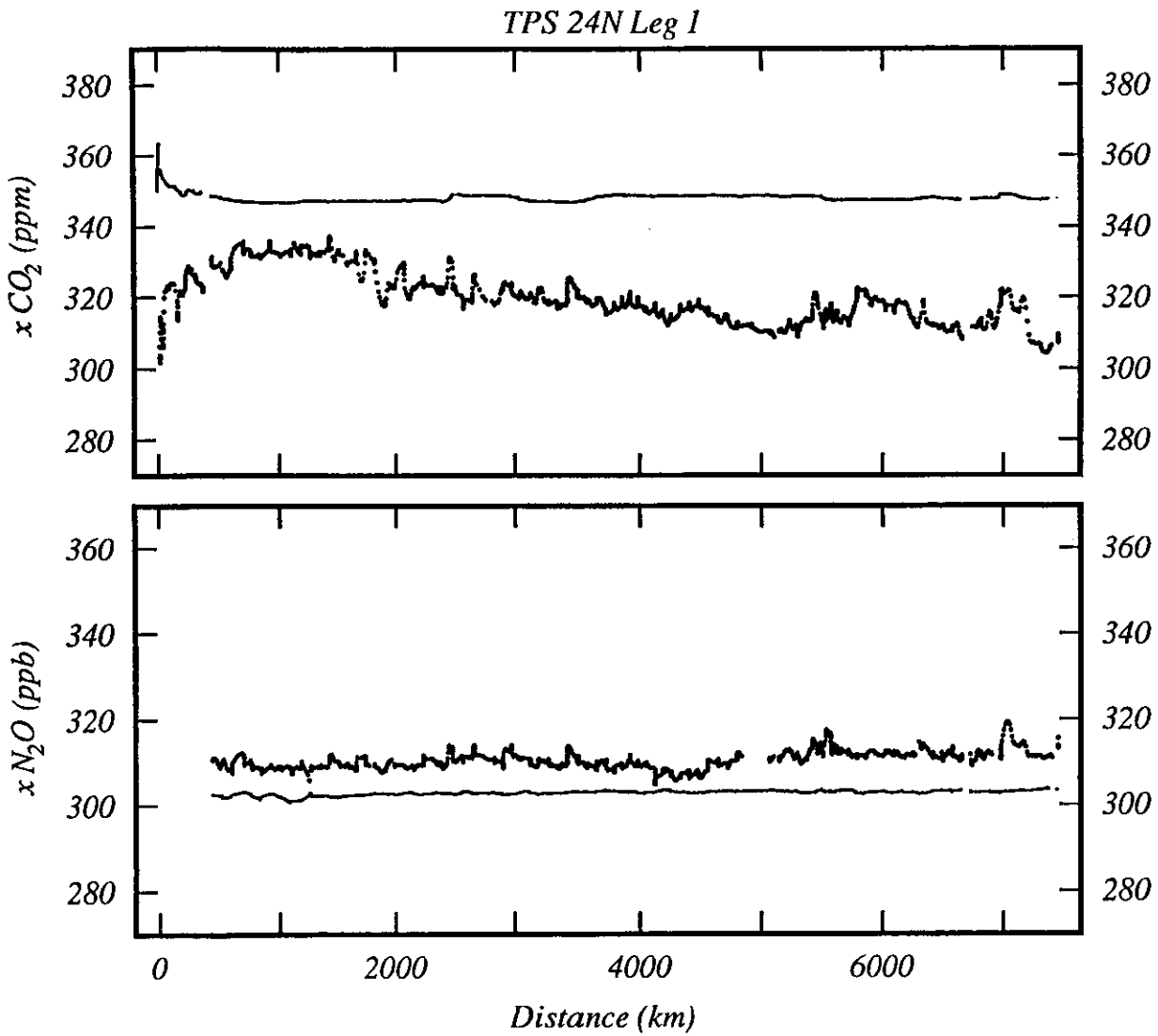

Figure 57. Data plot of xCO_2 and xN_2O (dry gas mole fractions), TPS24 Leg 1. Atmospheric measurements are plotted as a line (20 point running mean). Measurements of gas equilibrated with seawater are plotted as individual points after smoothing with a 5-point Gaussian smoother.

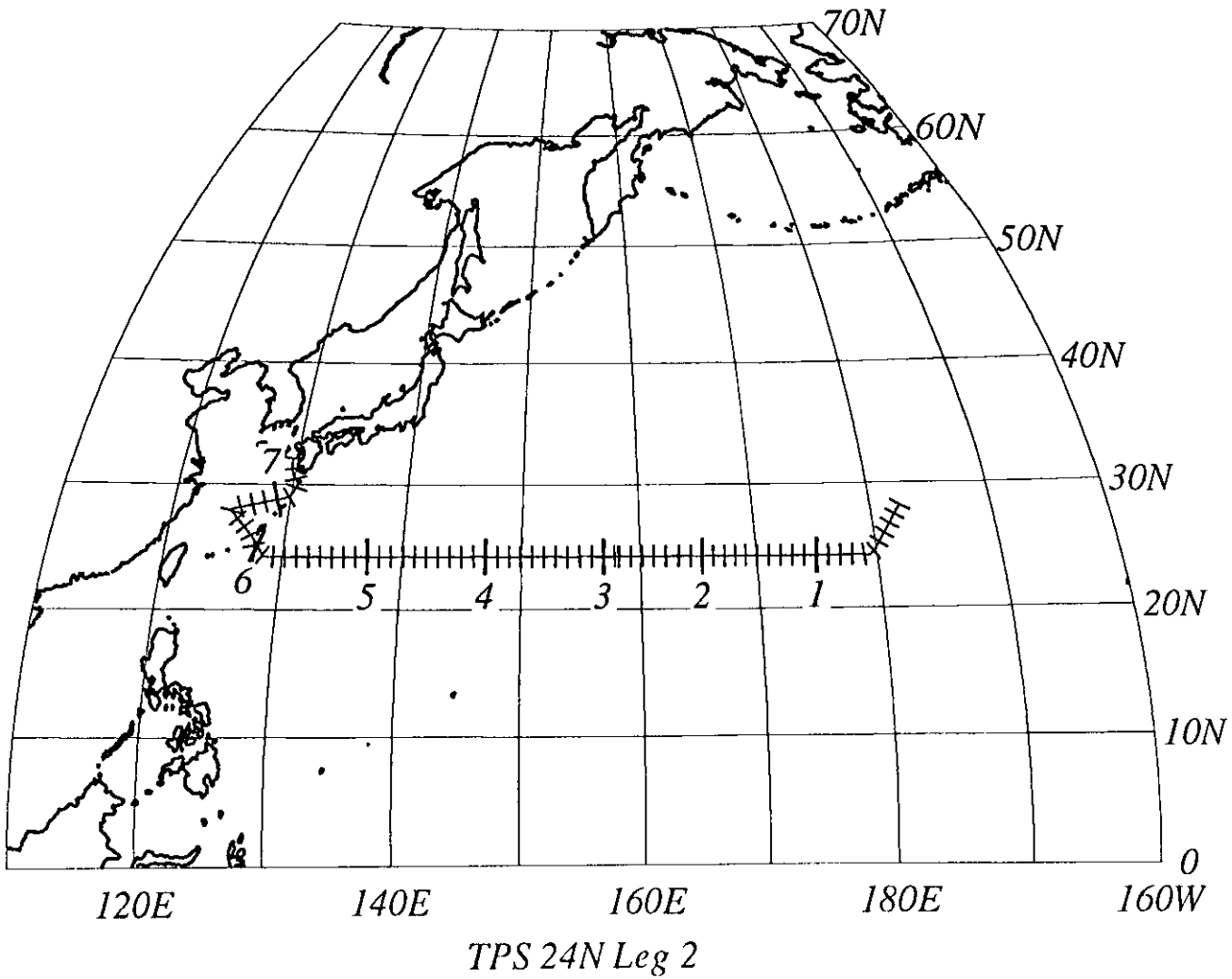

Figure 58. Cruise track plot, TPS24 Leg 2. Track indicates cumulative distance in 1000 km intervals, with subdivisions of 100 km.

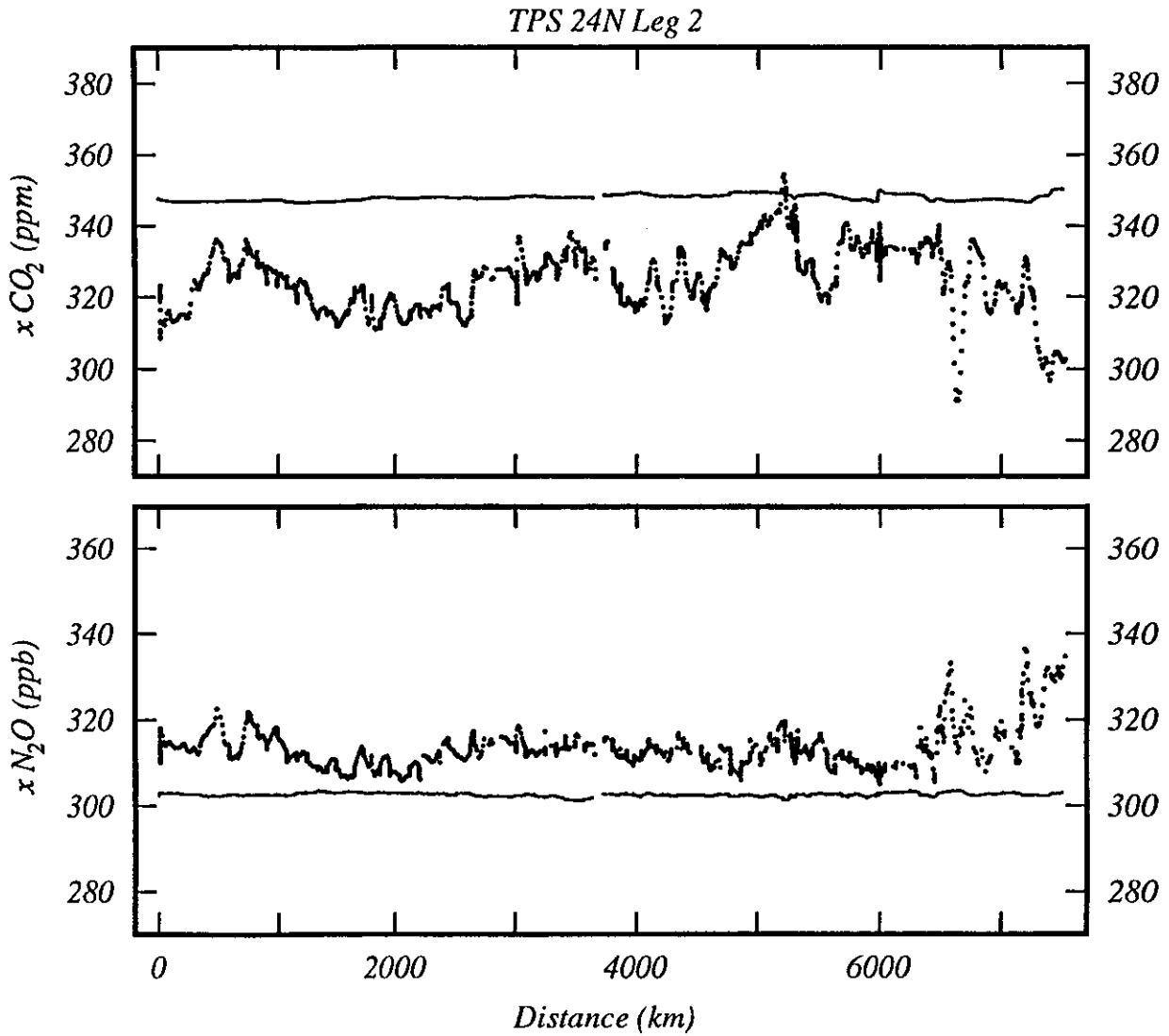

Figure 59. Data plot of xCO_2 and xN_2O (dry gas mole fractions), TPS24 Leg 2. Atmospheric measurements are plotted as a line (20 point running mean). Measurements of gas equilibrated with seawater are plotted as individual points after smoothing with a 5-point Gaussian smoother.

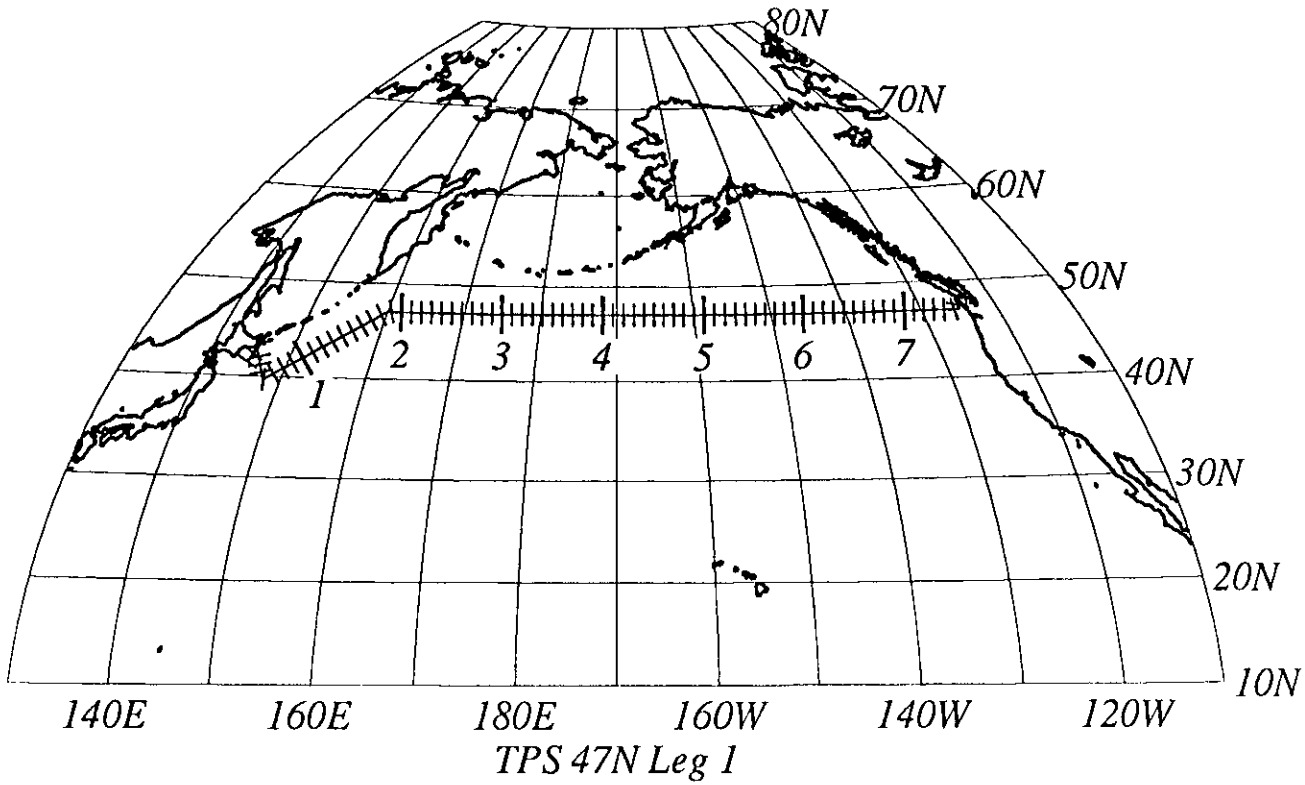

Figure 60. Cruise track plot, TPS47 Leg 1. Track indicates cumulative distance in 1000 km intervals, with subdivisions of 100 km.

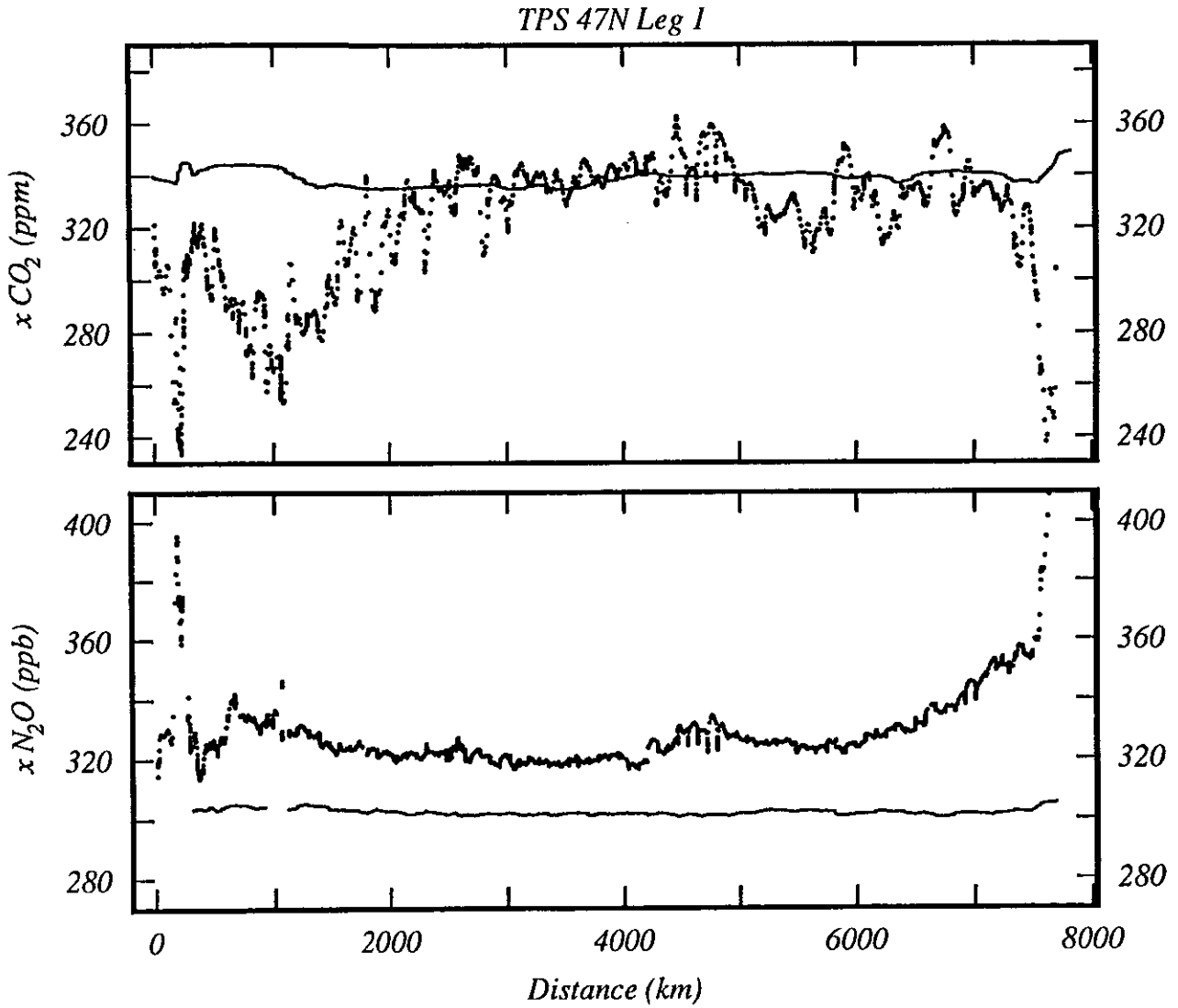

Figure 61. Data plot of xCO_2 and xN_2O (dry gas mole fractions), TPS47 Leg 1. Atmospheric measurements are plotted as a line (20 point running mean). Measurements of gas equilibrated with seawater are plotted as individual points after smoothing with a 5-point Gaussian smoother.

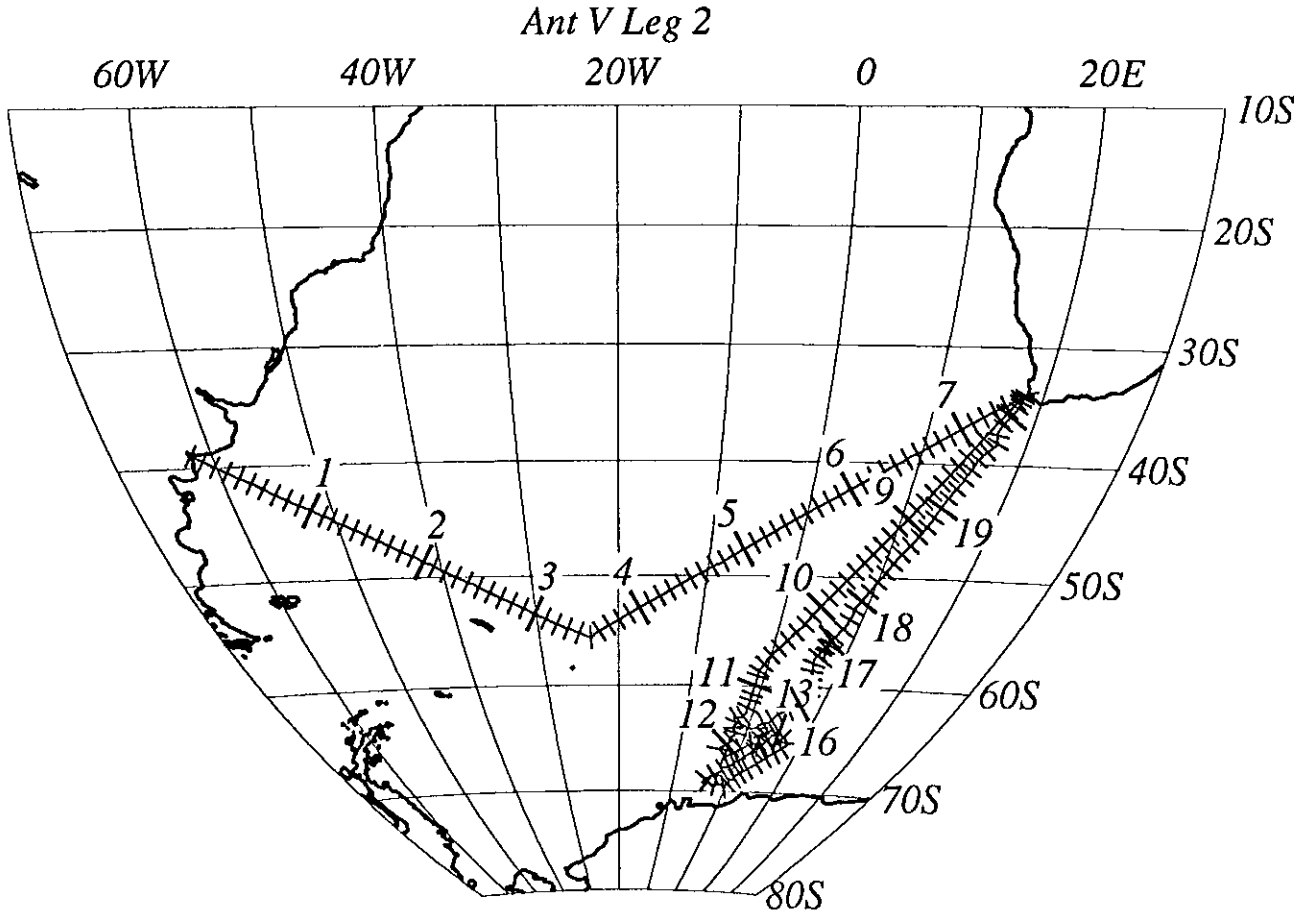

Figure 62. Cruise track plot, Ant V Leg 2. Track indicates cumulative distance in 1000 km intervals, with subdivisions of 100 km.

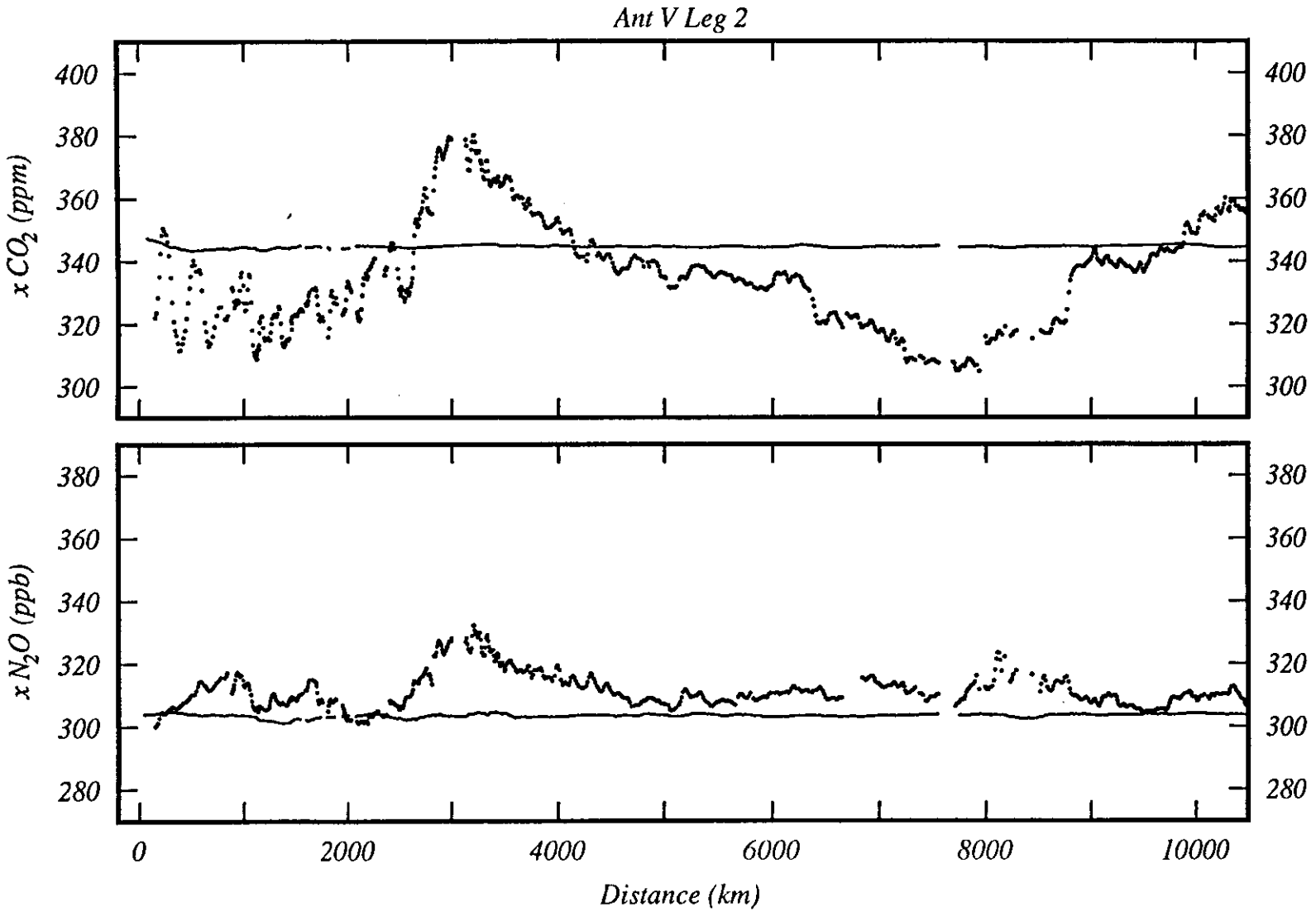

Figure 63. Data plot of xCO_2 and xN_2O (dry gas mole fractions), Ant V Leg 2. Atmospheric measurements are plotted as a line (20 point running mean). Measurements of gas equilibrated with seawater are plotted as individual points after smoothing with a 5-point Gaussian smoother.

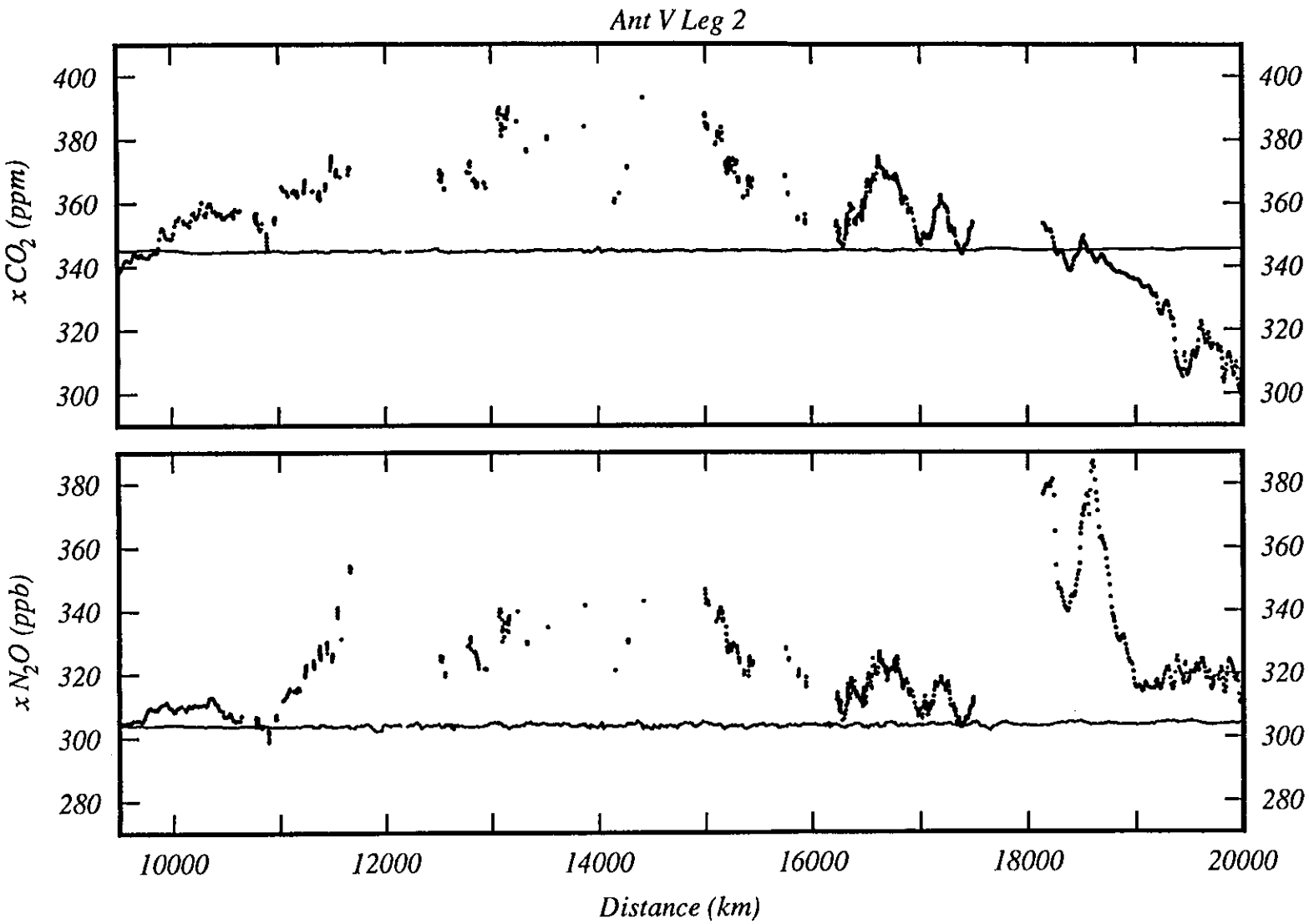

Figure 63. Continued

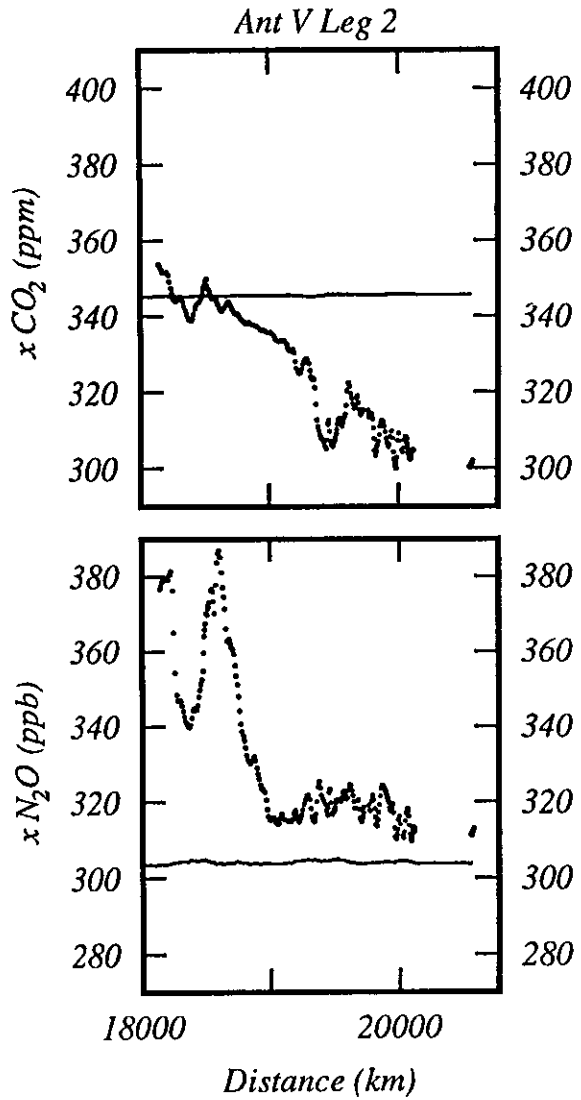

Figure 63. Continued

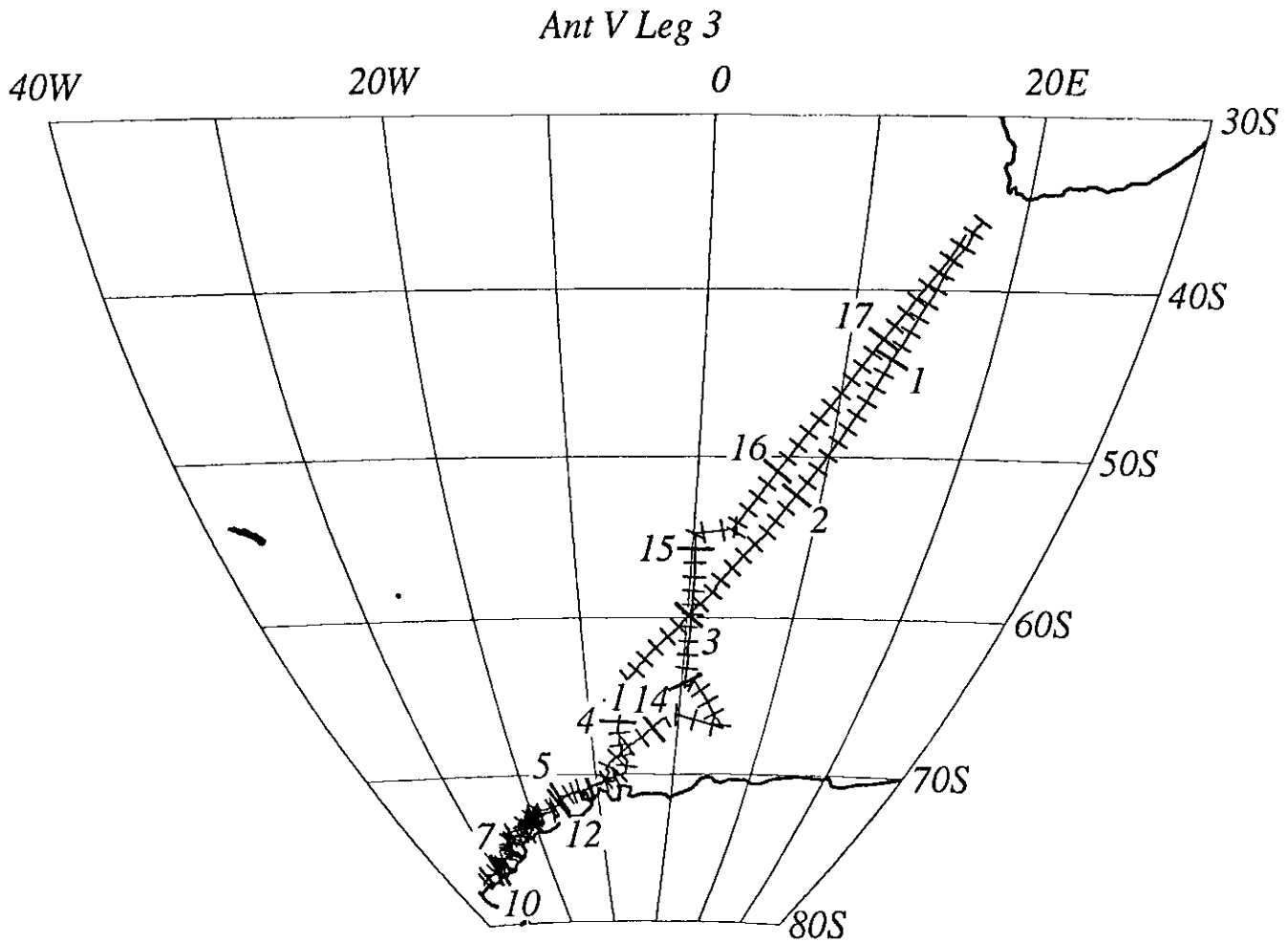

Figure 64. Cruise track plot, Ant V Leg 3. Track indicates cumulative distance in 1000 km intervals, with subdivisions of 100 km.

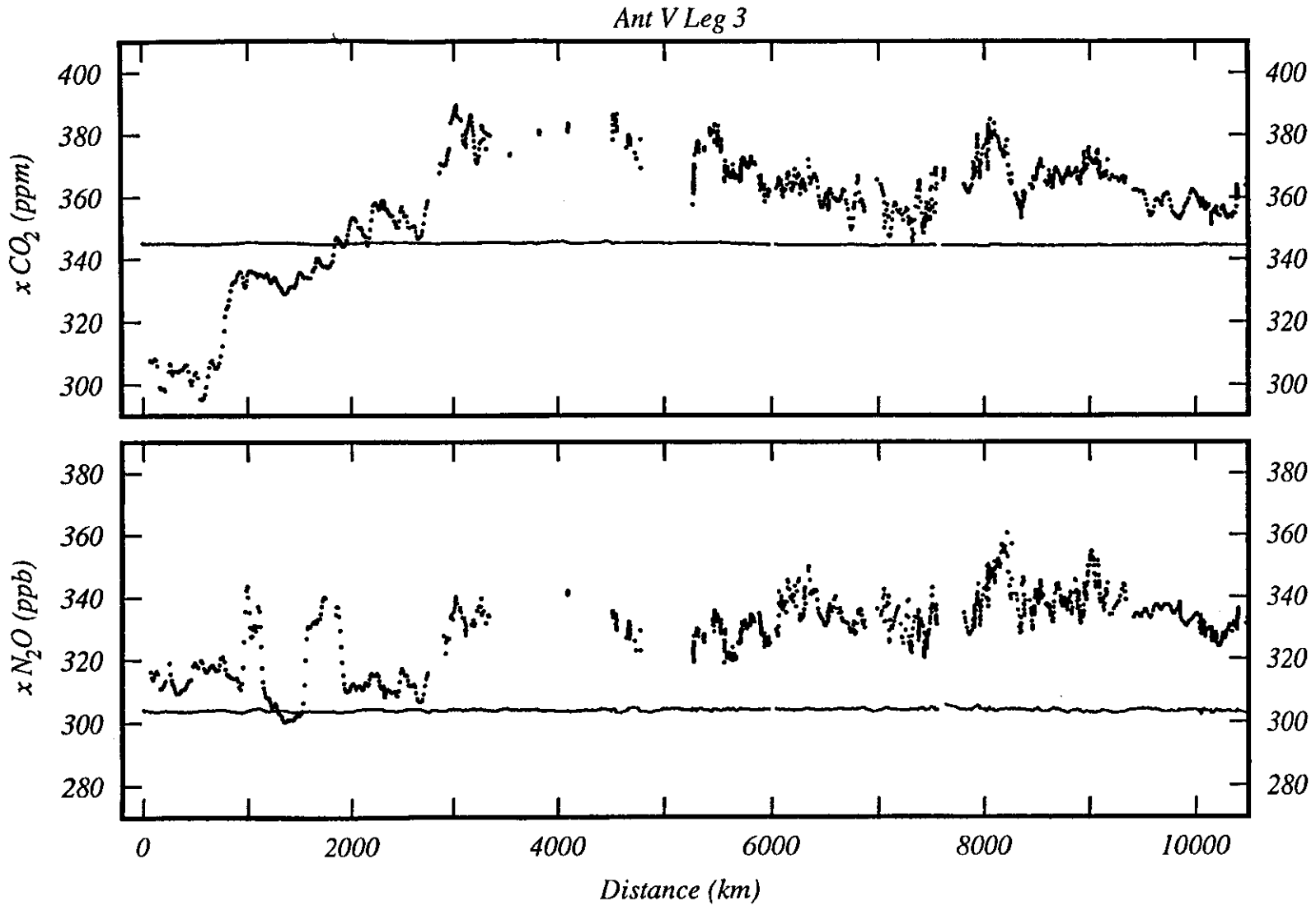

Figure 65. Data plot of xCO_2 and xN_2O (dry gas mole fractions), Ant V Leg 3. Atmospheric measurements are plotted as a line (20 point running mean). Measurements of gas equilibrated with seawater are plotted as individual points after smoothing with a 5-point Gaussian smoother.

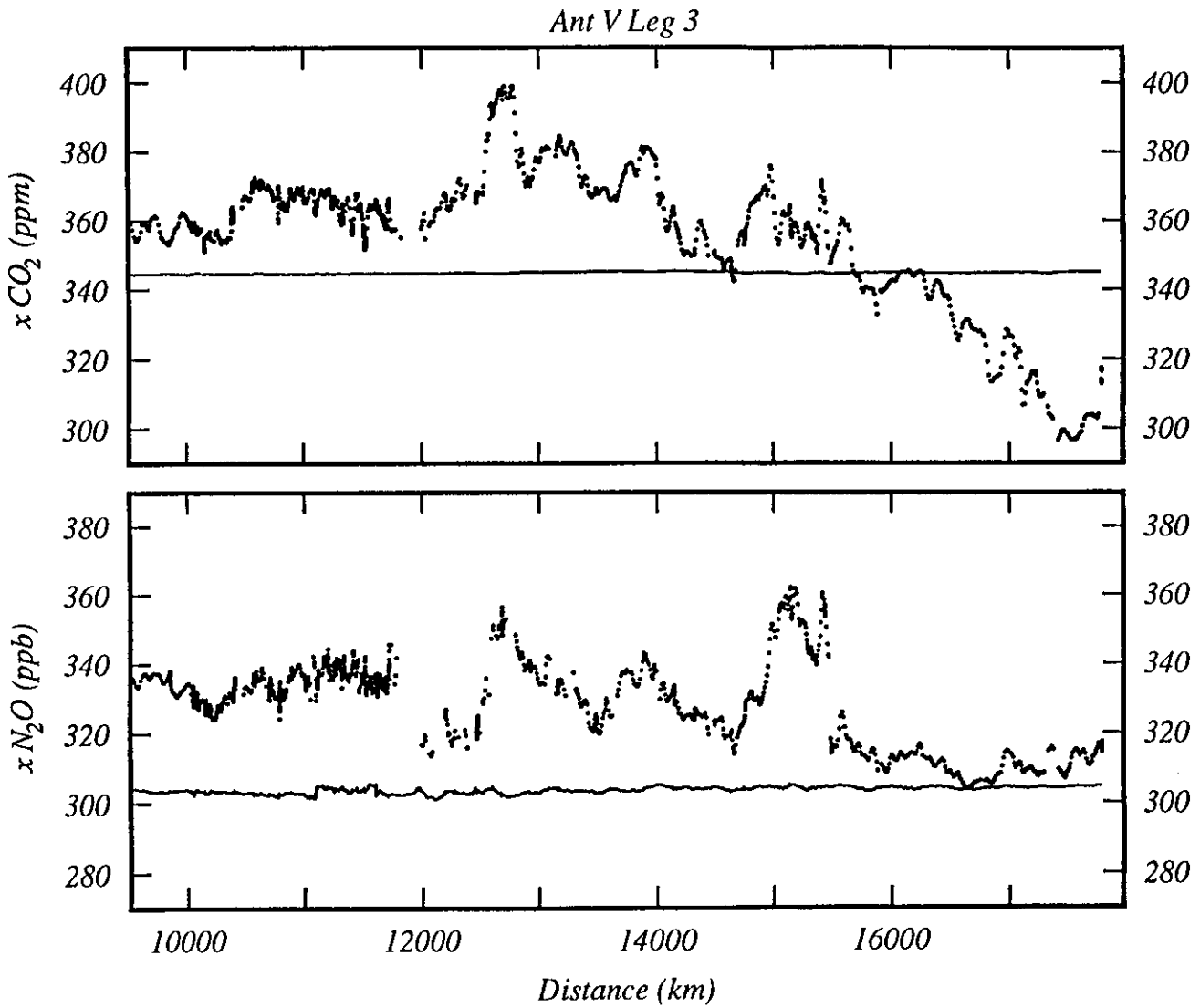

Figure 65. Continued

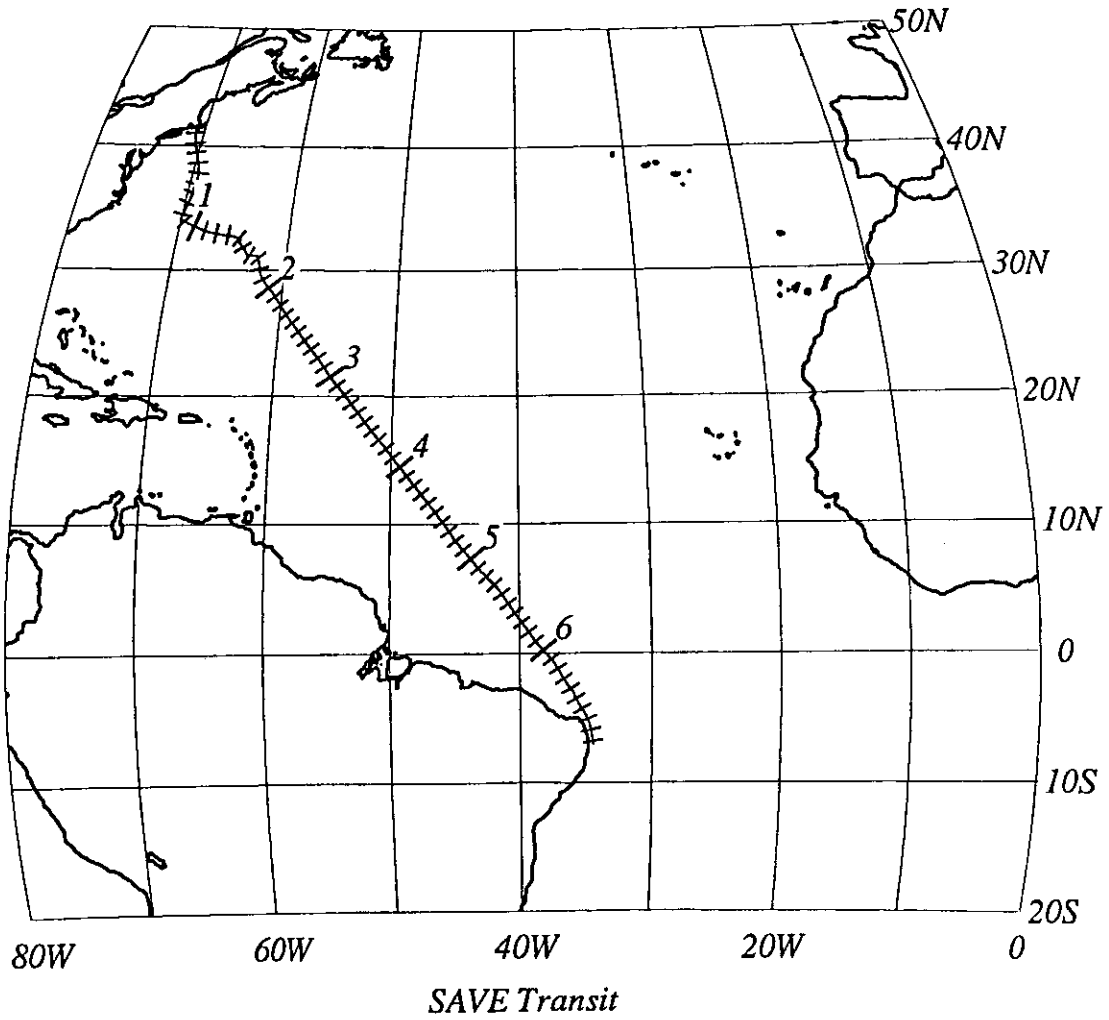

Figure 66. Cruise track plot, SAVE Transit. Track indicates cumulative distance in 1000 km intervals, with subdivisions of 100 km.

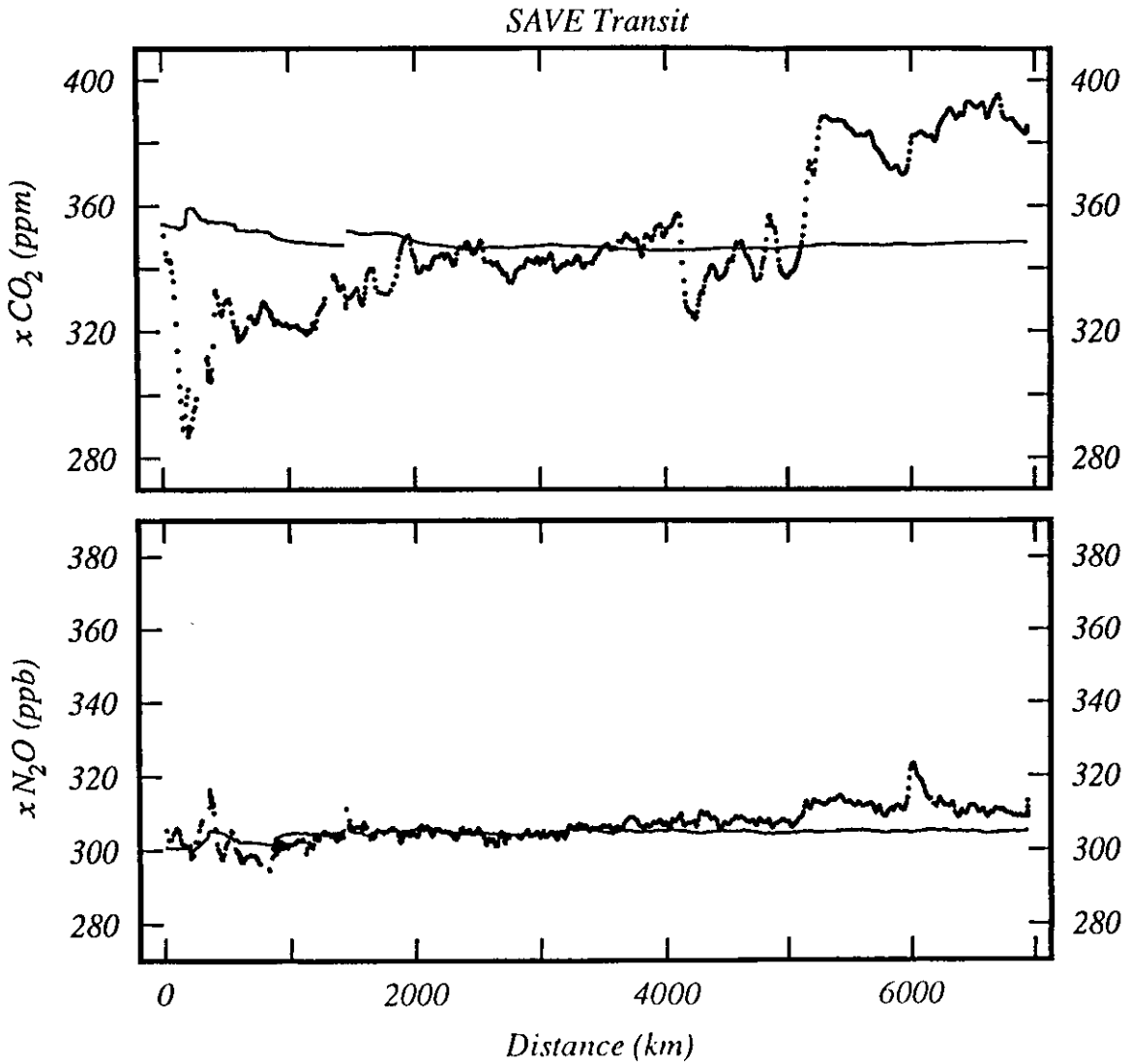

Figure 67. Data plot of xCO_2 and xN_2O (dry gas mole fractions), SAVE Transit. Atmospheric measurements are plotted as a line (20 point running mean). Measurements of gas equilibrated with seawater are plotted as individual points after smoothing with a 5-point Gaussian smoother.

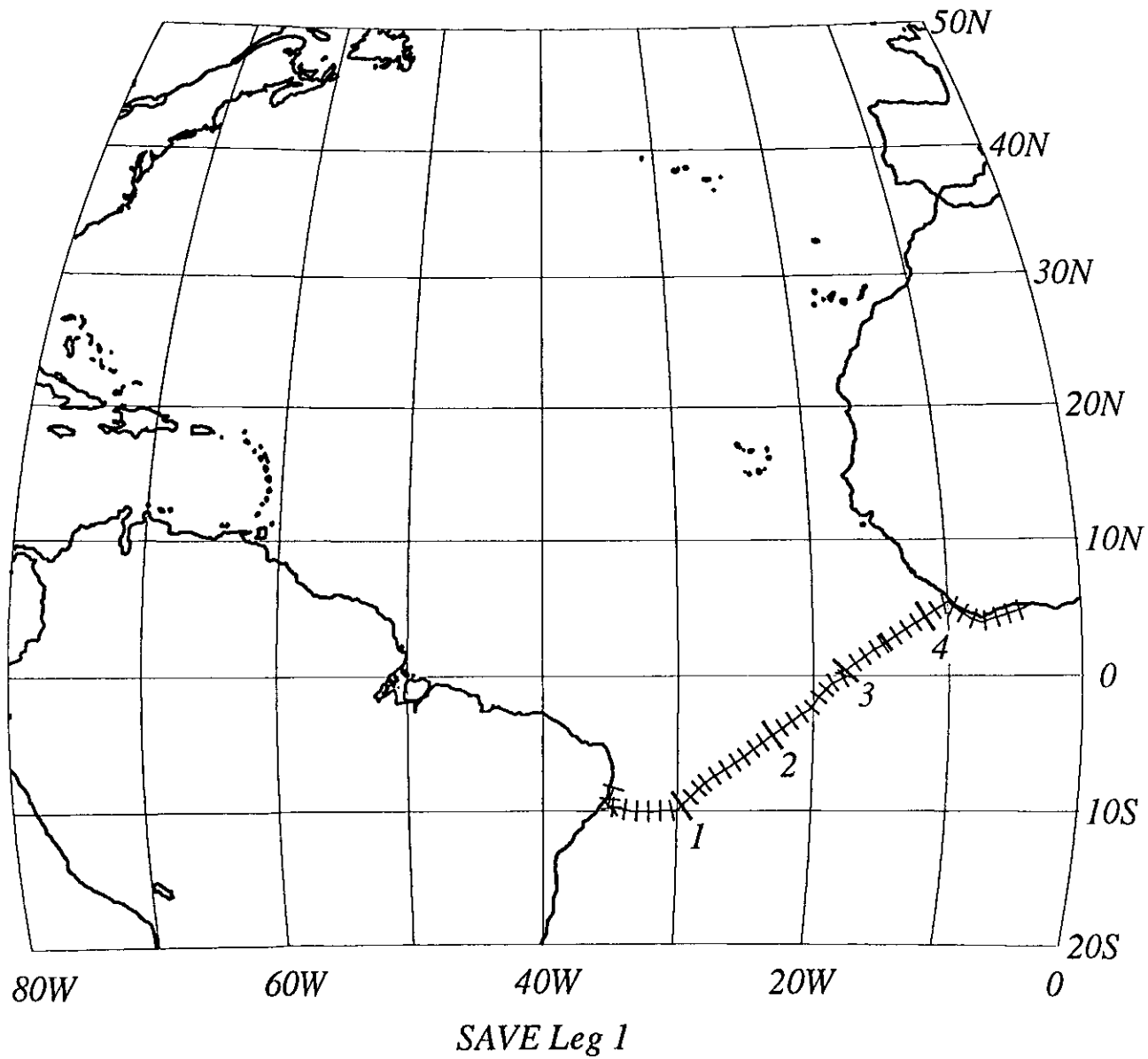

Figure 68. Cruise track plot, SAVE Leg 1. Track indicates cumulative distance in 1000 km intervals, with subdivisions of 100 km.

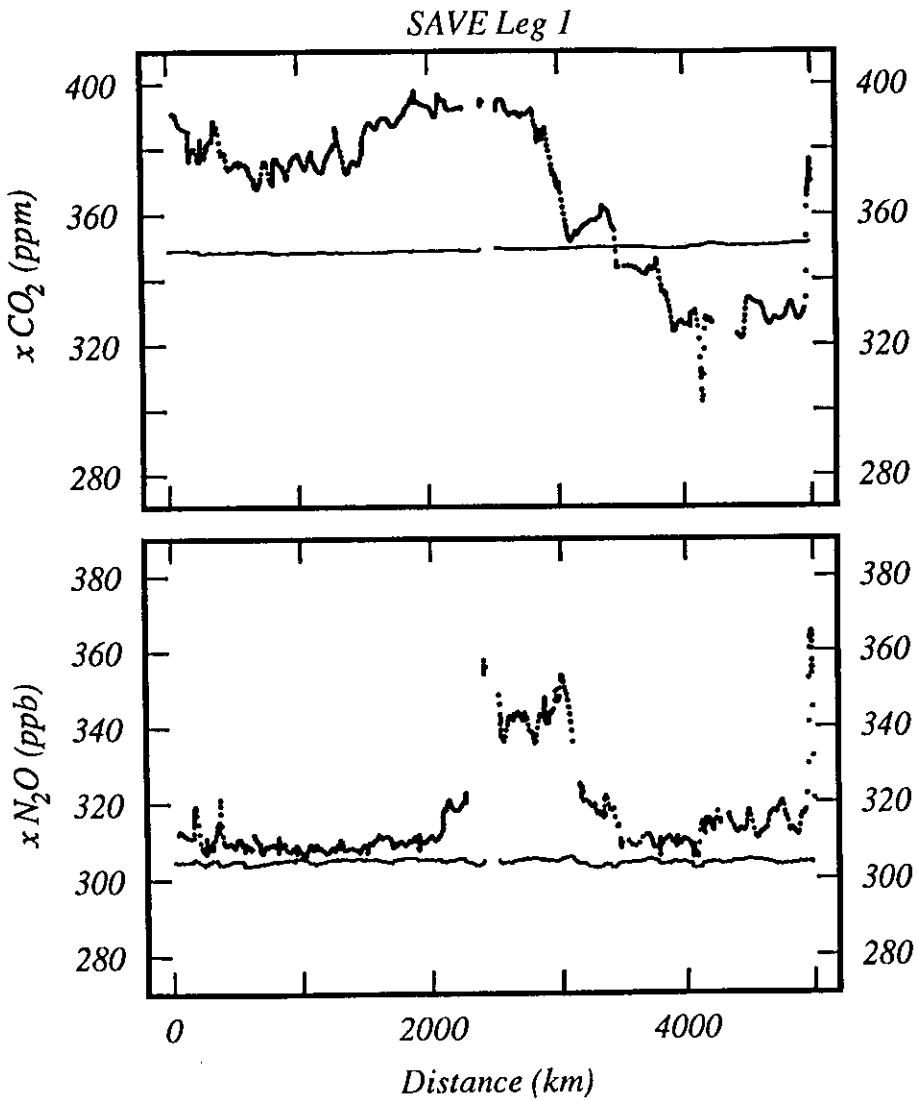

Figure 69. Data plot of xCO_2 and xN_2O (dry gas mole fractions), SAVE Leg 1. Atmospheric measurements are plotted as a line (20 point running mean). Measurements of gas equilibrated with seawater are plotted as individual points after smoothing with a 5-point Gaussian smoother.

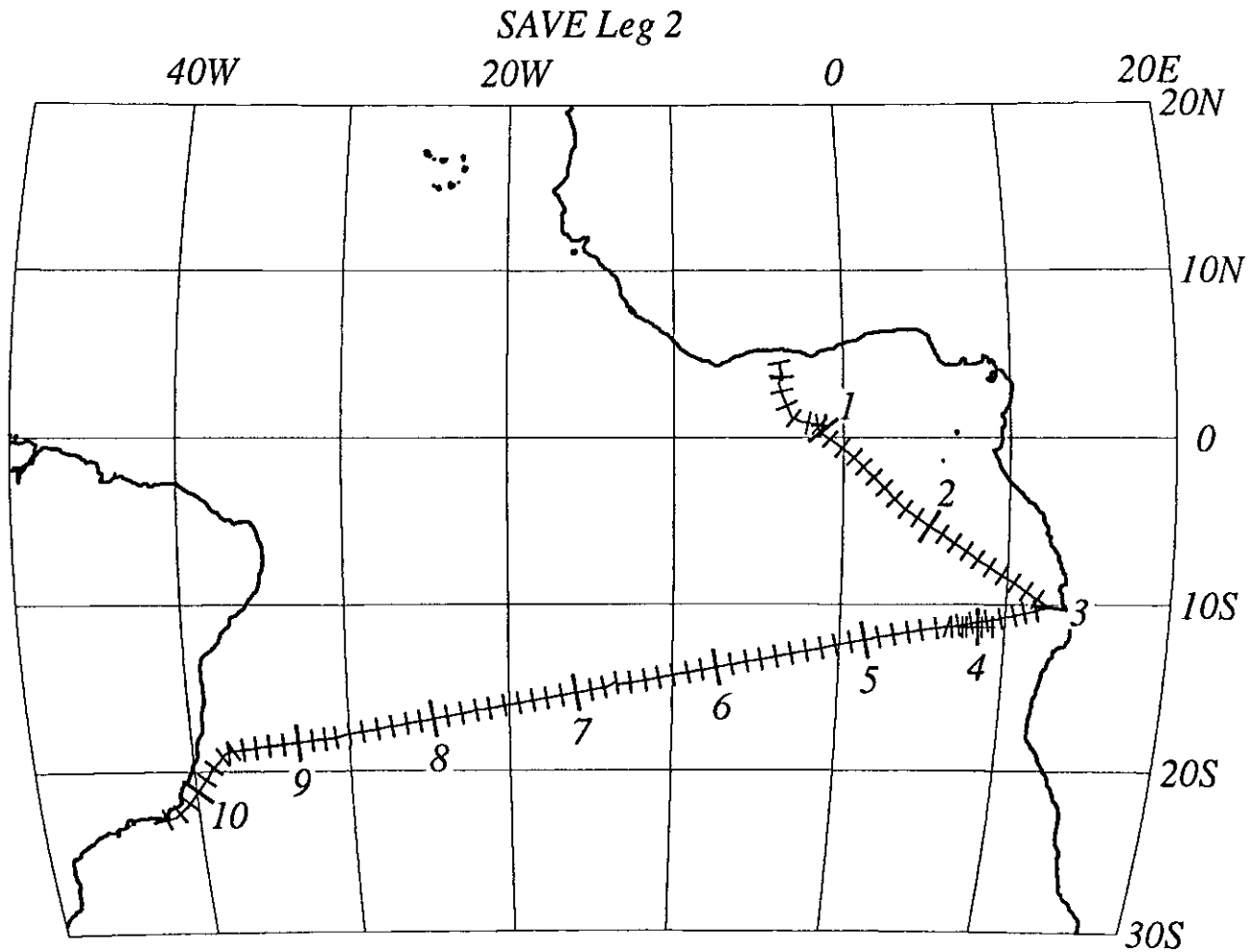

Figure 70. Cruise track plot, SAVE Leg 2. Track indicates cumulative distance in 1000 km intervals, with subdivisions of 100 km.

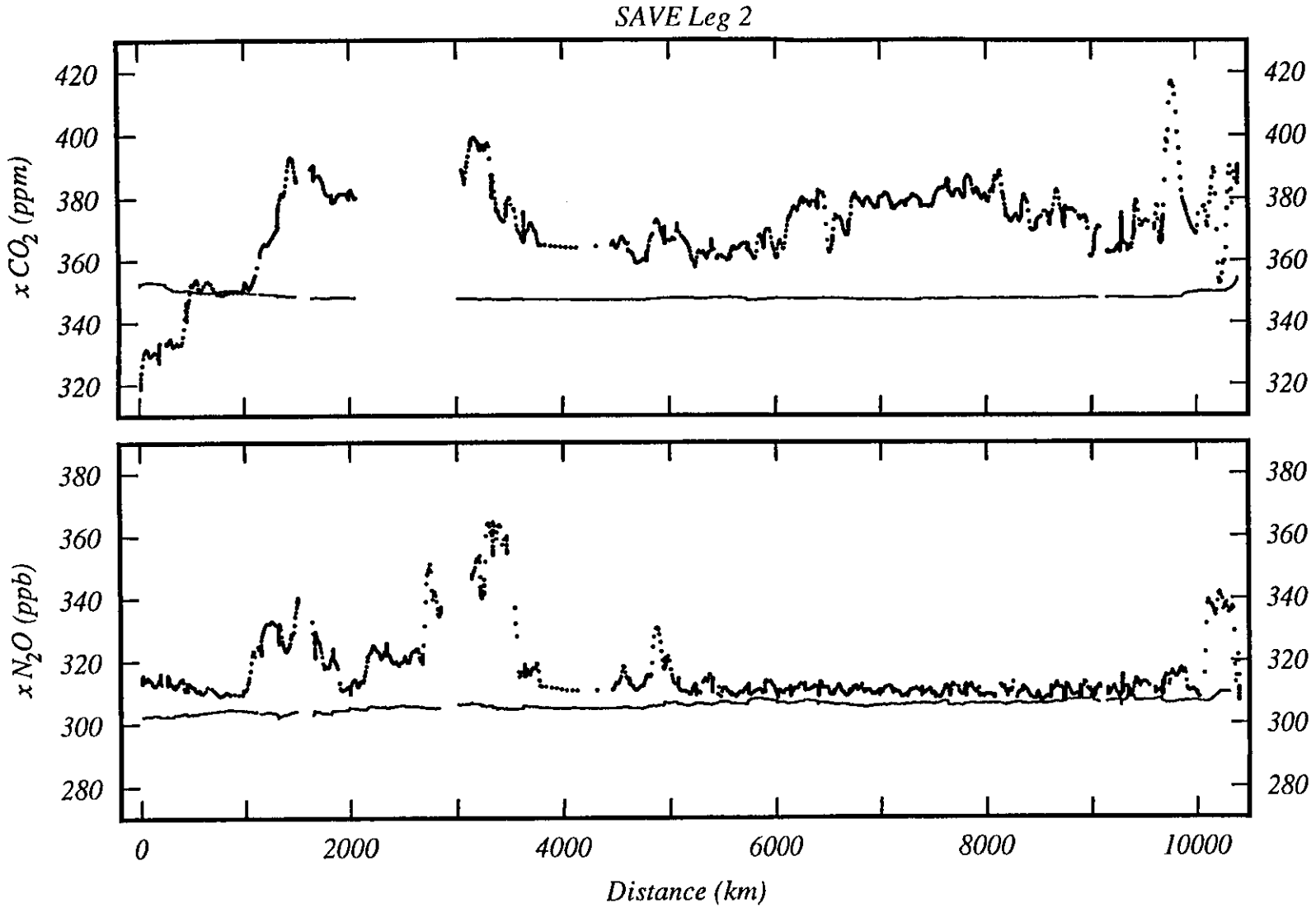

Figure 71. Data plot of xCO_2 and xN_2O (dry gas mole fractions), SAVE Leg 2. Atmospheric measurements are plotted as a line (20 point running mean). Measurements of gas equilibrated with seawater are plotted as individual points after smoothing with a 5-point Gaussian smoother.

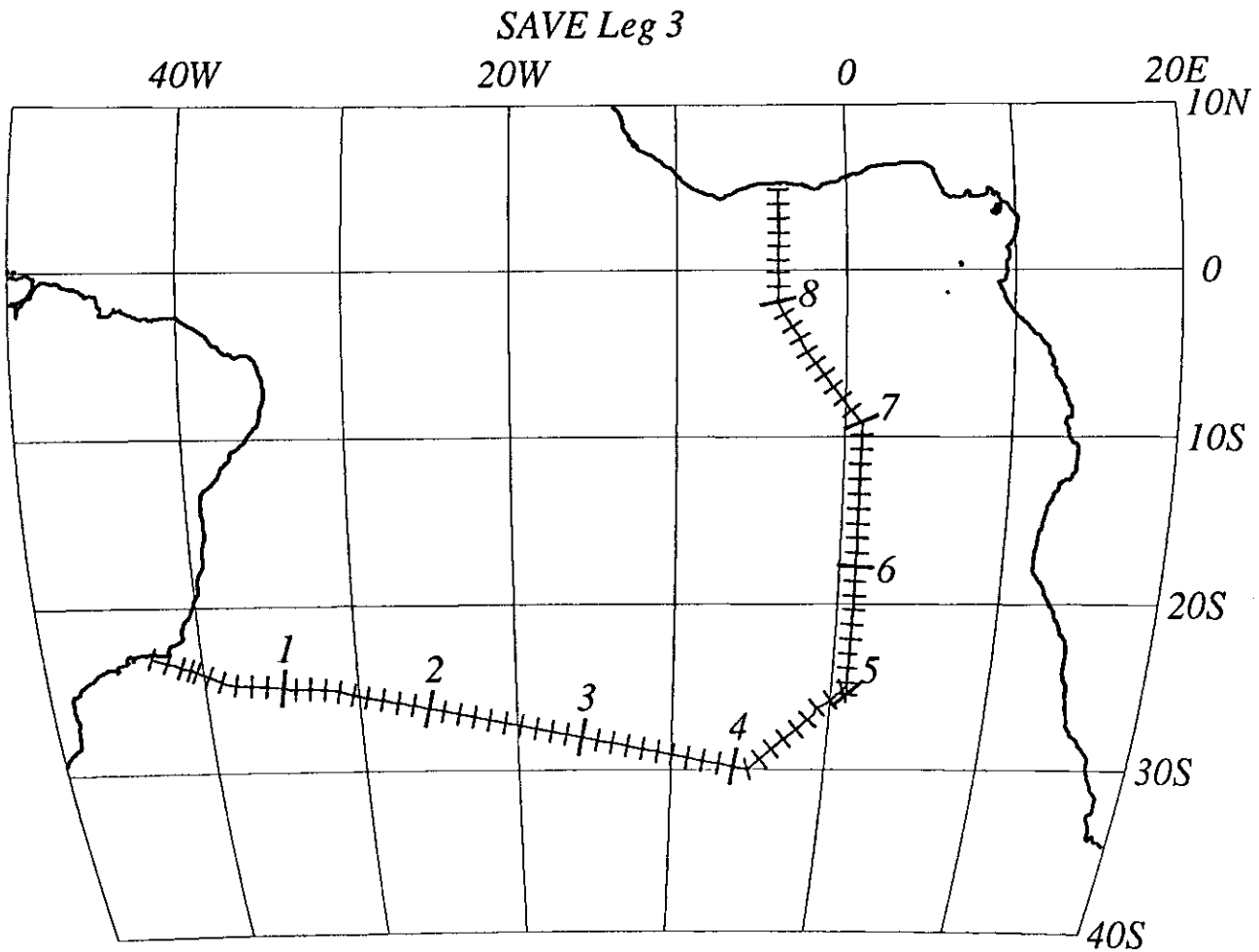

Figure 72. Cruise track plot, SAVE Leg 3. Track indicates cumulative distance in 1000 km intervals, with subdivisions of 100 km.

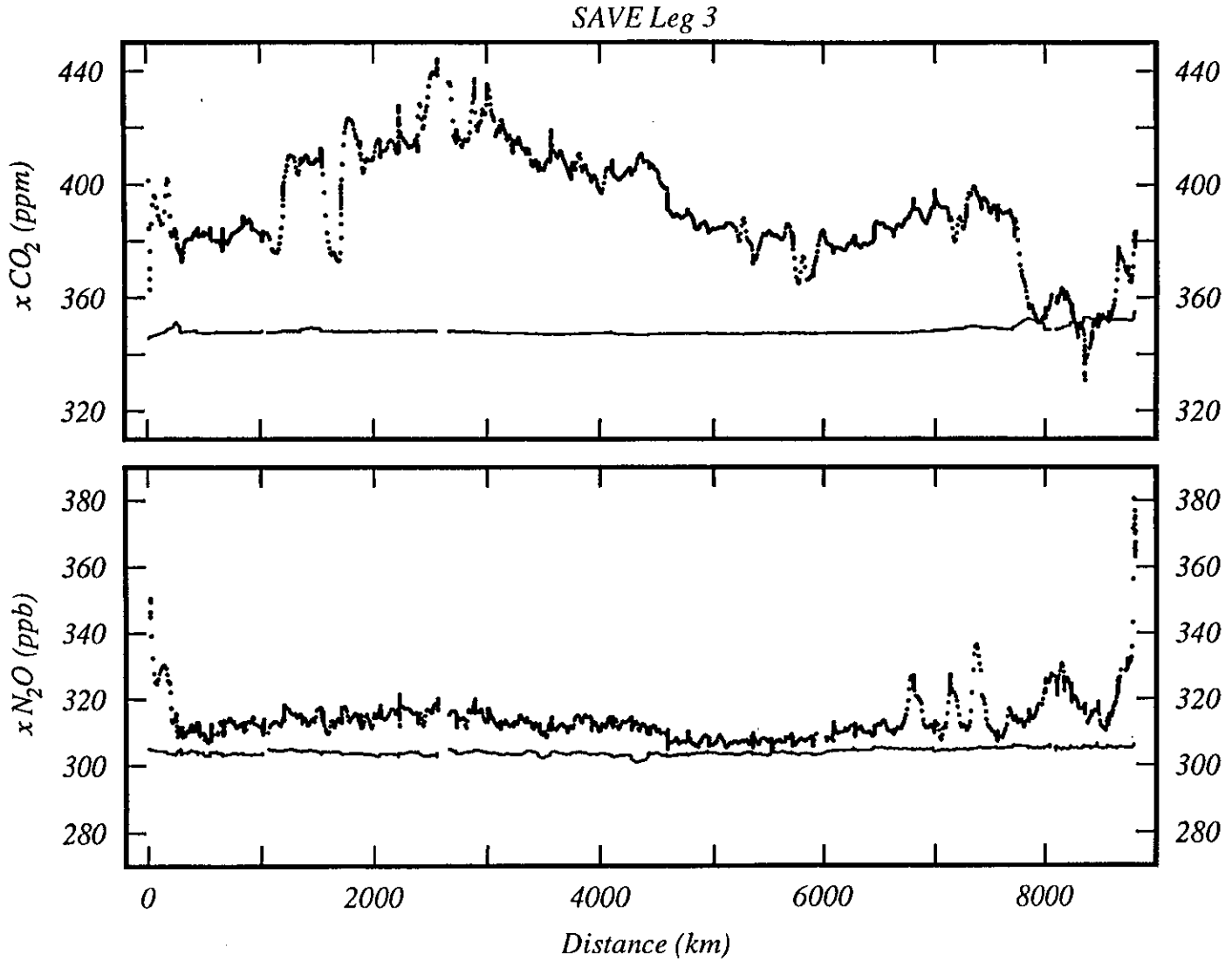

Figure 73. Data plot of xCO_2 and xN_2O (dry gas mole fractions), SAVE Leg 3. Atmospheric measurements are plotted as a line (20 point running mean). Measurements of gas equilibrated with seawater are plotted as individual points after smoothing with a 5-point Gaussian smoother.

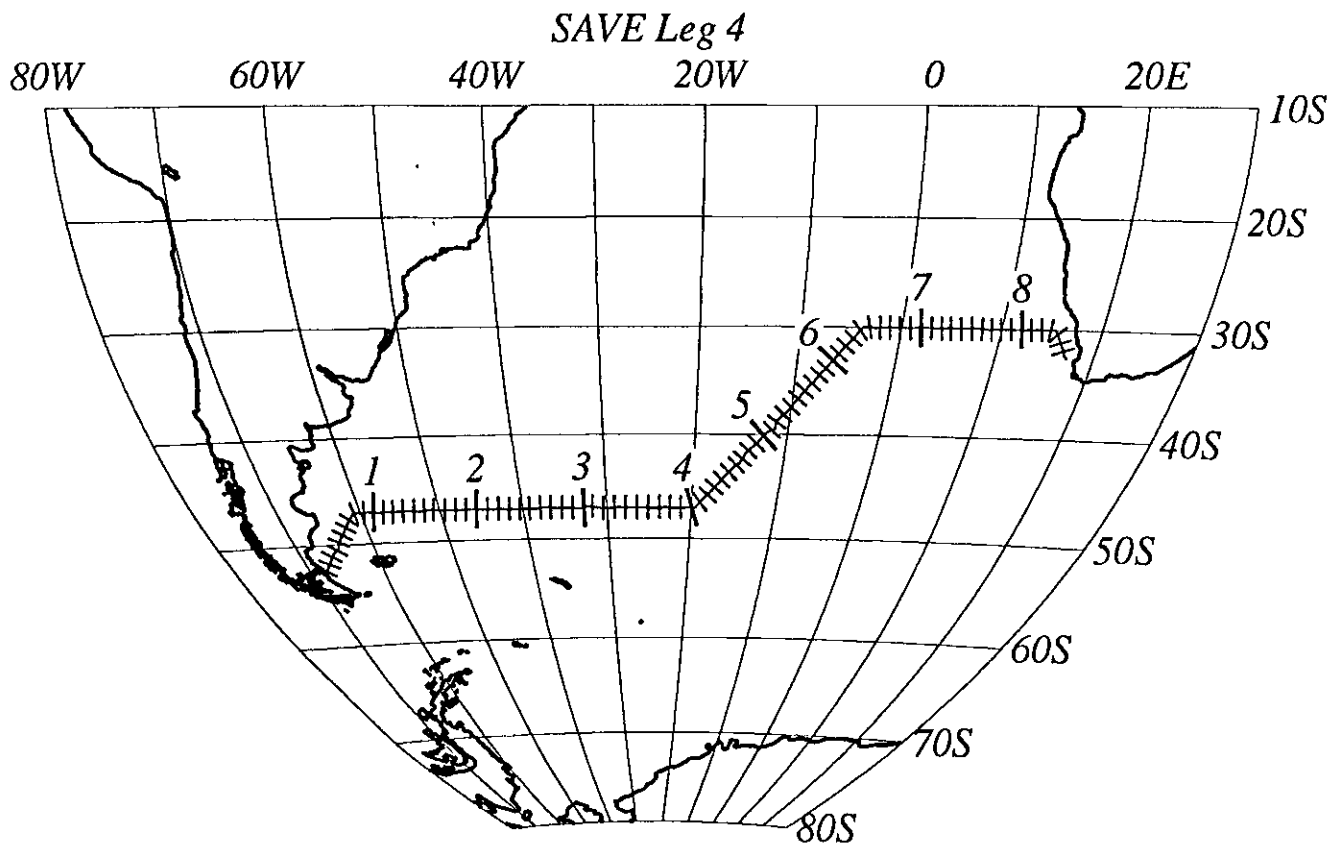

Figure 74. Cruise track plot, SAVE Leg 4. Track indicates cumulative distance in 1000 km intervals, with subdivisions of 100 km.

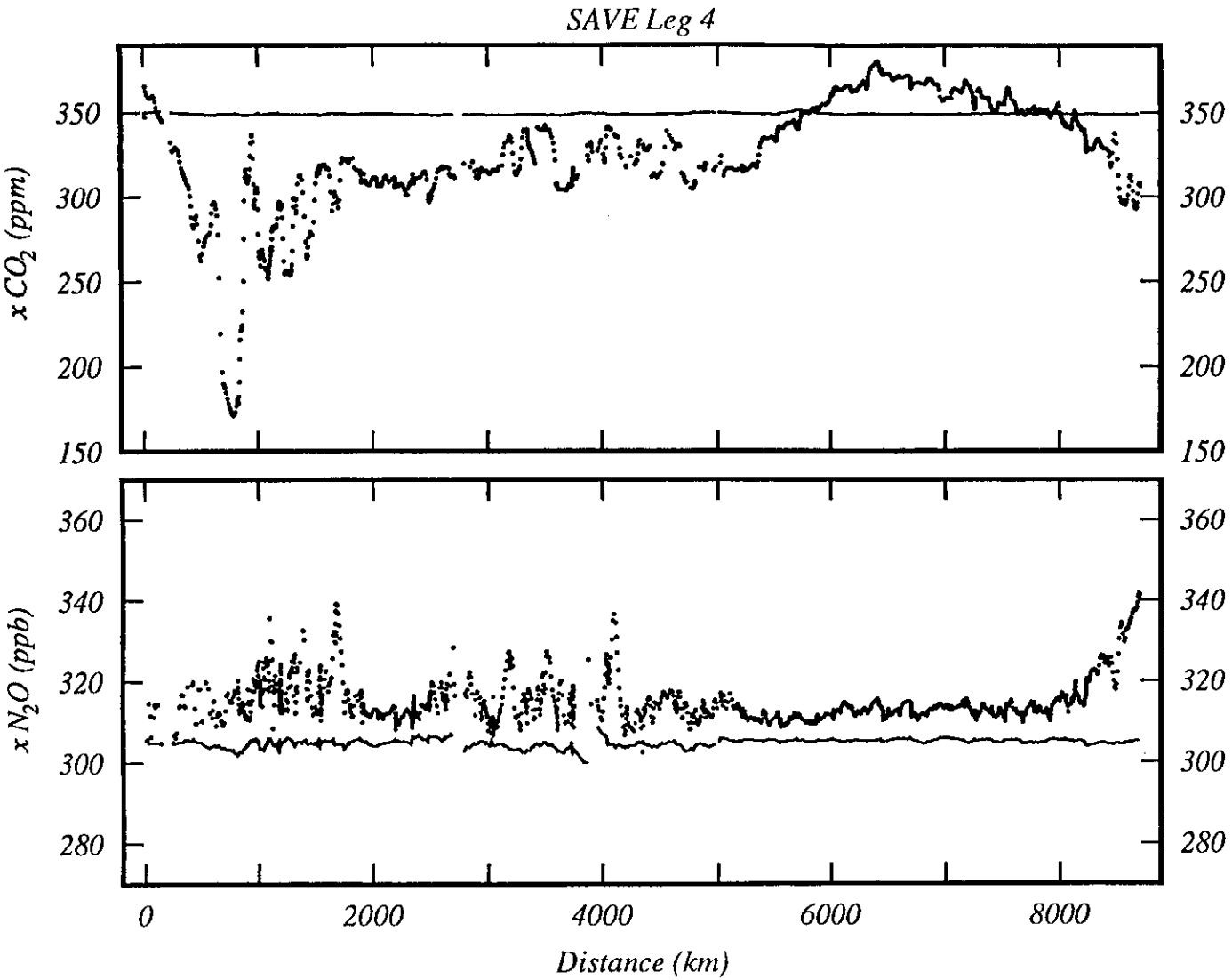

Figure 75. Data plot of xCO_2 and xN_2O (dry gas mole fractions), SAVE Leg 4. Atmospheric measurements are plotted as a line (20 point running mean). Measurements of gas equilibrated with seawater are plotted as individual points after smoothing with a 5-point Gaussian smoother.

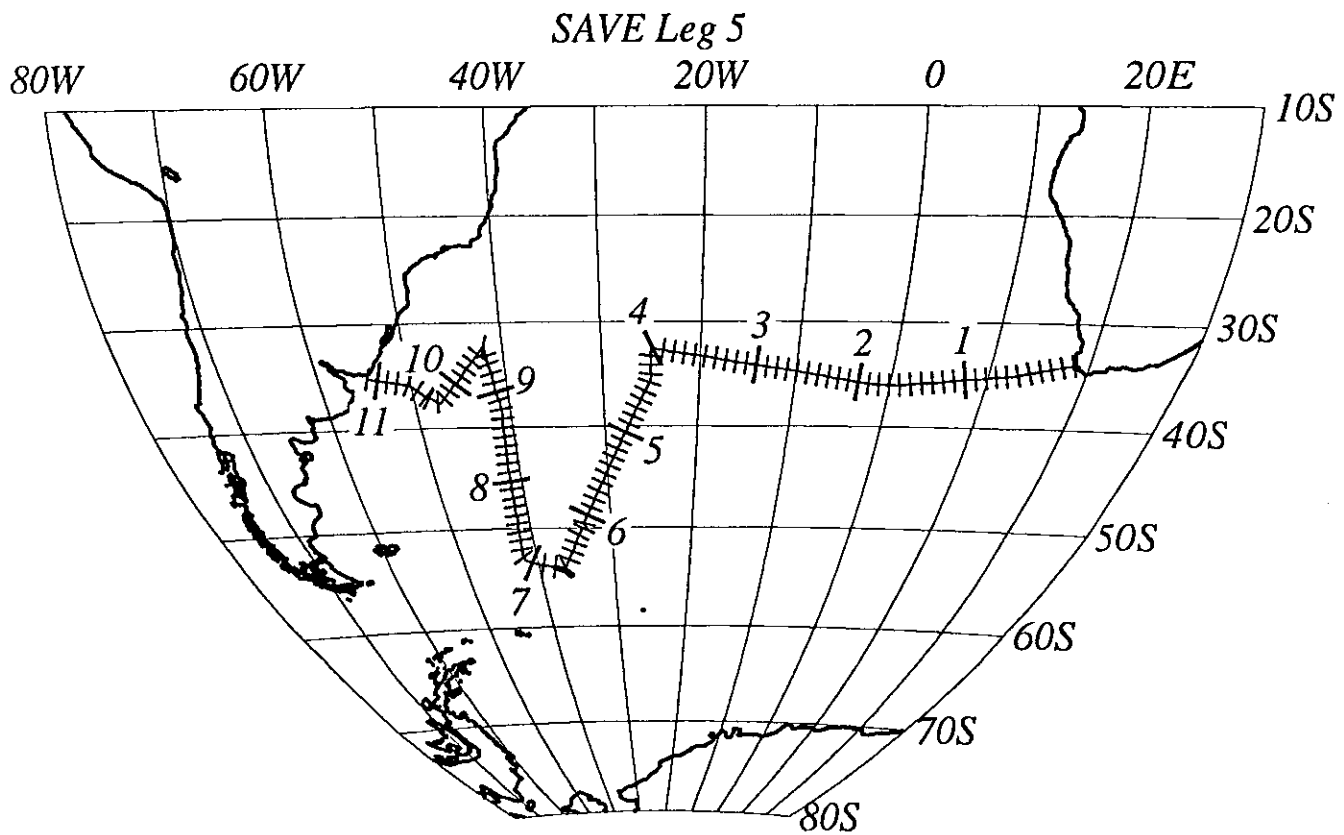

Figure 76. Cruise track plot, SAVE Leg 5. Track indicates cumulative distance in 1000 km intervals, with subdivisions of 100 km.

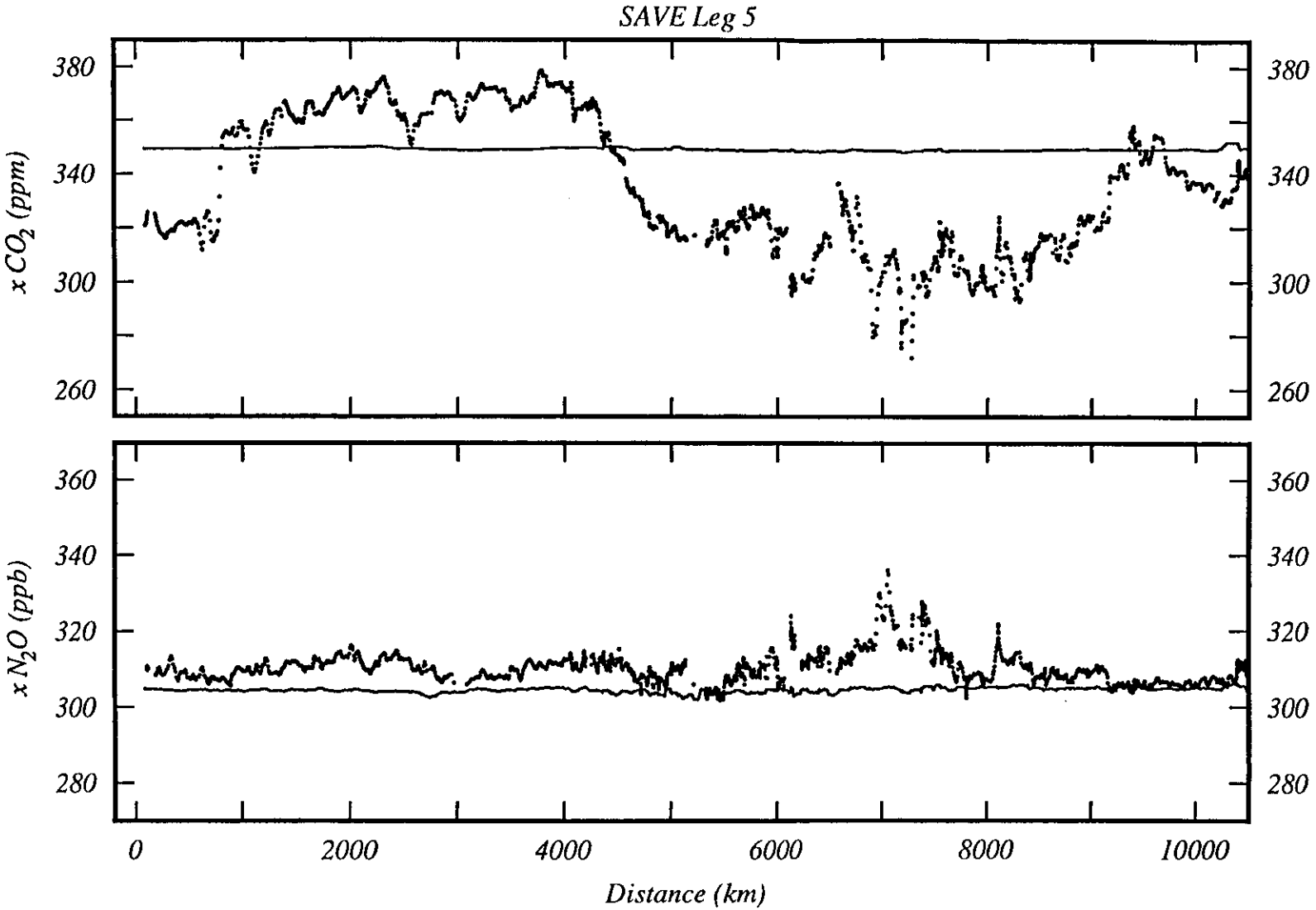

Figure 77. Data plot of xCO_2 and xN_2O (dry gas mole fractions), SAVE Leg 5. Atmospheric measurements are plotted as a line (20 point running mean). Measurements of gas equilibrated with seawater are plotted as individual points after smoothing with a 5-point Gaussian smoother.

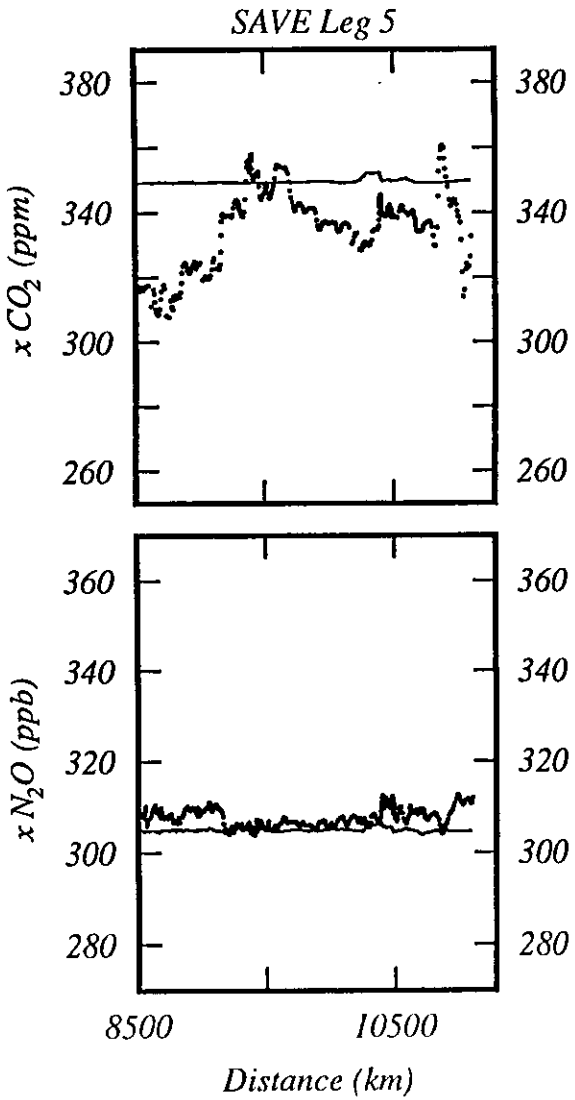

Figure 77. Continued

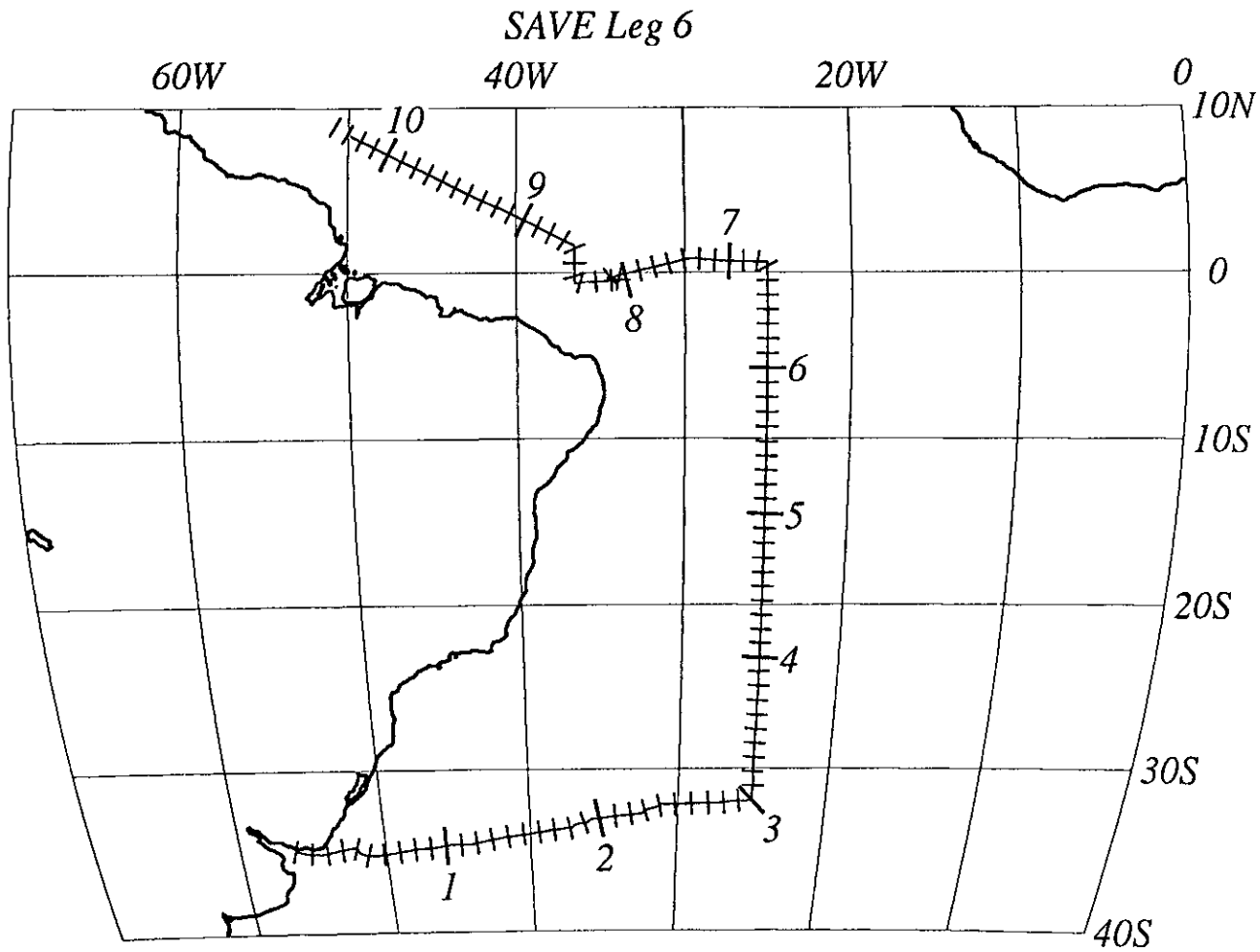

Figure 78. Cruise track plot, SAVE Leg 6. Track indicates cumulative distance in 1000 km intervals, with subdivisions of 100 km.

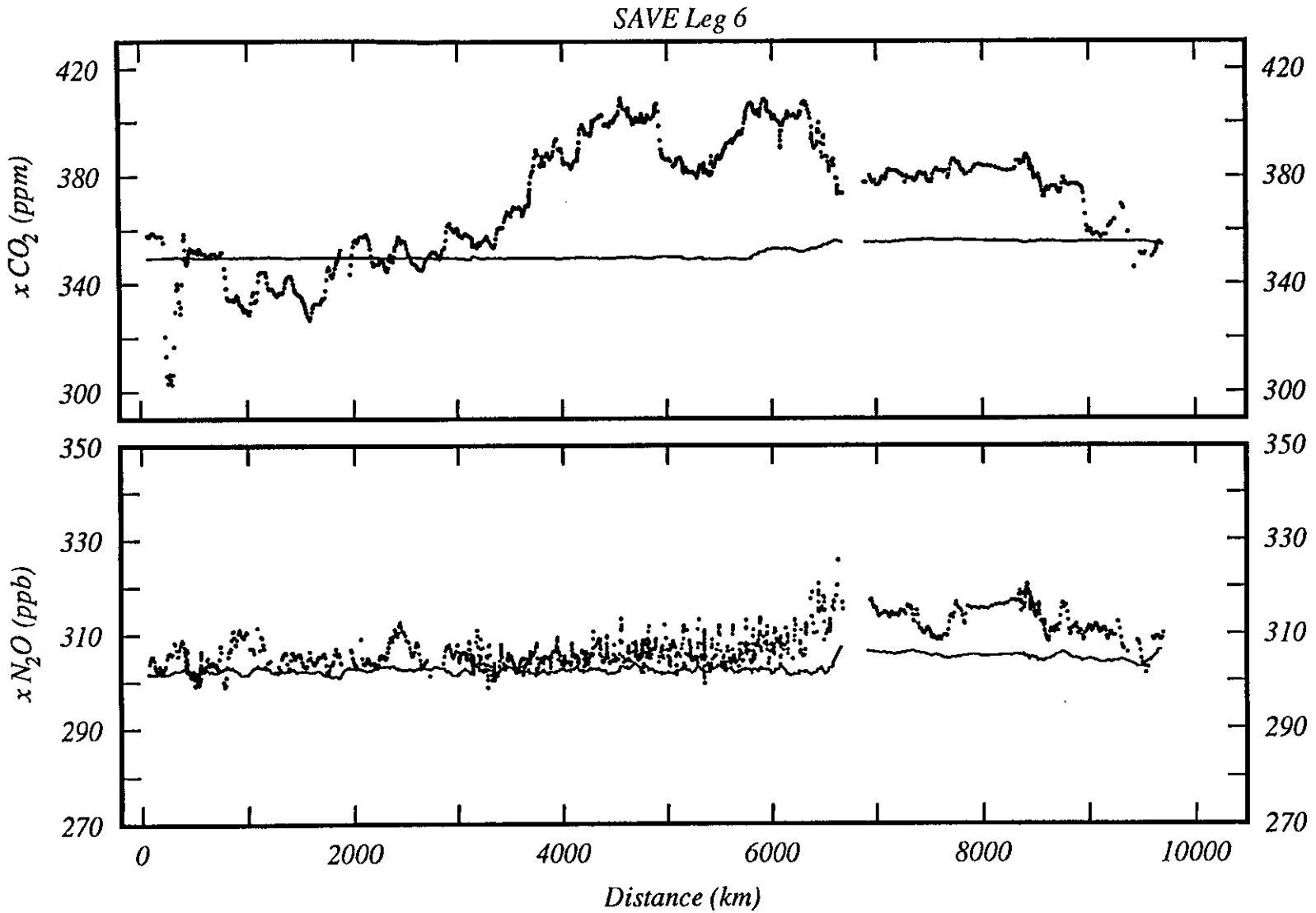

Figure 79. Data plot of xCO_2 and xN_2O (dry gas mole fractions), SAVE Leg 6. Atmospheric measurements are plotted as a line (20 point running mean). Measurements of gas equilibrated with seawater are plotted as individual points after smoothing with a 5-point Gaussian smoother.

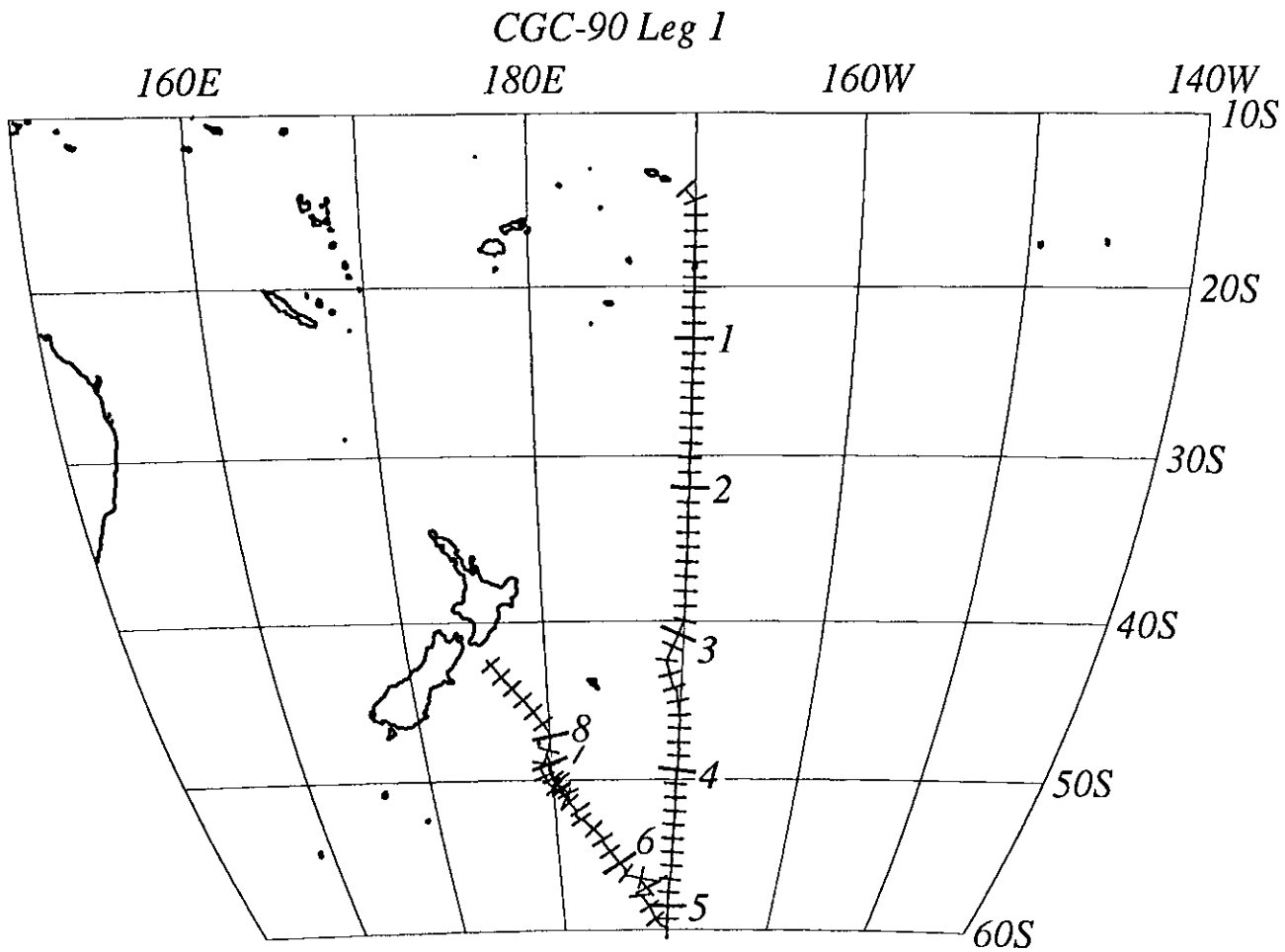

Figure 80. Cruise track plot, CGC-90 Leg 1. Track indicates cumulative distance in 1000 km intervals, with subdivisions of 100 km.

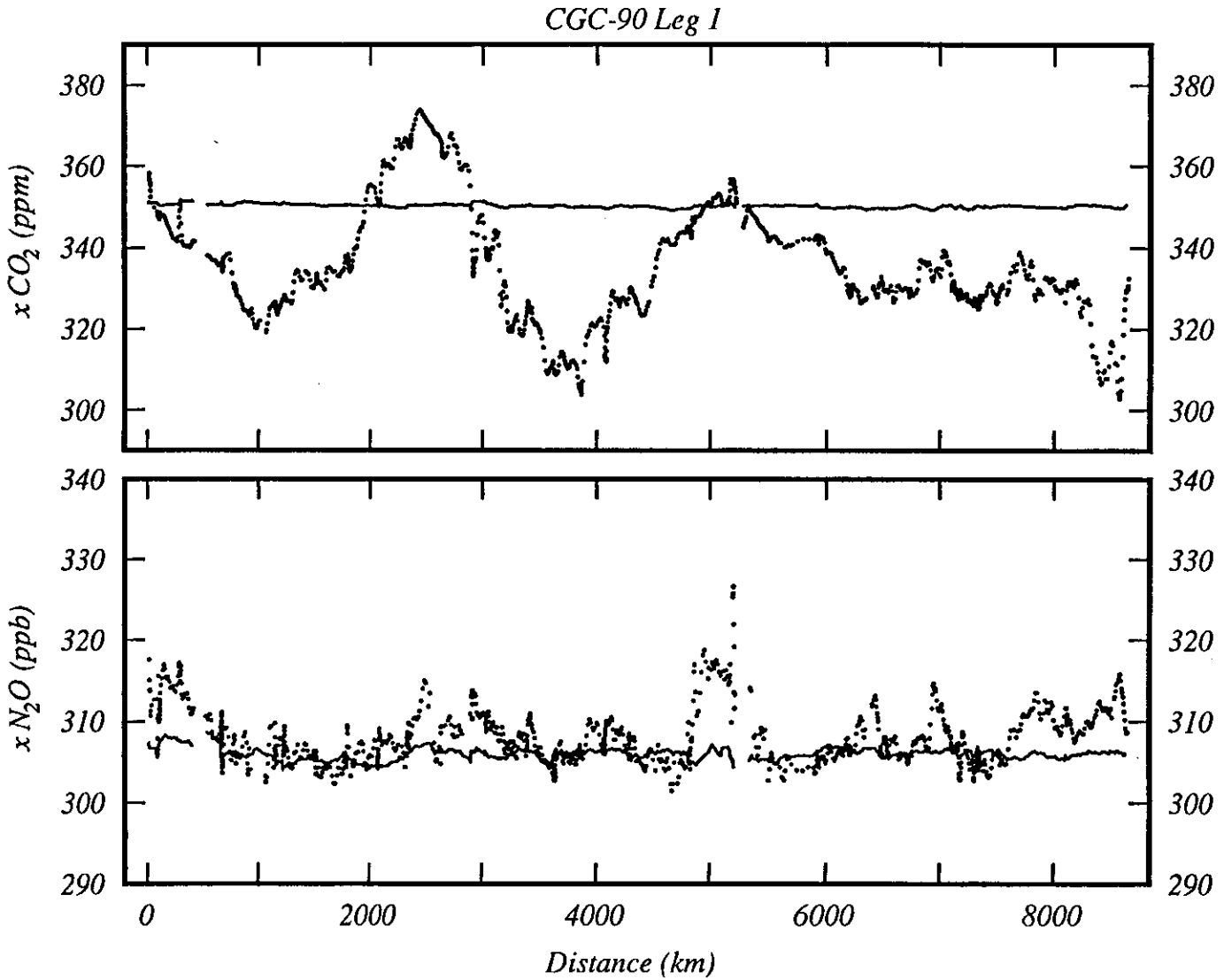

Figure 81. Data plot of xCO_2 and xN_2O (dry gas mole fractions), CGC-90 Leg 1. Atmospheric measurements are plotted as a line (20 point running mean). Measurements of gas equilibrated with seawater are plotted as individual points after smoothing with a 5-point Gaussian smoother.

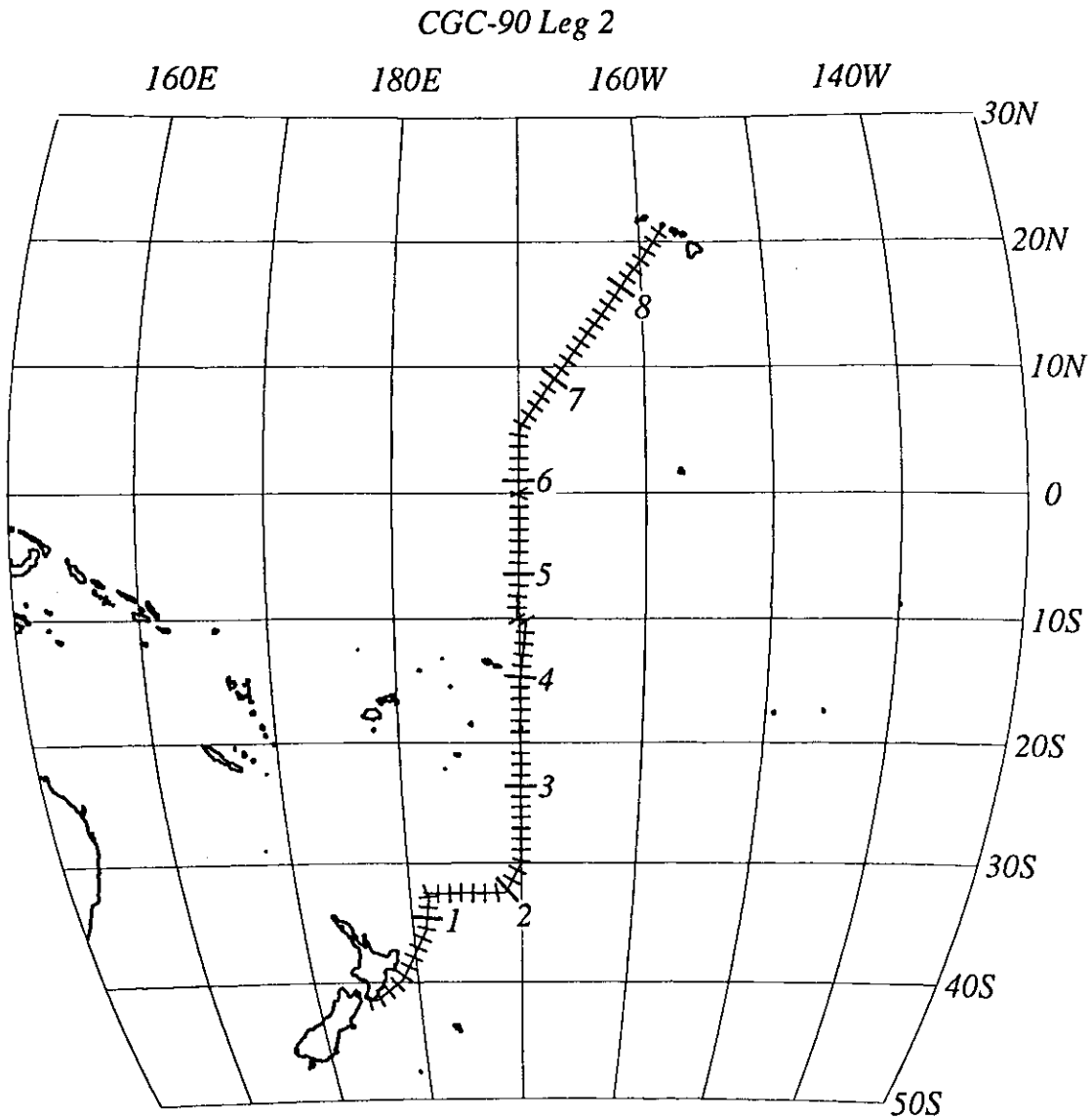

Figure 82. Cruise track plot, CGC-90 Leg 2. Track indicates cumulative distance in 1000 km intervals, with subdivisions of 100 km.

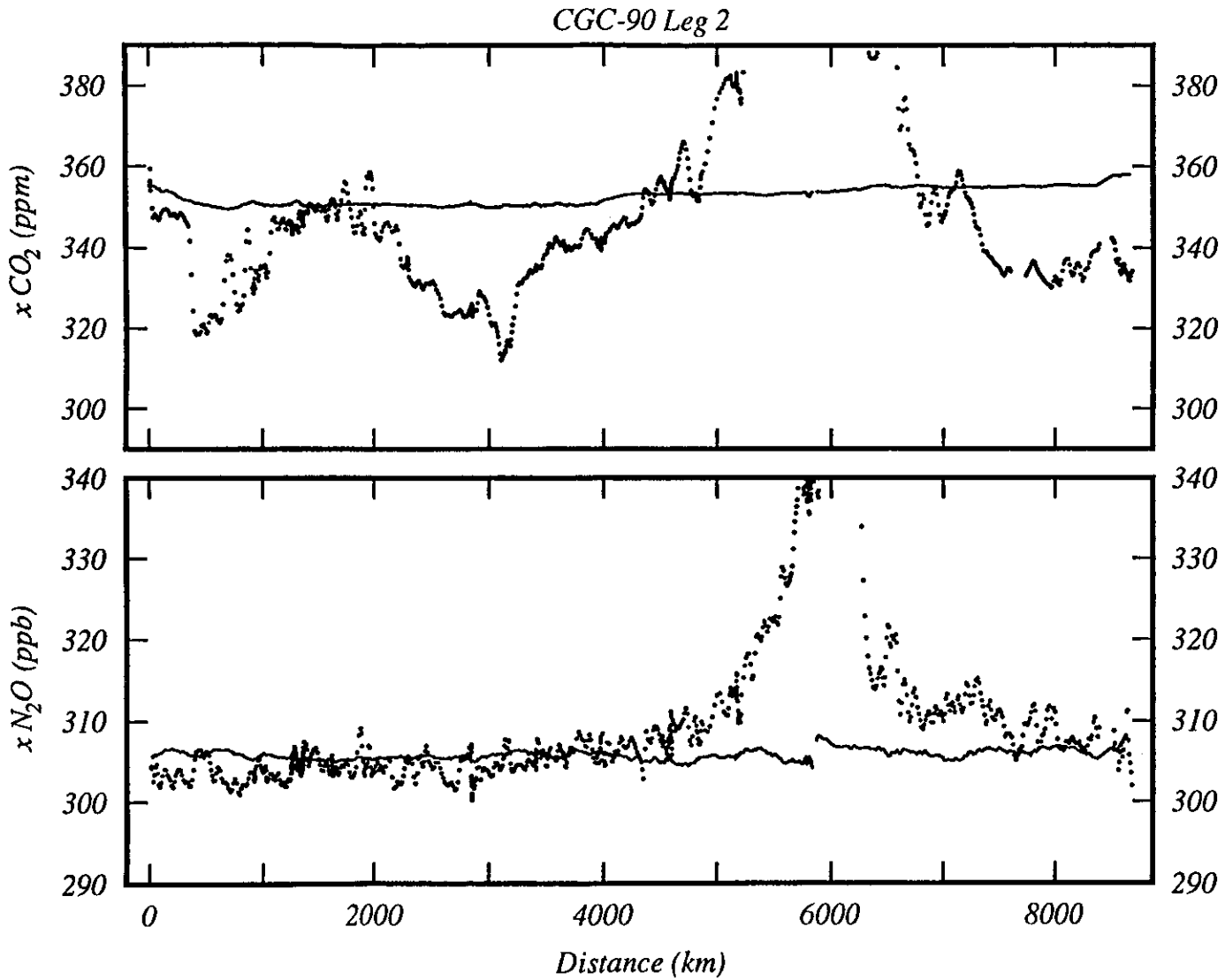

Figure 83. Data plot of xCO_2 and xN_2O (dry gas mole fractions), CGC-90 Leg 2. Atmospheric measurements are plotted as a line (20 point running mean). Measurements of gas equilibrated with seawater are plotted as individual points after smoothing with a 5-point Gaussian smoother.

5. METHODOLOGY

This document describes the results of surface water and atmospheric CO_2 and N_2O measurements carried out by shipboard gas chromatography over the period 1977–1990. The measurements were made by an automated high-precision shipboard gas chromatographic system developed during the late 1970s and used extensively over the intervening years. This instrument, which is described by Weiss (1981), measures CO_2 by flame ionization after quantitative reaction to methane in a stream of hydrogen using a reduced nickel catalyst preceded by a palladium catalyst to protect the nickel from oxygen and other atmospheric oxidants. Nitrous oxide is measured by a separate electron capture detector. (Methane is also measured by the flame ionization detector, although the system is not optimized for this gas. The methane results are not included in this data set because methane's equilibration time constant is long, and the results are therefore subject to contamination by biological activity in the ship's seawater pumping system.)

The chromatographic system measures 196 dry-gas samples a day, divided equally among the atmosphere, gas equilibrated with surface water, a low-range gas standard, and a high-range gas standard. Thus, the atmosphere and the ocean are each measured every half-hour, or 48 times a day. This corresponds to a spatial resolution of about 10 km when the ship is under way and gives several replicate measurements at each hydrographic station. The typical relative standard deviation of a single determination is about 0.04% for CO_2 and 0.3% for N_2O, but precision is occasionally affected adversely by shipboard operating conditions. The measurements are calibrated with dry-air secondary standards stored in Spectra-Seal aluminum cylinders. These standards are periodically calibrated for CO_2 against the Scripps Institution of Oceanography (SIO) manometric scale in the laboratory of C. D. Keeling and for N_2O against the calibration scale developed by Weiss *et al.* (1981). In addition to its accuracy, the chromatographic method for CO_2 offers the benefits over other commonly used techniques of being independent of oxygen concentration and using small amounts of sample and standard.

Surface seawater is pumped continuously from the bow of the ship (nominal depth approximately 3 m) at a rate of about 100 liters/min. This high pumping rate and the use of plastic polyvinylchloride (PVC) piping assure a minimal change in temperature and a minimal opportunity for chemical alteration of the water. The equilibrator is constructed of heavy acrylic plastic (for visibility and temperature insulation) and has an internal gas volume of about 20 liters. The equilibrator design consists of 2 concentric cylindrical stages, with a drain at the center to minimize volume changes as a result of ship motion. The water "rains" through the 2 stages of the equilibrator at a combined rate of about 20 liters/min, and a low 0.2-atm pressure head minimizes spraying, bubble entrapment, and other dynamic pressure effects. The 20-liter gas space is circulated by an air pump through a closed loop which provides the pressurized gas required by the chromatograph. Each half-hourly analysis removes about 75 ml of gas from this pumped loop. The first stage of the equilibrator is vented to the outside atmosphere so that the gas used for the analysis is replaced by clean marine air.

The temperature of the equilibrator is monitored and compared with the surface ocean temperatures measured at hydrographic stations to determine the thermal effect of the ship's pumping system as a function of intake temperature. The maximum amount of change, found for the coldest surface waters, is typically a warming of $<1°C$. As expected, this temperature difference decreases to zero when the water temperature reaches the mean inside temperature of the ship. The measured CO_2 values are corrected for this thermal effect (roughly 4% per degree) using an empirical equation (Weiss *et al.* 1982) which is dominated

by the temperature dependence of the CO_2 solubility coefficient (Weiss 1974). The measured N_2O values are also corrected for the solubility effect (Weiss and Price 1980).

The response time of the equilibrator has been evaluated theoretically and experimentally. For unbuffered gases such as nitrous oxide, oxygen and nitrogen, the theoretical response time (assuming complete exchange between water and gas) is given as FS/V, where F is the flux of water through the system, V is the volume of the equilibrated gas phase, and S is the Ostwald solubility coefficient. For the equilibrator used in the measurements presented here, this gives a characteristic ($1/e$) response time of about 1 min for N_2O, about 0.5 hr for oxygen and about 1 hr for nitrogen. For CO_2 the response time would be similar to N_2O if there were no chemical buffering, but with chemical buffering (see gas exchange discussion in Broecker and Peng 1982) the response time is enhanced by an order of magnitude to about 0.1 min. Laboratory experiments by Weiss *et al.* (1982) and by scientists at the National Oceanic and Atmospheric Administration (NOAA), Pacific Marine Environmental Laboratory (PMEL) and Climate Monitoring and Diagnostics Laboratory (CMDL), who have adopted this equilibrator design, have confirmed that the actual equilibration times are close to these theoretical values.

These differences in exchange times are important in understanding the performance of an equilibrator that is vented to atmospheric pressure. Since the major components of equilibrated gas — nitrogen, oxygen, and argon — have equilibration times that are much longer than those of the measured species, N_2O and CO_2, the effect will be for the equilibrium partial pressures of these latter two gases to be present in a water-saturated gas phase at a total pressure equal to the barometric pressure. This is exactly the condition that is satisfied by the actual atmosphere when it is in equilibrium with the ocean, since the gas-phase boundary layer is always saturated with water vapor and at the total barometric pressure. Since the chromatographic system measures the dry-gas mole fractions of these constituents, xCO_2 and xN_2O, in both the atmosphere and the equilibrated gas, and the total pressure is the same in both cases, the differences in xCO_2 between these phases are a close measure of the differences in CO_2 partial pressure (pCO_2), as long as the total pressure is near 1 atm:

$$\text{delta}(pCO_2) = \text{delta}(xCO_2)(P - pH_2O),$$

where delta signifies the difference between sea and air, P is the barometric pressure, and pH_2O is the water vapor pressure. Because the temperature and the barometric pressure are routinely recorded, the system is effectively completely constrained, but even without these variables delta(xCO_2) is a very good approximation of delta(pCO_2). The argument is, of course, the same for the partial pressure of N_2O.

Another question which is more difficult to answer is whether the equilibrium reached by the equilibrator is the true thermodynamic equilibrium that we wish to measure. This type of question is always very difficult to answer, but there is indirect evidence that it is very close. The discrete equilibrator pCO_2 measurements carried out by T. Takahashi's group at Lamont-Doherty Geological Observatory during the SAVE expeditions have shown agreement with the equilibrator values presented here to within 1 or 2 ppm (T. Takahashi, personal communication), even though their measurements are made at a fixed temperature and must be corrected to the surface water temperature. Also, the measurements of pN_2O in the central gyres of the major oceans presented here are generally within 1% of atmospheric saturation. If this were not the correct equilibrium value, one could not explain the constancy of these values over many thousands of kilometers in many different central gyres. Through continued use of the same equilibrator design during the World Ocean

Circulation Experiment (WOCE), it is hoped to obtain further verification that the measurements are being made at true equilibrium through comparisons with the discrete pCO_2 and carbon system measurements being carried out by other laboratories.

Concentrations of CO_2 and N_2O are calculated by fitting detector peak area response to a quadratic polynomial forced through the origin (zeroth order term is zero). The calculation is performed with the assumption that the linearity of the detector varies slowly compared with changes in detector sensitivity. Accordingly, the second order term of the quadratic polynomial (linearity of the detector) is determined from a running mean of the high standard to low standard response ratio over a range of plus and minus 20 runs, and the first order term (sensitivity of the detector) is determined from the immediately bracketing high and low standard runs. Further details concerning the methods of sample measurement and analysis are provided in Weiss (1981), a copy of which is provided in the appendix of this document.

The magnetic tape (or floppy diskettes) that accompanies this document includes a descriptive information file (File 1 on the magnetic tape or NDP044.DES on the floppy diskettes), a file (File 2 on the magnetic tape or TRACK.LST on the floppy diskettes) containing a list of the expedition legs on which measurements were made, and a file (File 3 on the magnetic tape or DATA.LST on the floppy diskettes) containing a list of the corresponding data filenames. The tape or diskettes also contain two data files for each expedition leg: one file containing the atmospheric results and one containing the surface seawater results for xCO_2 and xN_2O [in parts per million (ppm) and parts per billion (ppb), respectively].

6. APPLICATIONS OF THE DATA

The data in this package constitute one of the most extensive records available of xCO_2 and, particularly, xN_2O in marine air and surface seawater. These data will be useful in modeling applications dealing with the ocean's role in the global biogeochemical cycles of carbon and nitrogen. The combination of atmospheric and surface seawater sampling represented in these data should also make them useful in studies of ocean–atmosphere dynamics. In addition, since determinations of pCO_2 in the past were usually derived indirectly, these shipboard gas chromatographic analyses are especially valuable in that they represent direct measurements of seawater CO_2 and will be useful in studies evaluating other methodologies for determining pCO_2.

7. LIMITATIONS AND RESTRICTIONS

The locations, surface water temperatures, and barometric pressures presented in the surface water and atmospheric CO_2 and N_2O data set are all interpolated from the discrete values recorded on the ship, and therefore must be taken only as approximations. As noted in the list of expeditions presented in Table 1, only N_2O was measured on the first four expedition legs. Barometric pressure also was not measured on these first four expedition legs, but this should not be a significant impediment to the use of the data for most applications, as was discussed in the methodology section (Section 5). The reader should note that measurements on NORPAX leg 7 and before were made using anhydrous calcium sulfate drying agent to dry the measured samples, which may bias the CO_2 results slightly due to

acid-base reactions. This problem is discussed by Weiss (1981) and affects only these early legs. During the TPS-24 and TPS-47 expeditions, nitrogen carrier gas was used instead of argon-methane carrier gas for the N_2O determinations. Subsequent comparisons with flask atmospheric samples suggested that this may have produced a small bias of 1 or 2 ppb in the N_2O results from these legs, but no corrections have been applied.

The primary purpose of these data is to describe large-scale distributions of CO_2 and N_2O. The times of the measurements are accurate to within about 1 min, but the ancillary data such as position, sea surface temperature, and barometric pressure were interpolated from observations of extremely variable frequency and accuracy. The uncertainties resulting from these interpolations do not significantly increase the errors in the CO_2 and N_2O results. Ancillary data are reported for the sake of completeness but should not be used in their own right without a more thorough investigation of measurement and interpolation errors.

8. DATA CHECKS PERFORMED BY CDIAC

The Carbon Dioxide Information Analysis Center (CDIAC) endeavors to provide quality assurance (QA) of all data before their distribution. To ensure the highest possible quality in the data, CDIAC conducts extensive reviews for reasonableness, accuracy, completeness, and consistency of form. Although the reviews have common objectives, the specific form must be tailored to each data set; this tailoring process may involve considerable programming efforts. The entire QA process is an important part of CDIAC's effort to ensure accurate, usable CO_2-related data for researchers.

It is important to emphasize that the data were edited by the authors before submission to CDIAC to remove serious outliers and contaminated samples and to correct gross numerical errors. However, not all the data have yet been subjected to the level of scrutiny associated with careful interpretive work. Readers are therefore requested to draw to the attention of the authors any suspected inconsistencies in these data. Readers who have obtained this report directly from CDIAC will automatically receive notification of updates and corrections. *The authors also wish to encourage scientific collaborations with readers for the purpose of interpreting the results of these observations.*

The following summarizes the QA checks performed on the surface water and atmospheric CO_2 and N_2O data by CDIAC.

1. The format of all information, including header items, was checked to ensure consistency throughout each data file.

2. All numeric values were inspected for logical inconsistencies (*e.g.*, values of DATEDA <1 or >31; YEAR <1977 or >1990; TIME <0 or >2359; LAT <-90.0 or >90.0; LON <-180.0 or >180.0) and for the presence of outliers (*e.g.*, PRESS <900 or >1100; H2OTMP <-5 or >32).

The data distributed in this package are identical to the original data received by CDIAC. However, in order to enhance the ease of use of these data, the following alterations in format were made.

1. The data filenames were modified to conform to the two-level naming convention of DOS-based systems; for example, 05.INDOMED.LEG11A.WATER was changed to

INDOM11A.H2O. A complete listing of the filenames and the corresponding expedition legs is given in Section 11 of this document.

2. Within each data file, all header material was condensed into a single line. This involved removing blank lines and abbreviating the designations for sample type (*i.e.*, atmospheric data or surface seawater data). In addition, all descriptive column titles were removed.

3. Values of latitude and longitude were converted from degrees and minutes to decimal degrees, and signs were added to denote the hemisphere (Northern and Eastern Hemispheres were assigned "+" values; Southern and Western Hemispheres were assigned "-" values).

4. The designations for missing values, given as blanks in the original files, were changed to the following: -999.9 for missing values of barometric pressure; 99.99 for missing values of surface water temperature; and -99.9 for missing values of xN_2O and xCO_2.

9. REFERENCES

Broecker, W. S., and T.-H. Peng. 1982. *Tracers in the Sea.* Eldigio Press, Lamont-Doherty Geological Observatory of Columbia University, Palisades, New York.

Weiss, R. F. 1974. Carbon dioxide in water and seawater: The solubility of a non-ideal gas. *Marine Chemistry* 2:203–215.

Weiss, R. F., and B. A. Price. 1980. Nitrous oxide solubility in water and seawater. *Marine Chemistry* 8:347–359.

Weiss, R. F. 1981. Determinations of carbon dioxide and methane by dual catalyst flame ionization chromatography and nitrous oxide by electron capture chromatography. *Journal of Chromatographic Science* 19:611–616.

Weiss, R. F., C. D. Keeling, and H. Craig. 1981. The determination of tropospheric nitrous oxide. *Journal of Geophysical Research* 86:7197–7202.

Weiss, R. F., R. A. Jahnke, and C. D. Keeling. 1982. Seasonal effects of temperature and salinity on the partial pressure of carbon dioxide in seawater. *Nature* 300:511–513.

10. HOW TO OBTAIN THE DATA PACKAGE

This document describes a data set consisting of surface water and atmospheric CO_2 and N_2O measurements carried out by shipboard gas chromatography over the period 1977–1990. The data are available without charge upon request on nine-track magnetic tape, on floppy diskettes (IBM PC format, high- or low-density, 5.25- or 3.5-in. diskettes), or through File Transfer Protocol (FTP) from CDIAC. Requests for magnetic tapes should include any

specific instructions for transmitting the data as required by the user to access the data. Requests not accompanied by specific instructions will be filled on nine-track, 6250 BPI, standard-labeled tapes with characters written in Extended Binary Codes Decimal Interchange Code (EBCDIC), and files will be formatted as given in Section 11. Requests should be addressed to the following:

Carbon Dioxide Information Analysis Center
Oak Ridge National Laboratory
Post Office Box 2008
Oak Ridge, Tennessee 37831-6335
U.S.A.

The tape and documentation can be ordered by telephone, fax, or through electronic mail.

Telephone: (615) 574-0390

Fax: (615) 574-2232

Electronic mail: BITNET: CDP@ORNLSTC
OMNET: CDIAC
INTERNET: CDP@ORNL.GOV

PART 2

INFORMATION ABOUT THE DATA FILES PROVIDED ON MAGNETIC TAPE OR FLOPPY DISKETTES

11. CONTENTS OF THE MAGNETIC TAPE OR FLOPPY DISKETTES

The following is a list of files distributed on magnetic tape or floppy diskettes by CDIAC along with this documentation.

File number, description, and name	Logical records	Record format[a]	Block size	Record length
1. General descriptive information file: NDP044.DES	324	FB	8000	80
2. Track list of expedition legs: TRACK.LST	66	FB	9000	90
3. List of data filenames: DATA.LST	84	FB	8000	80
4. FORTRAN-77 data retrieval code to read and print the surface water and atmospheric CO_2 and N_2O data (Files 5–86): NDP044.FOR	21	FB	8000	80
5. SAS[b] input/output routine to read and print the surface water and atmospheric CO_2 and N_2O data (Files 5–86): NDP044.SAS	26	FB	8000	80
6. Atmospheric CO_2 and N_2O data for Indomed Leg 2: INDOM2.AIR	1080	FB	8000	80
7. Surface seawater CO_2 and N_2O data for Indomed Leg 2: INDOM2.H2O	1068	FB	8000	80
8. Atmospheric CO_2 and N_2O data for Indomed Leg 3: INDOM3.AIR	349	FB	8000	80
9. Surface seawater CO_2 and N_2O data for Indomed Leg 3: INDOM3.H2O	357	FB	8000	80
10. Atmospheric CO_2 and N_2O data for Indomed Leg 4: INDOM4.AIR	1607	FB	8000	80

File number, description, and name	Logical records	Record format[a]	Block size	Record length
11. Surface seawater CO_2 and N_2O data for Indomed Leg 4: INDOM4.H2O	1529	FB	8000	80
12. Atmospheric CO_2 and N_2O data for Indomed Leg 5: INDOM5.AIR	1233	FB	8000	80
13. Surface seawater CO_2 and N_2O data for Indomed Leg 5: INDOM5.H2O	1223	FB	8000	80
14. Atmospheric CO_2 and N_2O data for Indomed Leg 11A: INDOM11A.AIR	204	FB	8000	80
15. Surface seawater CO_2 and N_2O data for Indomed Leg 11A: INDOM11A.H2O	207	FB	8000	80
16. Atmospheric CO_2 and N_2O data for Indomed Leg 12: INDOM12.AIR	1520	FB	8000	80
17. Surface seawater CO_2 and N_2O data for Indomed Leg 12: INDOM12.H2O	1521	FB	8000	80
18. Atmospheric CO_2 and N_2O data for Indomed Leg 15: INDOM15.AIR	989	FB	8000	80
19. Surface seawater CO_2 and N_2O data for Indomed Leg 15: INDOM15.H2O	934	FB	8000	80
20. Atmospheric CO_2 and N_2O data for Indomed Leg 15A: INDOM15A.AIR	353	FB	8000	80
21. Surface seawater CO_2 and N_2O data for Indomed Leg 15A: INDOM15A.H2O	353	FB	8000	80
22. Atmospheric CO_2 and N_2O data for NORPAX Transit: NORPAX0.AIR	375	FB	8000	80
23. Surface seawater CO_2 and N_2O data for NORPAX Transit: NORPAX0.H2O	375	FB	8000	80
24. Atmospheric CO_2 and N_2O data for NORPAX Leg 7: NORPAX7.AIR	1115	FB	8000	80

File number, description, and name	Logical records	Record format[a]	Block size	Record length
25. Surface seawater CO_2 and N_2O data for NORPAX Leg 7: NORPAX7.H2O	1107	FB	8000	80
26. Atmospheric CO_2 and N_2O data for NORPAX Leg 9: NORPAX9.AIR	1141	FB	8000	80
27. Surface seawater CO_2 and N_2O data for NORPAX Leg 9: NORPAX9.H2O	1143	FB	8000	80
28. Atmospheric CO_2 and N_2O data for NORPAX Leg 13: NORPAX13.AIR	1130	FB	8000	80
29. Surface seawater CO_2 and N_2O data for NORPAX Leg 13: NORPAX13.H2O	1128	FB	8000	80
30. Atmospheric CO_2 and N_2O data for NORPAX Leg 15: NORPAX15.AIR	1301	FB	8000	80
31. Surface seawater CO_2 and N_2O data for NORPAX Leg 15: NORPAX15.H2O	1300	FB	8000	80
32. Atmospheric CO_2 and N_2O data for TTO/NAS Leg 1: NAS1.AIR	568	FB	8000	80
33. Surface seawater CO_2 and N_2O data for TTO/NAS Leg 1: NAS1.H2O	542	FB	8000	80
34. Atmospheric CO_2 and N_2O data for TTO/NAS Leg 2: NAS2.AIR	1201	FB	8000	80
35. Surface seawater CO_2 and N_2O data for TTO/NAS Leg 2: NAS2.H2O	1115	FB	8000	80
36. Atmospheric CO_2 and N_2O data for TTO/NAS Leg 3: NAS3.AIR	1300	FB	8000	80
37. Surface seawater CO_2 and N_2O data for TTO/NAS Leg 3: NAS3.H2O	1274	FB	8000	80
38. Atmospheric CO_2 and N_2O data for TTO/NAS Leg 4: NAS4.AIR	1119	FB	8000	80

File number, description, and name	Logical records	Record format[a]	Block size	Record length
39. Surface seawater CO_2 and N_2O data for TTO/NAS Leg 4: NAS4.H2O	933	FB	8000	80
40. Atmospheric CO_2 and N_2O data for TTO/NAS Leg 5: NAS5.AIR	1206	FB	8000	80
41. Surface seawater CO_2 and N_2O data for TTO/NAS Leg 5: NAS5.H2O	1109	FB	8000	80
42. Atmospheric CO_2 and N_2O data for TTO/NAS Leg 6: NAS6.AIR	1255	FB	8000	80
43. Surface seawater CO_2 and N_2O data for TTO/NAS Leg 6: NAS6.H2O	1212	FB	8000	80
44. Atmospheric CO_2 and N_2O data for TTO/NAS Leg 7: NAS7.AIR	1144	FB	8000	80
45. Surface seawater CO_2 and N_2O data for TTO/NAS Leg 7: NAS7.H2O	1089	FB	8000	80
46. Atmospheric CO_2 and N_2O data for Hudson 82-001 Leg 1: HUD1.AIR	1578	FB	8000	80
47. Surface seawater CO_2 and N_2O data for Hudson 82-001 Leg 1: HUD1.H2O	1590	FB	8000	80
48. Atmospheric CO_2 and N_2O data for Hudson 82-001 Leg 2: HUD2.AIR	544	FB	8000	80
49. Surface seawater CO_2 and N_2O data for Hudson 82-001 Leg 2: HUD2.H2O	496	FB	8000	80
50. Atmospheric CO_2 and N_2O data for TTO/TAS Leg 1: TAS1.AIR	953	FB	8000	80
51. Surface seawater CO_2 and N_2O data for TTO/TAS Leg 1: TAS1.H2O	947	FB	8000	80
52. Atmospheric CO_2 and N_2O data for TTO/TAS Leg 2: TAS2.AIR	1165	FB	8000	80

File number, description, and name	Logical records	Record format[a]	Block size	Record length
53. Surface seawater CO_2 and N_2O data for TTO/TAS Leg 2: TAS2.H2O	1133	FB	8000	80
54. Atmospheric CO_2 and N_2O data for TTO/TAS Leg 3: TAS3.AIR	905	FB	8000	80
55. Surface seawater CO_2 and N_2O data for TTO/TAS Leg 3: TAS3.H2O	904	FB	8000	80
56. Atmospheric CO_2 and N_2O data for Ajax Leg 1: AJAX1.AIR	1408	FB	8000	80
57. Surface seawater CO_2 and N_2O data for Ajax Leg 1: AJAX1.H2O	1407	FB	8000	80
58. Atmospheric CO_2 and N_2O data for Ajax Leg 2: AJAX2.AIR	1785	FB	8000	80
59. Surface seawater CO_2 and N_2O data for Ajax Leg 2: AJAX2.H2O	1748	FB	8000	80
60. Atmospheric CO_2 and N_2O data for TPS24 Leg 1: TPS241.AIR	1392	FB	8000	80
61. Surface seawater CO_2 and N_2O data for TPS24 Leg 1: TPS241.H2O	1485	FB	8000	80
62. Atmospheric CO_2 and N_2O data for TPS24 Leg 2: TPS242.AIR	1499	FB	8000	80
63. Surface seawater CO_2 and N_2O data for TPS24 Leg 2: TPS242.H2O	1513	FB	8000	80
64. Atmospheric CO_2 and N_2O data for TPS47 Leg 1: TPS471.AIR	1554	FB	8000	80
65. Surface seawater CO_2 and N_2O data for TPS47 Leg 1: TPS471.H2O	1595	FB	8000	80
66. Atmospheric CO_2 and N_2O data for Ant V Leg 2: ANT52.AIR	3641	FB	8000	80

File number, description, and name	Logical records	Record format[a]	Block size	Record length
67. Surface seawater CO_2 and N_2O data for Ant V Leg 2: ANT52.H2O	1697	FB	8000	80
68. Atmospheric CO_2 and N_2O data for Ant V Leg 3: ANT53.AIR	3592	FB	8000	80
69. Surface seawater CO_2 and N_2O data for Ant V Leg 3: ANT53.H2O	2797	FB	8000	80
70. Atmospheric CO_2 and N_2O data for SAVE Transit: SAVE0.AIR	825	FB	8000	80
71. Surface seawater CO_2 and N_2O data for SAVE Transit: SAVE0.H2O	816	FB	8000	80
72. Atmospheric CO_2 and N_2O data for SAVE Leg 1: SAVE1.AIR	930	FB	8000	80
73. Surface seawater CO_2 and N_2O data for SAVE Leg 1: SAVE1.H2O	888	FB	8000	80
74. Atmospheric CO_2 and N_2O data for SAVE Leg 2: SAVE2.AIR	1624	FB	8000	80
75. Surface seawater CO_2 and N_2O data for SAVE Leg 2: SAVE2.H2O	1618	FB	8000	80
76. Atmospheric CO_2 and N_2O data for SAVE Leg 3: SAVE3.AIR	1790	FB	8000	80
77. Surface seawater CO_2 and N_2O data for SAVE Leg 3: SAVE3.H2O	1785	FB	8000	80
78. Atmospheric CO_2 and N_2O data for SAVE Leg 4: SAVE4.AIR	1713	FB	8000	80
79. Surface seawater CO_2 and N_2O data for SAVE Leg 4: SAVE4.H2O	1697	FB	8000	80
80. Atmospheric CO_2 and N_2O data for SAVE Leg 5: SAVE5.AIR	2044	FB	8000	80

File number, description, and name	Logical records	Record format[a]	Block size	Record length
81. Surface seawater CO_2 and N_2O data for SAVE Leg 5: SAVE5.H2O	1927	FB	8000	80
82. Atmospheric CO_2 and N_2O data for SAVE Leg 6: SAVE6.AIR	1471	FB	8000	80
83. Surface seawater CO_2 and N_2O data for SAVE Leg 6: SAVE6.H2O	1466	FB	8000	80
84. Atmospheric CO_2 and N_2O data for CGC-90 Leg 1: CGC901.AIR	1175	FB	8000	80
85. Surface seawater CO_2 and N_2O data for CGC-90 Leg 1: CGC901.H2O	1197	FB	8000	80
86. Atmospheric CO_2 and N_2O data for CGC-90 Leg 2: CGC902.AIR	996	FB	8000	80
87. Surface seawater CO_2 and N_2O data for CGC-90 Leg 2: CGC902.H2O	1003	FB	8000	80
Total records	102,523	(or ~7.1 mB)		

[a] FB = fixed block.

[b] SAS is the registered trademark of SAS Institute, Inc., Cary, NC 27511-8000.

12. DESCRIPTIVE FILE ON THE TAPE/DISKETTES

The following is a listing of File 1 on the magnetic tape (or NDP044.DES on the floppy diskettes) distributed by CDIAC. This file is intended to complement the documentation and provide details (*i.e.*, variable descriptions, formats, and units) about the data files on the magnetic tape or floppy diskettes.

TITLE OF THE DATA SET

Surface Water and Atmospheric Carbon Dioxide and Nitrous Oxide Observations by Shipboard Automated Gas Chromatography: Results from Expeditions between 1977 and 1990.

DATA CONTRIBUTORS

R. F. Weiss F. A. Van Woy P. K. Salameh

Scripps Institution of Oceanography
University of California, San Diego
La Jolla, California

SOURCE AND SCOPE OF THE DATA

Note: The material provided on the magnetic tape or floppy diskettes for this section is essentially identical to the contents of Sections 4 (Source Information) and 5 (Methodology) of Part I of this documentation.

DATA FORMAT

Eighty-seven files are provided on this magnetic tape or these floppy diskettes, including (1) this descriptive file — File 1 on the magnetic tape or NDP044.DES on the floppy diskettes; (2) a file containing a list of expedition legs on which measurements were made — File 2 on the magnetic tape or TRACK.LST on the floppy diskettes; (3) a file containing a list of the data filenames corresponding (by number) to the expedition legs listed in File 2 (or TRACK.LST) — File 3 on the magnetic tape or DATA.LST on the floppy diskettes; (4) a FORTRAN-77 retrieval program to read and print any of the data files — File 4 on the magnetic tape or NDP044.FOR on the floppy diskettes; (5) a SAS input/output routine to read and print any of the data files — File 5 on the magnetic tape or NDP044.SAS on the floppy diskettes; and (6)–(87) 82 files containing the surface water and atmospheric CO_2 and N_2O data — Files 6–87 on the magnetic tape or *.AIR and *.H2O on the floppy diskettes [with full filenames as listed in File 3 (or DATA.LST)].

Table 2 (located in the documentation that accompanies this tape/diskettes) presents a partial listing of one of the surface water and atmospheric CO_2 and N_2O data files. The data files are formatted in the following way:

```
      CHARACTER SAMPTYP, HEADER*77, DATEMO*3, LATHEM, LONHEM
      INTEGER DATEDA, DATEYR, TIME
      REAL LAT, LON, PRESS, H2OTMP, XN2O, XCO2
      READ (5,500) SAMPTYP, HEADER
   10 READ (5,600,END=800) DATEDA, DATEMO, DATEYR, TIME,
     1  LAT, LATHEM, LON, LONHEM, PRESS, H2OTMP, XN2O, XCO2
      GOTO 10
  500 FORMAT (A1,2X,A77)
  600 FORMAT (I2,1X,A3,1X,I2,3X,I4,3X,F7.3,1X,A1,3X,F8.3,
     1        1X,A1,3X,F6.1,3X,F5.2,3X,F5.1,3X,F5.1)
  800 STOP
```

where

SAMPTYP is a one-character code describing the type of samples being presented in the data file: A = atmospheric samples, S = surface seawater (*i.e.*, gas equilibrated with surface seawater) samples;

HEADER is a descriptive character string consisting of (1) the name of the expedition (*e.g.*, AJAX Leg 1) and (2) the name of the research vessel (*e.g.*, R/V Knorr);

DATEDA is the numeric day of the month on which the sample was collected;

DATEMO is the three-letter abbreviation (Jan, Feb, etc.) for the month in which the sample was collected;

DATEYR is the final two digits of the year (since 1900) in which the sample was collected;

TIME is the Greenwich Mean Time at which the sample was collected, expressed in 24-hour time from 0000 to 2359;

LAT is the latitude (in decimal degrees) at which the sample was collected, with possible values from -90.000 to 90.000 (north latitudes are represented as positive);

LATHEM is the latitudinal hemisphere in which the sample was taken: N = Northern Hemisphere, S = Southern Hemisphere;

LON is the longitude (in decimal degrees) at which the sample was collected, with possible values from -180.000 to 180.000 (east longitudes are represented as positive);

LONHEM is the longitudinal hemisphere in which the sample was taken: E = Eastern Hemisphere, W = Western Hemisphere;

PRESS — is the approximate sea level barometric pressure in mBar, interpolated from discrete values recorded on the ship at hydrographic stations;

H2OTMP — is the approximate surface water temperature in degrees Celsius, interpolated from discrete values recorded on the ship at hydrographic stations;

XN2O — is the dry gas mole fraction of nitrous oxide (N_2O) in the sample, measured in parts per billion (ppb);

XCO2 — is the dry gas mole fraction of carbon dioxide (CO_2) in the sample, measured in parts per million (ppm);

Stated in tabular form, the contents include the following:

Variable[a]	Variable type	Variable width[b]	Line	Starting column	Ending column
SAMPTYP	Character	A1	1	1	1
HEADER	Character	A77	1	4	80
DATEDA	Numeric	I2	2...n	1	2
DATEMO	Character	A3	2...n	4	6
DATEYR	Numeric	I2	2...n	8	9
TIME	Numeric	I4	2...n	13	16
LAT	Numeric	F7.3	2...n	20	26
LATHEM	Character	A1	2...n	28	28
LON	Numeric	F8.3	2...n	32	39
LONHEM	Character	A1	2...n	41	41
PRESS	Numeric	F6.1	2...n	45	50
H2OTMP	Numeric	F5.2	2...n	54	58
XN2O	Numeric	F5.1	2...n	62	66
XCO2	Numeric	F5.1	2...n	70	74

[a] Missing values are represented as follows — PRESS: -999.9; H2OTMP: 99.99; XN2O: -99.9; XCO2: -99.9.

[b] Values for variable width are entered as FORTRAN 77 format codes.

Table 2. Partial listing of one of the surface water and atmospheric CO_2 and N_2O data files (File 23 on the magnetic tape or NORPAX0.H2O on the floppy diskettes)

S	NORPAX	Transit	R/V Wecoma					
6	Jul 79	2015	44.633 N	-124.050 W	1019.2	15.77	442.7	270.8
6	Jul 79	2045	44.605 N	-124.115 W	1019.6	15.48	445.8	273.5
6	Jul 79	2115	44.570 N	-124.193 W	1019.7	15.45	439.8	277.5
6	Jul 79	2145	44.537 N	-124.272 W	1019.6	15.60	350.6	244.5
6	Jul 79	2215	44.502 N	-124.350 W	1019.6	15.21	359.9	235.7
6	Jul 79	2245	44.467 N	-124.428 W	1019.6	14.82	343.9	248.2
6	Jul 79	2315	44.420 N	-124.547 W	1019.4	15.13	321.7	274.7
6	Jul 79	2345	44.362 N	-124.707 W	1019.2	15.58	321.0	269.7
7	Jul 79	0015	44.303 N	-124.868 W	1018.9	16.03	314.3	279.9
7	Jul 79	0045	44.245 N	-125.028 W	1018.7	16.15	320.2	274.4
7	Jul 79	0115	44.187 N	-125.188 W	1018.4	16.21	325.2	263.3
7	Jul 79	0145	44.128 N	-125.348 W	1018.1	16.06	327.6	264.0
7	Jul 79	0215	44.070 N	-125.510 W	1017.8	15.91	316.5	265.4
7	Jul 79	0245	44.012 N	-125.670 W	1017.4	15.88	313.0	274.4
7	Jul 79	0315	43.963 N	-125.795 W	1017.2	15.97	312.0	278.9
7	Jul 79	0345	43.923 N	-125.885 W	1016.8	16.06	309.8	297.8
7	Jul 79	0415	43.885 N	-125.973 W	1016.6	16.14	307.0	298.9
7	Jul 79	0445	43.845 N	-126.063 W	1016.3	16.21	308.7	296.1
7	Jul 79	0515	43.805 N	-126.153 W	1016.1	16.19	307.9	295.2
7	Jul 79	0545	43.765 N	-126.243 W	1015.8	16.07	308.9	316.0
7	Jul 79	0615	43.727 N	-126.332 W	1015.5	16.02	307.8	325.0
7	Jul 79	0645	43.687 N	-126.422 W	1015.1	16.02	308.4	333.8
7	Jul 79	0715	43.640 N	-126.528 W	1014.7	16.02	308.3	334.9
7	Jul 79	0745	43.588 N	-126.653 W	1014.3	16.02	309.1	336.2
7	Jul 79	0815	43.537 N	-126.778 W	1013.8	16.03	308.4	337.3
7	Jul 79	0845	43.485 N	-126.903 W	1013.3	16.09	308.8	338.1
7	Jul 79	0915	43.433 N	-127.028 W	1012.9	16.18	309.0	336.1
7	Jul 79	0945	43.382 N	-127.153 W	1012.4	16.27	307.0	330.1
7	Jul 79	1015	43.330 N	-127.278 W	1012.1	16.31	307.9	332.0
7	Jul 79	1045	43.278 N	-127.403 W	1012.0	16.28	311.6	338.1
7	Jul 79	1115	43.227 N	-127.528 W	1011.9	16.25	308.7	340.8
7	Jul 79	1145	43.175 N	-127.653 W	1011.8	16.27	310.9	341.8
7	Jul 79	1215	43.127 N	-127.778 W	1011.7	16.32	307.1	340.3
7	Jul 79	1245	43.082 N	-127.903 W	1011.6	16.37	-99.9	337.2
7	Jul 79	1315	43.035 N	-128.028 W	1011.5	16.39	308.2	339.4
7	Jul 79	1345	42.990 N	-128.153 W	1011.4	16.39	308.4	339.6
7	Jul 79	1415	42.943 N	-128.278 W	1011.3	16.32	305.8	340.8
7	Jul 79	1445	42.898 N	-128.403 W	1011.2	16.19	306.7	340.1
7	Jul 79	1515	42.852 N	-128.528 W	1011.1	16.05	307.1	342.5
7	Jul 79	1545	42.807 N	-128.653 W	1010.9	15.92	310.8	341.9
7	Jul 79	1615	42.762 N	-128.777 W	1010.2	15.78	310.8	344.7
7	Jul 79	1645	42.718 N	-128.898 W	1009.6	15.65	310.3	338.8
7	Jul 79	1715	42.673 N	-129.018 W	1008.8	15.51	310.4	341.2
7	Jul 79	1745	42.630 N	-129.140 W	1007.6	15.34	310.6	336.3
7	Jul 79	1815	42.587 N	-129.260 W	1007.2	15.30	310.6	333.6
7	Jul 79	1845	42.543 N	-129.382 W	1007.3	15.37	310.3	333.8
7	Jul 79	1915	42.498 N	-129.502 W	1007.4	15.43	309.9	337.7
7	Jul 79	1945	42.455 N	-129.623 W	1007.5	15.50	309.2	335.2
7	Jul 79	2015	42.412 N	-129.727 W	1007.7	15.54	311.0	342.5
7	Jul 79	2045	42.368 N	-129.815 W	1007.8	15.54	310.8	342.5
7	Jul 79	2115	42.323 N	-129.902 W	1007.9	15.54	310.9	342.0
7	Jul 79	2145	42.280 N	-129.990 W	1008.0	15.54	-99.9	344.6
7	Jul 79	2215	42.237 N	-130.077 W	1008.1	15.54	309.8	345.8
7	Jul 79	2245	42.193 N	-130.165 W	1008.2	15.55	310.9	345.0
7	Jul 79	2315	42.148 N	-130.252 W	1008.1	15.57	309.0	344.3
7	Jul 79	2345	42.105 N	-130.340 W	1008.0	15.58	307.6	343.8
8	Jul 79	0015	42.057 N	-130.428 W	1008.0	15.59	309.7	343.5
8	Jul 79	0045	42.005 N	-130.518 W	1008.2	15.60	310.2	343.5
8	Jul 79	0115	41.953 N	-130.607 W	1008.2	15.61	309.5	341.8

REFERENCES

Note: The material provided on the magnetic tape or floppy diskettes for this section is identical to the contents of Section 9 (References) of Part I of this documentation.

13. LISTING OF THE FORTRAN-77 DATA RETRIEVAL PROGRAM

The following is a listing of the FORTRAN-77 data retrieval program (File 4 on magnetic tape or NDP044.FOR on floppy diskette) provided by CDIAC to read and print the surface water and atmospheric CO_2 and N_2O data (Files 6–87 on magnetic tape or files *.AIR and *.H2O on floppy diskettes). The job control language (JCL) statements (preceded by // or /*) shown below are not provided in the file on the tape/diskette; requestors must add JCL statements themselves if required. The statements required will vary for each operating system. The JCL statements shown below are provided to illustrate the statements that an individual using an IBM mainframe (*e.g.*, IBM 3090) at ORNL would need to read these data from a nine-track, 6250 BPI, standard-labeled tape with characters written in EBCDIC.

```
//UIDCO2 JOB(12345),'USER ADDRESS'
//OUT OUTPUT DEFAULT=YES,JESDS=ALL,DEST=LOCAL
//EXEC FORTVCLG
//FORT.SYSIN DD *

C*****************************************************************
C A FORTRAN program to read and print the surface water and
C   atmospheric carbon dioxide and nitrous oxide data.
C*****************************************************************
      CHARACTER SAMPTYP, HEADER*77, DATEMO*3, LATHEM, LONHEM
      INTEGER DATEDA, DATEYR, TIME
      REAL LAT, LON, PRESS, H2OTMP, XN2O, XCO2
      READ (5,500) SAMPTYP, HEADER
      WRITE (6,500) SAMPTYP, HEADER
   10 READ (5,600,END=800) DATEDA, DATEMO, DATEYR, TIME, LAT,
     1  LATHEM, LON, LONHEM, PRESS, H2OTMP, XN2O, XCO2
      WRITE (6,650) DATEDA, DATEMO, DATEYR, TIME, LAT,
     1  LATHEM, LON, LONHEM, PRESS, H2OTMP, XN2O, XCO2
      GOTO 10
  500 FORMAT (A1,2X,A77)
  600 FORMAT (I2,1X,A3,1X,I2,3X,I4,3X,F7.3,1X,A1,3X,F8.3,1X,A1,
     1        3X,F6.1,3X,F5.2,3X,F5.1,3X,F5.1)
  650 FORMAT (I2,1X,A3,1X,I2,3X,I4.4,3X,F7.3,1X,A1,3X,F8.3,1X,
     1        A1,3X,F6.1,3X,F5.2,3X,F5.1,3X,F5.1,'      ')
  800 STOP
      END
/*
//GO.FT05F001 DD UNIT=TAPE62,VOL=SHR=TAPEVOL,DISP=(,PASS),
// LABEL=(4,SL,RETPD=0),
// DSN=TAB.NDP044.DATA
//GO.FT06F001 DD *
//
```

14. LISTING OF THE SAS INPUT/OUTPUT RETRIEVAL PROGRAM

The following is a listing of the SAS[a] data retrieval program (File 5 on magnetic tape or NDP044.SAS on floppy diskette) provided by CDIAC to read and print the surface water and atmospheric CO_2 and N_2O data (Files 6–87 on magnetic tape or files *.AIR and *.H2O on floppy diskettes). The JCL statements (preceded by // or /*) shown below are not provided in the file on the tape/diskette; requestors must add JCL statements themselves if required. The statements required will vary for each operating system. The JCL statements shown below are provided to illustrate the statements that an individual using an IBM mainframe (*e.g.*, IBM 3090) at ORNL would need to read these data from a nine-track, 6250 BPI, standard-labeled tape with characters written in EBCDIC.

```
//UIDCO2 JOB (12345),'USER ADDRESS'
//OUT OUTPUT DEFAULT=YES,JESDS=ALL,DEST=LOCAL
//STEP1 EXEC SAS,SASRGN=4096K,WORK=1600
//IN DD UNIT=TAPE62,VOL=SER=TAPEVOL,DISP=(,PASS),
// DSN=TAB.NDP044.DATA,LABEL=(4,SL,RETPD=0)
//FT06F001 DD SYSOUT=A
//SYSIN DD *

* A SAS program to read and print the surface water and
   atmospheric carbon dioxide and nitrous oxide data;
DATA WEISS(DROP=X);
  INFILE IN;
  INPUT X $ 2 @;
  IF X EQ ' ' THEN DO;
    INPUT SAMPTYP $ 1 @4 HEADER $CHAR77.;
    RECCODE=1;
    END;
  ELSE DO;
    INPUT DATEDA 1-2 DATEMO $ 4-6 DATEYR 8-9 TIME 13-16 LAT 20-26
      LATHEM $ 28 LON 32-39 LONHEM $ 41 PRESS 45-50 H2OTMP 54-58
      XN2O 62-66 XCO2 70-74;
    RECCODE=2;
    END;
DATA PRINT;
  SET WEISS;
  FILE PRINT;
  OPTIONS MISSING=' ';
  IF RECCODE=1 THEN
    PUT SAMPTYP 1 HEADER 4-80;
  ELSE IF RECCODE=2 THEN
    PUT DATEDA 1-2 DATEMO 4-6 DATEYR 8-9 @13 TIME z4. @20 LAT 7.3
    LATHEM 28 @32 LON 8.3 LONHEM 41 @45 PRESS 6.1 @54 H2OTMP 5.2
      @62 XN2O 5.1 @70 XCO2 5.1 @75 '      ';
RUN;
/*
//
```

[a] SAS is the registered trademark of SAS Institute, Inc., Cary, NC 27511-8000.

15. VERIFICATION OF DATA TRANSPORT

The surface water and atmospheric CO_2 and N_2O data can be read by using the FORTRAN or SAS input/output routines provided. Users should verify that the data file has been correctly transported to their systems by generating some or all of the statistics presented in Table 3. These statistics were generated in FORTRAN but can be duplicated in other languages or statistical packages. If the statistics generated by the user differ from those presented here, the data files may have been corrupted in transport.

These statistics are presented only as a tool to ensure proper reading of the data files. They are not to be construed as summarizing the surface water and atmospheric CO_2 and N_2O data.

Table 3. Characteristics of numeric variables in the collective surface water and atmospheric CO_2 and N_2O data files

Variable	Number of observations	Mean	Minimum value	Maximum value
DATEDA	101920	14.991	1.000	31.000
DATEYR	101920	83.469	77.000	90.000
TIME	101920	1176.071	0.000	2359.000
LAT	101920	-2.444	-77.177	79.005
LON	101920	-36.570	-179.998	179.998
PRESS	101920	843.456	-999.900	1035.400
H2OTMP	101920	18.075	-2.130	99.990
XN2O	101920	279.027	-99.900	725.600
XCO2	101920	291.289	-99.900	737.900

The following is a listing of the FORTRAN program used to generate the statistics described in Table 3:

```
      CHARACTER DATAFIL*12, VARNAME(9)*6
      INTEGER DATEDA, DATEYR, TIME, I, J, N
      REAL LAT, LON, PRESS, H2OTMP, XN2O, XCO2, DATA(9,5)
      VARNAME(1)='DATEDA'
      VARNAME(2)='DATEYR'
      VARNAME(3)='TIME  '
      VARNAME(4)='LAT   '
      VARNAME(5)='LON   '
      VARNAME(6)='PRESS '
      VARNAME(7)='H2OTMP'
      VARNAME(8)='XN2O  '
      VARNAME(9)='XCO2  '
      DO 10 I=1,9
        DO 5 J=1,5
          DATA(I,J)=0
    5   CONTINUE
   10 CONTINUE
      N=0
      OPEN (UNIT=2, FILE='DATA.LST', ACCESS='SEQUENTIAL',
     1  FORM='FORMATTED', STATUS='OLD')
      OPEN (UNIT=4, FILE='SUMSTATS.OUT', ACCESS='SEQUENTIAL',
     1  FORM='FORMATTED', STATUS='NEW')
   15 READ (2,100,END=45) DATAFIL
      OPEN (UNIT=3, FILE=DATAFIL, ACCESS='SEQUENTIAL',
     1  FORM='FORMATTED', STATUS='OLD')
      READ (3,200)
   20 READ (3,300,END=40) DATEDA, DATEYR, TIME, LAT, LON, PRESS
     1  H2OTMP, XN2O, XCO2
      DATA(1,1)=REAL(DATEDA)
      DATA(2,1)=REAL(DATEYR)
      DATA(3,1)=REAL(TIME)
      DATA(4,1)=LAT
      DATA(5,1)=LON
      DATA(6,1)=PRESS
      DATA(7,1)=H2OTMP
      DATA(8,1)=XN2O
      DATA(9,1)=XCO2
```

```
      IF(N.EQ.0) THEN
        DO 30 I=1,9
          DO 25 J=4,5
            DATA(I,J)=DATA(I,1)
 25       CONTINUE
 30     CONTINUE
      END IF
      DO 35 I=1,9
        DATA(I,2)=DATA(I,2)+DATA(I,1)
        IF(DATA(I,1).LT.DATA(I,4)) DATA(I,4)=DATA(I,1)
        IF(DATA(I,1).GT.DATA(I,5)) DATA(I,5)=DATA(I,1)
 35   CONTINUE
      N=N+1
      GOTO 20
 40   CLOSE (UNIT=3)
      GOTO 15
 45   CLOSE (UNIT=2)
      DO 50 I=1,9
        DATA(I,3)=DATA(I,2)/REAL(N)
 50   CONTINUE
      DO 55 I=1,9
        WRITE (4,400) VARNAME(I), N, DATA(I,3), DATA(I,4),
     1    DATA(I,5)
 55   CONTINUE
      CLOSE (UNIT=4)
      STOP
100   FORMAT (4X,A12)
200   FORMAT (1X)
300   FORMAT (I2,5X,I2,3X,I4,3X,F7.3,5X,F8.3,5X,F6.1,3X,F5.2,
     1  3X,F5.1,3X,F5.1)
400   FORMAT (1X,A6,2X,I6,2X,F8.3,2X,F8.3,2X,F8.3)
      END
```

APPENDIX

REPRINTS OF PERTINENT LITERATURE

Journal of Chromatographic Science, Vol. 19, December, 1981

Determinations of Carbon Dioxide and Methane by Dual Catalyst Flame Ionization Chromatography and Nitrous Oxide by Electron Capture Chromatography

Ray F. Weiss

Scripps Institution of Oceanography, A-020, University of California, San Diego, La Jolla, California 92093

Abstract

An automated gas chromatographic (GC) system has been developed for the measurement of carbon dioxide, methane, and nitrous oxide in air and other gases. Carbon dioxide is measured by a flame ionization detector (FID) after conversion to methane in pure hydrogen carrier gas, using palladium and nickel dual catalysts which permit direct on-line injection of oxygen-containing samples. The detector measures methane in the same sample, although the system has not been optimized for this gas. Nitrous oxide is measured in a separate aliquot of the sample using a hot electron capture detector (ECD) and argon-methane carrier gas. Typical relative standard deviations of the calculated results are 0.04% for carbon dioxide, 0.4% for methane, and 0.3% for nitrous oxide.

Introduction

The GC measurement of trace quantities of carbon dioxide by catalytic conversion to methane, followed by FID, has become commonplace. In this method, carbon dioxide as well as carbon monoxide are reduced to methane by passing over a reduced nickel catalyst at elevated temperature in the presence of excess hydrogen (1-3). Although the method has been demonstrated to be quantitative for both CO_2 and CO (3), the catalyst has been found to be susceptible to oxidation by oxygen, with a resulting drop in conversion efficiency (4). This problem has traditionally been approached by the use of in-line switching valves, which are used to shunt the oxidizing components of the sample around the catalyst instead of through it. The principal disadvantages of this approach lie in its complexity and in the effects on instrument stability of flow interruptions associated with the switching process.

The instrument described in this paper has been developed for the automated repetitive analysis of carbon dioxide, methane, and nitrous oxide in the atmosphere and in air equilibrated with ocean water. Because the magnitude of natural variations in these samples is often exceedingly small, every effort has been made to achieve the highest possible precision. In the case of carbon dioxide, a new dual catalyst technique has been developed, in which the nickel catalyst is protected by a palladium catalyst that reduces oxygen to water, thus permitting the entire sample to flow through the system without the use of in-line switching valves. Methane is unaffected by the two catalysts, and is also measured by FID. The measurement of nitrous oxide is by electron capture chromatography (5,6) using a separate aliquot of the sample. Because of the highly specific nature of the ECD, and because of the importance of selective interference effects in the electron capture process (7), the separating column and injection sequencing have been selected to optimize the separation of nitrous oxide. The detailed design of the system, its performance, and maintenance are described in the following sections.

Experimental

The configuration of the instrument is shown schematically in Figure 1. Its major components include a custom made gas

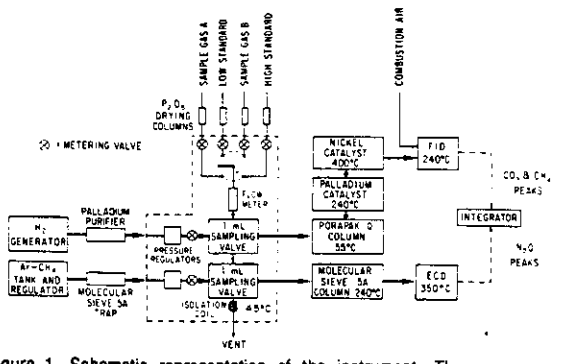

Figure 1. Schematic representation of the instrument. The components enclosed in the thermostated gas sampling module are surrounded by a dashed line. Heavy solid lines denote the two carrier gas flow paths. The CO_2 and CH_4 peaks are detected by FID and the N_2O peaks by ECD. The operations of the instrument are controlled automatically by the integrator.

sampling module, a Perkin-Elmer (Norwalk, Connecticut) model 3920B chromatograph which has been modified extensively to provide the necessary heated areas and improve temperature stability, and a Spectra-Physics (Santa Clara, California) model SP4100 integrator which acquires, processes, and records the data and controls the automatic operation of the system.

Sampling

The automated sampling module has been designed to sample sequentially from four separate gas streams which are supplied to the instrument at ca. 0.6 atm above ambient pressure. In its usual configuration, the sequence of gases is arranged to alternate between samples and standards, each of which passes through its own drying column so that the instrument measures directly the composition of the dry gas. This approach is preferable for applications in atmospheric studies in which the composition on a dry basis is the quantity of interest, but the instrument can also tolerate the injection of moist samples without interference in the analyses. Although the compressed gas standards are already dried, they too are fitted with drying columns so that any unforeseen consequences of these columns will affect the samples and standards equally. Similarly, the pressures of the samples and standards in the drying columns should be equal and constant to minimize the effect of any partitioning between the drier and the gas phase. For the samples, this is done by constantly purging the sampling line through a back-pressure regulator which fixes the pressure at the inlet to the drying column. The samples are pressurized by a stainless steel bellows pump, and the purge rate is typically ca. 5 l/min. It is important to avoid the use of permeable materials in the plumbing of the sampling system, since the permeation rates of nitrous oxide and carbon dioxide in such materials are typically very high.

The selection of an absorbent for the drying columns is most critical for carbon dioxide because this gas is measured most precisely, and is involved in acid-base reactions. For example, the neutral absorbent anhydrous calcium sulfate performs adequately as a drying agent for methane and nitrous oxide measurements, but initially removes small quantities of carbon dioxide from the sample stream. As the absorbent is gradually moistened, this CO_2 is apparently reliberated, and the sample stream becomes slightly enriched in CO_2. Such difficulties are avoided by the use of an acidic absorbent such as P_2O_5. After some experimentation, the best solution for this application has been found to be Aquasorb (Mallinckrodt, St. Louis, Missouri) consisting of a solid support impregnated with P_2O_5 and containing a colored indicator, which gives a dew point of -96°C. With Aquasorb drying columns packed in Pyrex tubes so that the colored indicator can be observed, the results for carbon dioxide, nitrous oxide, and methane have been found to be reproducible and unaltered within the analytical limits of the instrumentation.

Inside the thermostated sampling module, each of the four sample inlets is connected through a metering valve to a Carle Instruments (Anaheim, California) model 2025 4-port stream selector valve, fitted with an 8-position rotary electric actuator which allows the valve to be indexed to the four ports and four intermediate off-port positions. After the stream selector valve, the sample gases flow through a Brooks (Emerson Electric, Hatfield, Pennsylvania) flowmeter, which has been rebuilt to remove dead volume in the end fittings, and is used to set the four inlet metering valves to give the same flow. The sample gases then flow through two Carle model 2021 6-port rotary gas sampling valves, each of which is fitted with a 1 ml sample loop and an electric actuator. The effluent gas is then vented to the atmosphere through an isolation coil made of 2 m x 2.1 mm i.d. stainless steel tubing.

Prior to each sample injection, the stream selector valve is indexed to the next sample port, and the system is purged with sample at 75 ml/min for 90 sec. Considerably less sample could be used, but even at these excessive flushing rates, a single tank of standard will last for over one year of continuous operation. At the end of the flushing period, the stream selector valve is indexed to the next intermediate off-port position, and the gas in the two sampling valves is allowed to equilibrate with atmospheric pressure through the isolation coil before injection.

The effectiveness of the isolation coil was tested by injecting pure N_2 samples and adjusting the equilibration time following the flushing to see if back-mixing of the trace constituents of room air could be detected in the analyses. No such contamination was found at the longest tested equilibration time of 150 sec. The time required for pressure equilibration was tested by measuring the effect on peak area of reducing the equilibration time using normal air samples. No effect was observed with equilibration times as short as 2 sec. From the results of these tests, a 10 sec equilibration time was selected for routine use.

Because the amount of gas in the sampling loops depends directly on the absolute temperature of the sampling loops and on barometric pressure, the accuracy of the results is limited by the changes in these quantities which occur between the injection of a sample and the two adjacent standards. Variations in barometric pressure can generally be neglected, but precise temperature control is essential. In addition, conventional pressure regulators and needle valves used to control the flow of carrier gas are significantly affected by temperature variations. These components are therefore installed within the thermostated sampling module.

The temperature of the sampling module is maintained at ca. 45°C by a high velocity air bath. The recirculation time for air within the closed sampling module is about 1 sec, and the temperature within the module is sensed by a micro-thermistor bead mounted near the two sampling loops. The thermistor is connected through a bridge and a high gain amplifier to a zero-crossing solid state switch which controls the power to the heating element. Because the thermistor has a low thermal mass and the circuit is sensitive to changes of a few thousandths of a degree, the cycling time for the entire heating system is also on the order of 1 sec. Thus, components within the sampling module which are larger than the thermistor and have longer thermal exchange times will experience correspondingly smaller temperature variations. The estimated temperature stability of the gas sampling loops is better than 0.02°C.

Standards and Carrier Gases

For applications involving atmospheric analyses, the instrument is calibrated using compressed air working standards doped to contain a range of concentrations of the measured constituents. Although standards prepared in nitrogen, helium, or other diluent gases may also be used, it is preferred practice, especially with detectors such as the ECD

which are prone to interference effects (7), to use standards which reflect the composition of the unknown samples as closely as possible. The standards used with this instrument are prepared by compressing clean marine air at La Jolla and are stored in aluminum cylinders. By using selective absorbents, or by doping the cylinders prior to the addition of the compressed air, it is possible to vary the trace gas composition of this air over a wide range. Typically, the low range working standard is prepared with near-ambient concentrations of CO_2 (~335 ppm), CH_4 (~1.5 ppm), and N_2O (~300 ppb), and the high range standard is prepared with these constituents enriched by 50 to 75%. In addition, a suite of comparison standards covering a wide range of concentrations is used to check linearity. All the compressed air standards are dried to a dew point of less than -80°C at 1 atm.

The compressed air standards are calibrated independently, and their concentrations are reported as mole fractions of the dry gas. For CO_2, the calibrations are performed in the laboratory of C.D. Keeling at Scripps, using nondispersive infrared analysis and manometric techniques (8). Alternatively, the chromatograph itself can be used to calibrate the compressed air standards against the Keeling CO_2 standards. In either case, the CO_2 calibrations have an accuracy of up to ±0.1 ppm, or about 0.03 relative percent at near ambient concentrations, depending upon how directly the comparisons are tied to the Keeling primary manometric standards. The N_2O concentration in the standards is given by the product of the CO_2 concentration and the N_2O-CO_2 ratio as measured by ultrasonic phase shift GC (9). This method offers the benefit of a nonspecific detector which is relatively immune to interference effects, and also allows N_2O in the 300 ppb concentration range to be calibrated using mixtures of N_2O in CO_2, which need not be diluted more than about 1 ppt. Using this "bootstrap" technique, the calibrations of ambient N_2O concentrations have an accuracy of about ±0.2 relative percent. The calibrations of CH_4 in the standards are still in progress using classical manometric and static dilution techniques.

The approximately 50 ml/min flow of hydrogen carrier gas for the flame ionization measurement of CO_2 and CH_4 is prepared electrolytically from distilled water by a General Electric (Wilmington, Massachusetts) hydrogen generator. The gas is further purified by an Aadco (Rockville, Maryland) hydrogen purifier employing a palladium diffusion thimble operated at 420°C. Without this final step of purification the precision of the methane analysis is significantly degraded.

The carrier gas for the electron capture measurement of N_2O is a 95% argon/5% methane mixture, supplied at a rate of ca. 20 ml/min through a molecular sieve 5A (Coast Engineering, Gardena, California) trap, which is activated at 300°C and is operated at room temperature. Initially, a chemical oxygen scrubber was also used to purify the Ar-CH_4 carrier gas. However, the small amounts of oxidant apparently present in most cylinders of high purity Ar-CH_4 was found to enhance the sensitivity and the stability of the N_2O measurement; thus, best results are obtained with the molecular sieve trap alone.

Separation, Catalysis, and Detection

The separation of the CO_2 and CH_4 peaks is carried out at ca. 55°C on a 3 m x 2.2 mm i.d. stainless steel column packed with 80/100 mesh Porapak Q (Waters Associates, Framingham, Massachusetts). The CO_2 separation can be carried out equally well, with a lower pressure drop but without adequate resolution for CH_4, on a 1.8 m column of Porapak T at 50°C.

Following the separation column, the gases enter the palladium catalyst for the conversion of oxygen to water by reaction with the hydrogen carrier (10). The catalyst is prepared using -60 mesh palladium metal (Alfa Inorganics, Danvers, Massachusetts) mixed in a 1.4 volume ratio with 80/100 mesh acid-washed Chromosorb W (Johns-Manville, Denver, Colorado) as an inert support to prevent the fine palladium powder from blocking the gas flow. A 37 cm length of this mixture is packed into a 2.2 mm i.d. stainless steel tube. By using pure palladium metal (11), the catalytic surfaces are kept strongly reducing, not only by gas phase H_2 but also by hydrogen dissolved in the metal. The reaction is further enhanced by operating the catalyst at elevated temperature, 240°C having been selected as a convenient choice because it is the temperature of the molecular sieve separating column used in the N_2O measurement. Because of the high temperature of this catalyst and of the nickel catalyst which follows, the water produced by the reaction is rapidly eluted through the two catalysts and the detector before the elution of the methane and carbon dioxide peaks from the separating columns.

The reduced nickel catalyst for conversion of CO_2 to CH_4 is prepared from nickelous nitrate deposited on Chromosorb W (3). A 13 cm length of this catalyst is packed into a 2.2 mm i.d. stainless steel tube. After first oxidizing the catalyst by purging with air at ca. 500°C for approximately 30 min, the nickel surface is reduced by purging with H_2 at 500 to 525°C for several hours. The catalyst is then operated at 400°C. Because of the high temperatures involved, quartz wool, rather than the usual Pyrex wool, is used to hold the packing inside the stainless steel tube. If the machine is shut down, or occasionally after prolonged use, it is necessary to reactivate the catalyst using the oxidation and reduction procedures described above.

By using this new dual catalyst technique, it is possible to carry out repetitive on-line measurements of CO_2 in oxygen-containing gases by methane conversion without need of column switching or backflushing during the analysis. The water formed by the palladium catalyst passes through the nickel catalyst without reaction, carbon dioxide is unaffected by the palladium catalyst, and methane passes through both catalysts without reaction.

The CH_4 and CO_2 as CH_4 peaks are detected by the Perkin-Elmer 3920B FID using the approximately 50 ml/min flow of H_2 carrier gas as the source of combustion fuel. The usual hydrogen inlet port of the detector is blocked off in this application. Hydrocarbon-free oxidizing gas is provided at ca. 550 ml/min by an Aadco model 737-1-B "clean air generator," a preparative chromatograph which purifies room air (12). This instrument also enriches the O_2 concentration in the effluent to ca. 40%. The flows of carrier gas and combustion air have been selected to optimize combustion efficiency. The use of normal air for the detector, as opposed to oxygen enriched air, reduces the detection sensitivity by ca. 6%. Although the method described here is greatly simplified, as opposed to the usual flame ionization technique which requires separate supplies of carrier gas and fuel hydrogen, the choice of carrier gas flow rate is fixed by the flame burning characteristics, and is not necessarily the ideal choice for the best column performance. Fortunately, the separations performed here are not terribly demanding, and a relatively high

flow rate for this column diameter is tolerable. If necessary, the flow rate in the separating column can be reduced by introducing additional fuel hydrogen before the palladium catalyst.

The separation of the N_2O peak is carried out at approximately 240°C on a 1.8 m x 2.2 mm i.d. stainless steel column packed with 60/80 mesh molecular sieve 5A. This choice of column packing offers several advantages over Porapak or Porasil columns often used for this analysis (6). The molecular sieve 5A column is highly selective for N_2O, thus reducing the probability that other trace constituents with high electron capture cross sections or significant interference effects will be eluted together with N_2O. Unlike most other column packings, molecular sieves do not produce progressively longer retention times with increasing molecular size. Molecules which are too large to interact with the structure of the molecular sieve pass through the column relatively rapidly. Thus, the interference of such compounds during subsequent analyses is minimized in applications which require repetitive analyses without the benefit of backflushing. The Perkin-Elmer 3920B ^{63}Ni ECD is operated at elevated temperature (350°C) for enhanced sensitivity to N_2O (5,6).

Data Processing and System Automation

A Spectra-Physics SP4100 computing integrator with BASIC program control is used to integrate the peaks with a sensitivity of 0.5 μV·sec per count. Valve operations required for the sampling procedure are controlled through zero-crossing solid state switches activated by the integrator. In addition to sampling and injection, this includes returning the sampling valves to the load position 30 sec after the start of the analysis so that the next sample can be prepared for injection while the analysis is being completed. Because the analyses are highly repetitive, the integration parameters are specifically tailored for each of the three peaks. The instrument begins each analysis by recording the signal from the FID. Following the elution of the CO_2 peak, the integrator activates reed switches to transfer the input signal to the ECD before the elution of the N_2O peak.

At the end of each run, the sample identification, injection time and date, retention times, peak areas, and baseline correction codes are printed and recorded automatically by a solenoid-controlled Hitachi (Tokyo, Japan) model D-980 magnetic cassette recorder interfaced to the integrator using frequency shift keying at a rate of 1200 baud. In the laboratory, the tapes are replayed through a similar tape deck which is fitted with a decoding circuit so that the data may be played directly into a computer through an RS-232C interface for final processing and interpretation. For real time observation of the data, the integrator calculates the concentrations of the unknown samples using the two bracketing standard calibration runs. The results of multiple standard calibration have shown that the performance of the detectors is best represented by a linear fit of the sensitivity against concentration, which is equivalent to fitting peak area against concentration with a quadratic fit forced through the origin. The integrator also calculates the concentration intercept of a linear fit to the two standards as a way of monitoring detector linearity. The linearity of the responses and tuning for optimum linearity are discussed below.

Results and Discussion

A typical chromatogram for a 1 ml air sample, measured under shipboard conditions, is shown in Figure 2. The peaks have been recorded at various attenuation factors as labeled along the baseline and opposite each peak. The labeled peak areas are in units of 0.5 μV·sec per count for the unattenuated signal connected to the 1.0 V full-scale output of the electrometers. The retention times for CH_4, CO_2, and N_2O are about 110, 195, and 360 sec, respectively. Under automatic operation an analysis is repeated every 450 sec, or exactly eight times per hour. Thus, the cycle of the four inlet gases requires 30 min. For samples which do not require the measurement of N_2O, the measurement of CH_4 and CO_2 can be repeated every 220 sec.

Two instruments of this design have been operated a total of more than 8000 hr of continuous analyses under conditions ranging from an air-conditioned shorebased laboratory, to shipboard operation in the tropics with substantial vibration, ship motion, and laboratory temperature variations. The precision of these measurements, expressed as the relative standard deviation of the calculated results for the sample analyses, ranges from 0.02 to 0.08% for CO_2, 0.2 to 0.7% for CH_4, and 0.2 to 0.5% for N_2O. The individual analyses, as opposed to the calculated values which include the results of both sample and standard analyses, are more precise by a factor of 1.4. Although extreme variations in environmental conditions can affect instrumental precision adversely, the

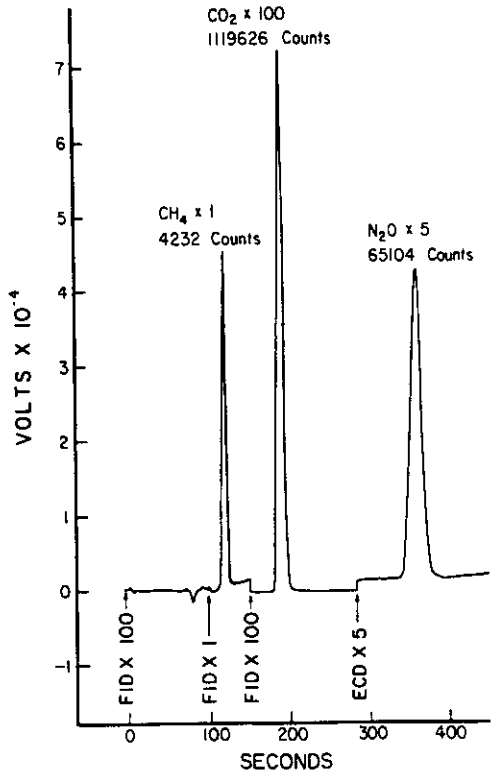

Figure 2. Shipboard chromatogram of a 1 ml air sample.

instrument generally performs as well under shipboard conditions as it does in a well controlled shorebased laboratory. The typical relative standard derivations of the calculated results are 0.04% for CO_2, 0.4% for CH_4, and 0.3% for N_2O.

The very high precision which has been achieved for CO_2 is due to the precision of the gas sampling operations, the quality of the integrating electronics, and the integrating nature of the FID. Unlike concentration detectors such as the thermal conductivity detector, the integrated response of the FID does not show a first-order dependence on carrier flow rate. Rather, the flow of carrier gas is only important insofar as it affects ionization and collection efficiencies. The precision for CH_4 is limited by the small sample size and by less than ideal column separation, both of which are selected solely to optimize the precision for CO_2. The precision achieved for N_2O is equivalent to the best precisions for this analysis reported in the literature. Unlike the FID, the ECD most closely approximates a concentration detector, and its precision is therefore dependent on flow control. The precision for N_2O is probably also limited by the signal-to-noise ratio of the detector.

The linearity of the instrument has been investigated in detail for the measurement of CO_2 in the concentration range of 320 to 450 ppm through analysis of a number of standard tanks provided by the Keeling laboratory. If the detector is properly cleaned and tuned, the results are completely linear. There is no significant difference at the 0.1 ppm confidence level between linear and quadratic fits of the peak area data against concentration for these standards. However, experience has shown that after several months of continuous operation the FID can become significantly nonlinear, either by contamination of the collector surface or by misadjustment of the air inlet orifice. In this case, as discussed above, the results are still closely represented by a quadratic fit of peak area against concentration. The linearity of the detector is easily restored by cleaning the collector in strong base and then in strong acid or by adjusting the air inlet orifice.

Occasionally, after months of operation, the nickel catalyst has been found to deteriorate in a way which will not respond to the usual activation procedures. This deterioration results in a broadening of the CO_2 peak and a reduction in CO_2 precision. This problem is best cured by replacement of the nickel catalyst. A search for alternate forms of nickel catalyst is now in progress.

The long-term performance of the ECD has been excellent despite its high operating temperature. Although the linearity of this detector has not been studied as carefully as the FID, no significant nonlinearities have been detected within the limits of instrumental precision over the 300 to 600 ppb concentration range.

An example of instrumental performance for continuous atmospheric analyses is shown in Figure 3. The data were measured aboard ship in the equatorial Pacific Ocean during a 24 day period in the fall of 1979. Dry air mole fractions are plotted against time (Figure 3) with 48 separate measurements plotted for each gas each day. Approximate latitudes are labeled along the upper axis, showing that the ship's track is divided into northbound and southbound segments, crossing the Intertropical Convergence Zone at about five degrees north three separate times. Thus, the data demonstrate not only the precision of the measurements over an extended period at sea, but also show reproducibly the interhemispheric differences in CO_2 and CH_4 concentrations. The existence of a possible small interhemispheric gradient in N_2O is not well demonstrated by the limited geographical coverage of these data, but is now being investigated using similar data covering a broader geographical range.

Conclusion

The dual catalyst GC technique for the measurement of CO_2 has been demonstrated to be comparable in precision to the best infrared analysis techniques now in use. In addition, the chromatograph has several distinct advantages over the infrared method. The 1 ml sample size, as compared to as much as 1 liter for the infrared analysis, makes possible the analysis of small samples, such as those equilibrated with, or extracted from, small samples of seawater or other natural waters. Efforts to exploit this capability are now in progress. Another consequence of this smaller sample size is that the consumption of standards in long-term monitoring is no longer a practical limitation. The chromatographic analysis is rapid and easily automated. The linearity of the chromatographic response exceeds that of the infrared analyzer, making calibration less tedious, especially when samples cover a wide range of CO_2 concentrations. Finally, the response for CO_2 is essentially independent of the gross composition of the gas, so that there are no corrections analogous to the pressure broadening correction which is required by the presence of oxygen in the infrared analyzer.

Although the electron capture results for N_2O are of high precision, the specific nature of the detector and its susceptibility to interference effects argue against its use for long-term monitoring unless the composition of standards, samples, and carrier gases with respect to all major and minor components can be rigidly maintained. These long-term measurements are best carried out by more direct, nonspecific methods such as the ultrasonic phase shift technique (9). However, the precision of the electron capture technique makes this method

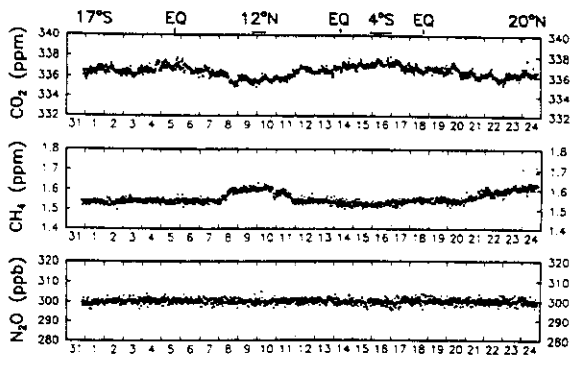

Figure 3. Atmospheric concentrations of CO_2, CH_4, and N_2O measured between October 31 and November 24, 1979 aboard the Research Vessel **Wecoma** during Leg 9 of the NORPAX Equatorial Experiment between Tahiti and Hawaii. The data are expressed as mole fractions of the dry gas plotted against time, with the days of the month labeled along the lower axis of each plot. In the case of CH_4, the concentration scale is provisional pending calibration. Approximate latitudes are labeled across the top of the figure, and the latitudinal dependences of the data are discussed briefly in the text.

ideal for the measurement of spatial or short-term variations such as those made from a moving platform.

After the measurement of tens of thousands of samples in the laboratory and on ships around the world, the reliability and serviceability of the instrumentation have been well demonstrated. The data recovery rate for both the flame ionization and electron capture systems has been well above 99%, the only losses having been due to the failure of two power supply capacitors. The instrumentation has also proven to be relatively portable and well suited for extended operation in remote areas, not only because of its low rate of consumption of standard gases, but also because it generates its own hydrogen carrier gas and hydrocarbon-free combustion air. The dual catalyst flame ionization technique is now being implemented for the measurement of atmospheric carbon dioxide at remote, clean-air global monitoring sites.

Acknowledgements

The author is indebted to a number of persons who have contributed to the development of this instrumentation. The shipboard operations and much of the laboratory testing were carried out by F.A. Van Woy, whose patience and perseverance have led to a better understanding of the system and its idiosyncracies. The calibration of the instrument for CO_2, and the verification of its performance for this gas, have depended directly on the generous assistance of C.D. Keeling, P. Guenther, and D. Moss of the Scripps CO_2 Laboratory. Finally, the author thanks N. Andersen and L. Machta for their interest and support. This work was supported by the Marine Chemistry and Atmospheric Chemistry Programs of the U.S. National Science Foundation. Additional testing and development work during the NORPAX Equatorial Experiment was supported by the U.S. Department of Energy.

References

1. F.W. Hightower and A.H. White. Synthesis of methane from water gas. *Ind. Eng. Chem.* **20**: 10-15 (1928).
2. K. Porter and D.H. Volman. Flame ionization detection of carbon monoxide for gas chromatographic analysis. *Anal. Chem.* **34**: 748-49 (1962).
3. F.W. Williams, F.J. Woods, and M.E. Umstead. Determination of carbon dioxide in the parts-per-million range with gas chromatography. *J. Chromatogr. Sci.* **10**: 570-72 (1972).
4. Carle Instruments, unpublished operating instructions for the "Methanizer" catalytic converter.
5. W.E. Wentworth and R. Freeman. Measurement of atmospheric nitrous oxide using an electron capture detector in conjunction with gas chromatography. *J. Chromatogr.* **79**: 322-23 (1973).
6. R.A. Rasmussen, J. Krasnec, and D. Pierotti. N_2O analysis in the atmosphere via electron capture-gas chromatography. *Geophys. Res. Lett.* **3**: 615-18 (1976).
7. R.E. Sievers, M.P. Phillips, R.M. Barkley, M.A. Wizner, M.J. Bollinger, R.S. Hutte, and F.C. Fehsenfeld. Selective electron-capture sensitization. *J. Chromatogr.* **186**: 3-14 (1979).
8. C.D. Keeling, R.B. Bacastow, A.E. Bainbridge, C.A. Ekdahl Jr., P.R. Guenther, L.S. Waterman, and J.F. Chin. Atmospheric carbon dioxide variations at Mauna Loa Observatory, Hawaii. *Tellus.* **28**: 538-51 (1976).
9. R.F. Weiss, C.D. Keeling, and H. Craig. The determination of tropospheric nitrous oxide. *J. Geophys. Res.* **86**: 7197-202 (1981).
10. M. Krejci, K. Tesarik, and J. Janak. Rapid chromatophic separation and determination of helium-neon-argon and nitrogen-krypton-methane mixtures and determination of argon in the presence of oxygen at room temperature. In *Gas Chromatography*. H.J. Noebels, R.F. Wall, and N. Brenner, eds. Academic press, New York, New York, 1961, pp. 255-61.
11. R.F. Weiss and H. Craig. Precise shipboard determination of dissolved nitrogen, oxygen, argon, and total inorganic carbon by gas chromatography. *Deep-Sea Res.* **20**: 291-303 (1973).
12. W.H. King Jr. Generation of clean air to permit gas chromatography without cylinders. *Anal. Chem.* **43**: 984 (1971).

Manuscript received February 2, 1981;
revision received July 1, 1981.

INTERNAL DISTRIBUTION

1. T. A. Boden
2. J. B. Cannon
3. J. H. Cushman
4. R. M. Cushman
5. M. P. Farrell
6. D. E. Fowler
7. C. W. Gehrs
8. S. G. Hildebrand
9. P. Kanciruk
10. T. H. Peng
11. D. E. Reichle
12. R. J. Sepanski
13. F. E. Sharples
14. D. S. Shriner
16. S. H. Stow
17. R. I. Van Hook

18-317. CDIAC

318. Central Research Library

319-323. ESD Library

324. Information Analysis Library

325-326. Laboratory Records Department

327. Laboratory Records, RC

328. ORNL Patent Office

329. ORNL Y-12 Technical Library

EXTERNAL DISTRIBUTION

330. S. S. Alexander, Pennsylvania State University, Department of Geosciences, 503 Deike Building, University Park, PA 16802

331. J. H. Allen, National Oceanic and Atmospheric Administration, National Geophysical Data Center Code E/GC2, 325 Broadway, Boulder, CO 80303

332. D. Alvic, EERC/UT, Pellissippi Office, Ste. 100, 10521 Research Drive, Knoxville, TN 37932

333. N. Andersen, National Science Foundation, OCE, 1800 G. Street, Washington, DC 20550

334. R. C. Barry, University of Colorado, World Data Center A, Glaciology, CIRES,

Campus Box 449, Boulder, CO 80309-0449

335. P. Brewer, Monterey Bay Aquariam Res. Inst., 160 Central Avenue, Pacific Grove, CA 93950

336. M. A. Chinnery, National Oceanic and Atmospheric Administration, National Geophysical Data Center Code E/GC2, 325 Broadway, Boulder, CO 80303

337. Roger C. Dahlman, Global Change Research Program, Environmental Sciences Division, Office of Health and Environmental Research, ER-74, U.S. Department of Energy, Washington, DC 20585

338. W. Draeger, EROS Data Center, U.S. Geological Survey, Sioux Falls, SD 57198

339. M. Dryer, National Oceanic and Atmospheric Administration, Space Environmental Lab., ERL/OAR, R/E/SE, 320 Broadway, Boulder, CO 80303

340. R. Feely, National Oceanic and Atm. Adm., Pacific Marine and Enviro. Lab, 7600 Sand Point Way, NE, Seattle, WA 98115

341. J. Filson, National Earthquake Information Center, U.S. Geological Survey, Denver Federal Center, P.O. Box 20546, Denver, CO 80225

342. Jerry F. Franklin, Bloedel Professor of Ecosystem Analysis, College of Forest Resources, University of Washington, Anderson Hall (AR-10), Seattle, WA 98195

343. David J. Galas, Office of Health and Environmental Research, ER-70, U.S. Department of Energy, Washington, DC 20585

344. S. Graves, National Aeronautics and Space Administration Headquarters Code SED, 600 Independence Avenue, Washington, DC 20546

345. J. L. Green, National Space Science Data Center, NASA Goddard Space Flight Center, Code 630.2, Greenbelt, MD 20771

346. Thomas J. Gross, Global Change Research Program, Environmental Sciences Division, Office of Health and Environmental Research, ER-74, U.S. Department of Energy, Washington, DC 20585

347. K. D. Hadeen, National Oceanic and Atmospheric Administration, NESDIS/NCDC, Federal Building MC E/CC, Asheville, NC 28801

348. R. C. Harriss, Institute for the Study of Earth, Oceans, and Space, Science and Engineering Research Building, University of New Hampshire, Durham, NH 03824

349-353. G. Heimerdinger, Woods Hole Oceanographic Institution, McLean Building, Woods Hole, MA 02543

354. W. J. Hinze, Purdue University, Department of Earth and Atmospheric Sciences, West Lafayette, IN 47907

355. G. Y. Jordy, Director, Office of Program Analysis, Office of Energy Research, ER-30, G-226, U.S. Department of Energy, Washington, DC 20585

356. D. Lauer, EROS Data Center, U.S. Geological Survey, Sioux Falls, SD 57198

357. S. Levitus, NOAA/National Oceanographic Data Center, 1825 Connecticut Avenue, NW, Washington, DC 20235

358. M. S. Loughridge, National Oceanic and Atmospheric Administration, National Geophysical Data Center, Code E/GC3, 325 Broadway, Boulder, CO 80303

359. H. M. McCammon, Acting Deputy Director, Environmental Sciences Division, Office of Health and Environmental Research, Office of Energy Research, ER-74, U.S. Department of Energy, Washington, DC 20585

360. L. Merlivat, Universite Pierre et Marie Curie, LODYC, 2 Etage, 4 place Jussieu, 75252 Paris Cedex 05

361. R. H. Olsen, Vice President for Research, University of Michigan, Medical Science Building II, #5605, 1301 East Catherine Street, Ann Arbor, MI 48109-0620

362. J. T. Overpeck, National Oceanic and Atmospheric Administration, National Geophysical Data Center, Paleoclimatology Program, 325 Broadway E/EC, Boulder, CO 80303

363. Ari Patrinos, Director, Environmental Sciences Division, Office of Health and Environmental Research, ER-74, U.S. Department of Energy, Washington, DC 20585

364. S. Ichtiaque Rasool, IGBP Data and Information System Office, Universite Paris, Tour 26, 4 Etage, Aile 26-16, 4 Place Jussieu, 75230 Paris, Cedex 06, France

365. Michael R. Riches, Global Change Research Program, Environmental Sciences Division, Office of Health and Environmental Research, ER-74, U.S. Department of Energy, Washington, DC 20585

366. S. Ruttenberg, Univ. Corporation for Atmospheric Research, CSNET, P. O. Box 3000, Boulder, CO 80307-3000

367-371. Peter K. Salameh, Scripps Institution of Oceanography, 8602 La Jolla Shores Drive, La Jolla, CA 92037

372. A. L. Shumbera, National Oceanic and Atmospheric Administration, WDC-A for Meteorology, National Climatic Data Center, Federal Building MC E/CC, Asheville, NC 28801

373-377. F. A. Van Woy, Scripps Institution of Oceanography, 8602 La Jolla Shores Drive, La Jolla, CA 92037

378-382. SIO Library, 8602 La Jolla Shores Drive, La Jolla, CA 92037

383-389. SIO Reference Series Contribution, 8602 La Jolla Shores Drive, La Jolla, CA 92037

390-391. SIO Technical Publications, 8602 La Jolla Shores, La Jolla, CA 92037

392. T. Takahashi, Columbia University, Lamont-Doherty Geological Obs., Palisades, NY 10964

393. P. Tans, National Oceanic and Atm. Adm., Mailcode R/E/CG1, 325 Broadway, Boulder, CO 80304

394. F. Webster, University of Delaware, College of Marine Studies, Lewes, DE 19958

395-409. Ray F. Weiss, Scripps Institution of Oceanography, 2271 Ritter Hall, 8602 La Jolla Shores Drive, La Jolla, CA 92037

410. F. J. Wobber, Environmental Sciences Division, Office of Health and Environmental Research, Office of Energy Research, ER-74, U.S. Department of Energy, Washington, DC 20585

411. L. W. Wolf, National Research Council, Commission on Geosciences, Environment, and Resources, 2101 Constitution Avenue, Washington, DC 20418

412. Office of Assistant Manager for Energy Research and Development, U.S. Department of Energy Oak Ridge Field Office, P. O. Box 2001, Oak Ridge, TN 37831-8600

413-414. Office of Scientific and Technical Information, P. O. Box 62, Oak Ridge, TN 37831